ABSTRACT

Title of Document: **FUNCTIONAL CHARACTERIZATION OF PAPAIN-LIKE PROTEASE p48 REQUIRED FOR REPLICATION OF HYPOVIRUS CHV-1 RESPONSIBLE FOR VIRULENCE-ATTENTUATION OF THE CHESTNUT BLIGHT FUNGUS**

Kenneth S. Jensen, Jr.,
Doctor of Philosophy, 2014

Directed By: Professor Donald L. Nuss,
Institute for Bioscience &
Biotechnology Research
Department of Cell Biology &
Molecular Genetics

The prototypic hypovirus CHV-1/EP713, responsible for virulence attenuation (hypovirulence) of the chestnut blight fungus *Cryphonectria parasitica*, encodes two leader papain-like proteases, p29 and p48, at the N-terminus of ORF A and ORF B, respectively. Protease p29 has been shown to be dispensable for hypovirus RNA replication, whereas protease p48 is essential for hypovirus RNA replication. The p48 protein can also act *in trans* to complement a mutant CHV-1/EP713, p48 deficient virus (Δp48). The Δp48 mutant virus retained replication competence in the apparent absence of p48 following transmission to wild-type *C. parasitica* and

successive subculturing. It was concluded that p48 plays an essential role in the initiation but not the maintenance of virus RNA propagation. Here, I report efforts to identify the mechanisms by which the CHV-1 p48 papain-like protease contributes to virus replication. Mutational analyses of the p48 catalytic and cleavage site residues defined the requirements for p48/ORF B processing *in vivo* and revealed its functional importance in the context of viral replication and RNA accumulation. In addition, the ability of ORF B to undergo processing through an alternative pathway was identified. Mutation of either of the p48 catalytic residues eliminated the capability of p48 to complement the Δp48 mutant virus, suggesting that these residues are essential for *in trans* rescue (Chapter 2). Extensive deletion/addition analyses identified two independent but redundant p48 functional domains that are essential for virus replication. The first functional domain is between amino acids Thr169-Glu302 and the second functional domain is between amino acids 330-418. The requirements for p48 function were found to be different when p48 was provided *in trans* than when provided *in cis*. Whereas only one functional domain is required for viral replication when p48 is supplied *in cis*, neither functional domain alone is sufficient for complementation of the Δp48 mutant virus (Chapter 3). The information gained from these studies has significantly increased our knowledge of the requirements and role of p48 in hypovirus replication and provided new insights into the diversity of replication strategies employed by positive strand RNA viruses.

FUNCTIONAL CHARACTERIZATION OF PAPAIN-LIKE PROTEASE p48 REQUIRED FOR REPLICATION OF HYPOVIRUS CHV-1 RESPONSIBLE FOR VIRULENCE-ATTENTUATION OF THE CHESTNUT BLIGHT FUNGUS

By

Kenneth S. Jensen Jr.

Dissertation submitted to the Faculty of the Graduate School of the
University of Maryland, College Park, in partial fulfillment
of the requirements for the degree of
Doctor of Philosophy
2014

Advisory Committee:
Dr. Donald L. Nuss, Chair
Dr. Jeffrey DeStefano
Dr. Jonathan Dinman
Dr. David Straney
Dr. James Culver, Dean's Representative

Dedication

I would like to dedicate this dissertation to my wonderful wife, Lindsay, my amazing son, Carter, and to my parents, Ken and Patty, for their unconditional love, support, and encouragement.

Acknowledgements

I would like to take this opportunity to express my profound gratitude to my mentor Dr. Donald Nuss for his guidance, teachings, and encouraging advice. Your support was vital to my growth as a scientist and for that, I will be forever grateful. I am truly fortunate to have had such a wonderful mentor.

I would also like to thank all of my committee members: Dr. Jonathan Dinman, Dr. James Culver, Dr. David Straney, and Dr. Jeffrey DeStefano, for their support and valuable advice. I appreciate their time and efforts in reviewing and discussing my dissertation.

In addition, I would like to extend my gratitude to all past and present members of the Nuss laboratory: Xuemin Zhang, Diane Shi, Dongxiu Zhang, Martin Speiring, and Gil Choi. Thank you all for the guidance, support, help, and discussions over the course of my graduate career it is very much appreciated.

I am also grateful to Dr. Daniel Nelson and his lab, especially Yang Shen, for all of their help in teaching me the finer points of protein purification, and to Dr. Larik Turko and his lab, specifically Kyle Anderson for the introduction into the world of mass spectrometry.

Special thanks go to my family, especially my wife, Lindsay, parents Ken and Patty, and parents-in-law Mike and Genny. You have all always been there for me, supporting me, and made this possible.

Table of Contents

Abbreviations

aa	Amino Acids
Arg	Arginine
agl	Argonaute like gene
Asp	Aspartic Acid
CHAP	Cysteine, histidine-dependent amidohydrolase/ peptidase
CHV	*Cryphonectria parasitica* hypovirus
CThTV	*Curvularia* thermal tolerance virus
Cys	Cysteine
dcl	Dicer like gene
D1	Domain 1
D2	Domain 2
DI RNA	Defective Interfering RNA
dsDNA	Double-stranded DNA
dsRNA	Double-stranded RNA
eGFP	Enhanced green fluorescence protein
FgHV1	*Fusarium gramminearum* hypovirus 1
Glu	Glutamic acid
GLRaV-2	Grapevine Leafroll-associated Virus-2
Gly	Glycine
GyH	Glycosyl hydrolase
HC-Pro	Helper Component Proteinase
His	Histidine
HvV190S	*Helminthosporium Victoriae* Virus 190S
IEF	Isoelectric Focusing
IRES	Internal Ribosomal Entry Site
kb	Kilobases
kbp	Kilobase pairs
kDa	Kilodaltons

LC/MS	Liquid Chromatography Mass Spectrometry
MHV	Murine Hepatitis Virus
MS/MS	Tandem Mass Spectrometry
nm	Nanometers
nt	nucleotides
ORF	Open Reading Frame
PCD	Programmed Cell Death
PDA	Potato Dextrose Agar
PDB	Potato Dextrose Broth
PlHV1	*Phomopsis longicolla* hypovirus 1
PLP1	Papain-like Protease 1 of MHV
PMF	Peptide Mass Fingerprint
qRT-PCR	Quantitative Real-Time PCR
RDRP	RNA Dependent RNA Polymerase
RISC	RNA Induced Silencing Complex
RNAi	RNA interference
ScV-L-A	*Saccharomyces cerevisiae* virus L-A
SDS	Sodium Dodecyl Sulfate
Ser	Serine
ssDNA	Single-stranded DNA
SsHV1	*Sclerotinia sclerotiorium* hypovirus 1
ssRNA	Single-stranded RNA
TEV	Tobacco Etch Virus
Thr	Threonine
UGT	UDP-Glucose/sterol glucosyltranserase
UTR	Untranslated Region
VcHV1	*Valsa ceratosperma* hypovirus 1
vic	Vegetative incompatibility
vsRNA	Small virus-derived RNAs
WT	Wild-type
ZYMV	Zucchini Yellow Mosaic Virus

List of Figures

Chapter 1: Introduction and Literature Review

1.1 Statement of Purpose

Positive-stranded RNA viruses have the ability to replicate in numerous hosts, including, but not limited to, fungi, plants, insects, and animals. These viruses employ similar replication mechanisms, including rearrangement of host membranes to support viral replication, alteration of the host signaling pathways, and suppression or alteration of anti-viral responses. The main difference between mycoviruses and viruses that infect plants and animals is that, with one exception, mycoviruses have an exclusively intracellular lifecycle, and members of *Hypoviridae* family, in particular, do not encode structural proteins and lack the ability to form virions.

Infection of the chestnut blight fungus, *Cryphonectria parasitica* (*C. parasitica*), with the prototypical hypovirus CHV-1/EP713, a single-strand RNA virus of positive polarity, results in the reduction of fungal virulence, termed hypovirulence, as a result of virus-mediated alterations of host-signaling pathways. CHV-1/EP713 has two open reading frames (ORFs), A and B, each encoding a papain-like leader protease at the N-terminus, that are believed to have arisen from a gene duplication event. The ORF B protease, p48, has been demonstrated to be essential for viral replication, whereas the ORF A protease, p29, is dispensable for viral replication. In addition, p48 was detected when intracellular vesicles associated with viral RNA were extracted from a CHV-1 infected EP155 isolate (Wang et al., 2013). When supplied *in trans*, p48 was shown to complement a Δp48 mutant virus.

Surprisingly, once rescued, the Δp48 mutant virus continued to replicate in the absence of p48, suggesting a novel 'hit and run' mechanism.

The goal of this study was to investigate mechanisms by which CHV-1 p48 papain-like protease contributes to virus replication. Mutational analyses defined the requirements for p48 cleavage, previously studied only *in vitro*, and determined its functional importance in the context of viral replication, revealing a contribution to viral RNA accumulation and an alternative p48-processing pathway. Extensive deletion/addition analyses identified two independent but redundant p48 functional domains required for viral replication. In addition, requirements for p48 function were found to be different when p48 was provided *in trans* than when provided *in cis*. The information gained from these studies add to our understanding of the role of p48 in viral replication and provide further insight into the diversity of replication mechanisms employed by positive-sense RNA viruses.

1.2 Mycoviruses

Overview

Viruses that infect fungi are referred to as mycoviruses and are found in all major fungal taxonomic groups (Buck, 1998; Hollings, 1978). While fundamentally similar to viruses of plants and animals, mycoviruses do have several distinguishing features. Mycoviruses generally lack any extracellular routes of infection and they are not known to have any natural vectors (Ghabrial and Suzuki, 2009; Nuss, 2010). With the exception of a recently identified Gemini-like virus (Yu et al., 2013), mycovirus infection cannot be initiated by exposing uninfected fungal mycelia to cell extracts prepared from an infected strain. Rather, mycoviruses use two main transmission

methods, hyphal anastomosis, or fusion of the hyphae, and dissemination via asexual fungal spores, depending upon the host. This exclusive intracellular lifecycle is characterized generally by persistent infections without severe symptoms or cell death and, in the case of several mycovirus families, the absence of a structural protein or formation of distinct virions (Reviewed in Nuss, 2010).

Mycovirology has a much more recent history than the study of animal and plant viruses, with the first description of a fungal virus, the agent responsible for a mushroom die back disease known as La France disease, appearing in 1962 (Hollings, 1962). The application of molecular techniques over the subsequent decades has provided a basic understanding of the genome organizations, structures and replication strategies employed by mycoviruses. These advances have contributed to a basic taxonomic framework that is rapidly expanding as new fungal viruses are identified and characterized. A majority of mycoviruses isolated from filamentous fungi have RNA genomes, either single-stranded (ssRNA) or double-stranded (dsRNA), with 2 exceptions being a double-stranded DNA (dsDNA) virus isolated from the aquatic fungus *Rhizidiomyces* (Dawe and Kuhn, 1983) and a single-stranded DNA (ssDNA) virus isolated from *Sclerotinia sclerotiorum* (Yu et al., 2013). RNA mycoviruses currently fall within seven primary taxonomic families: *Totiviridae*, *Partitiviridae*, *Chrysoviridae*, *Reoviridae*, *Endornaviridae*, *Narnaviridae*, and *Hypoviridae* (Nuss, 2010).

Members of the *Totiviridae*, *Partitiviridae, Chrysoviridae* and *Reoviridae* families have dsRNA genomes, form isometric particles, and viruses in related genera have the ability to infect organisms other than fungi (Ghabrial and Suzuki, 2009).

Members of the family *Totiviridae* form icosahedral virions approximately 33-40 nanometers (nm) in diameter, and the genome ranges from 4.6- to 7-kbp (Figure 1.1) (Wickner et al., 2012). Totiviruses have a monopartite genome that encodes a capsid protein and RNA-dependent RNA polymerase (RDRP). Three different strategies for RDRP expression have been identified: (1) through -1 ribosomal frameshifting as observed in *Saccharomyces cerevisiae* virus L-A (ScV-L-A) (Dinman et al., 1991; Dinman and Wickner, 1994); (2) through proteolytic processing pathways, as in *Ustilago maydis* virus H1 (Kang et al., 2001); and (3) through a termination/re-initiation mechanism as demonstrated by *Helminthosporium Victoriae* Virus 190S (HvV190S) (Huang and Ghabrial, 1996; Huang et al., 1997).

Members of the family *Partitiviridae* form icosahedral virions 34-42 nm in diameter, however the genome consists of two dsRNA fragments ranging from 1.4- to 2.3-kbp, which are individually packaged (Ghabrial and Suzuki, 2009). One dsRNA encodes the capsid protein and the second encodes the RDRP, with both virions needing to be present to establish an infection. Three genera of *Partitiviridae* have been identified with one infecting fungi and the other two infecting plants (Ghabrial et al., 2005A).

Members of the family *Chrysoviridae* form icosahedral virions 30-40 nm in diameter with a multipartite genome consisting of four separately encapsidated dsRNA fragments ranging from 2.4- to 3.6-kbp (Figure 1.1) (Ghabrial et al., 2005B). Of the four dsRNA fragments, two have been shown to encode the capsid and RDRP proteins while the functions of the proteins encoded by the other two dsRNAs have not been determined (Nuss, 2010).

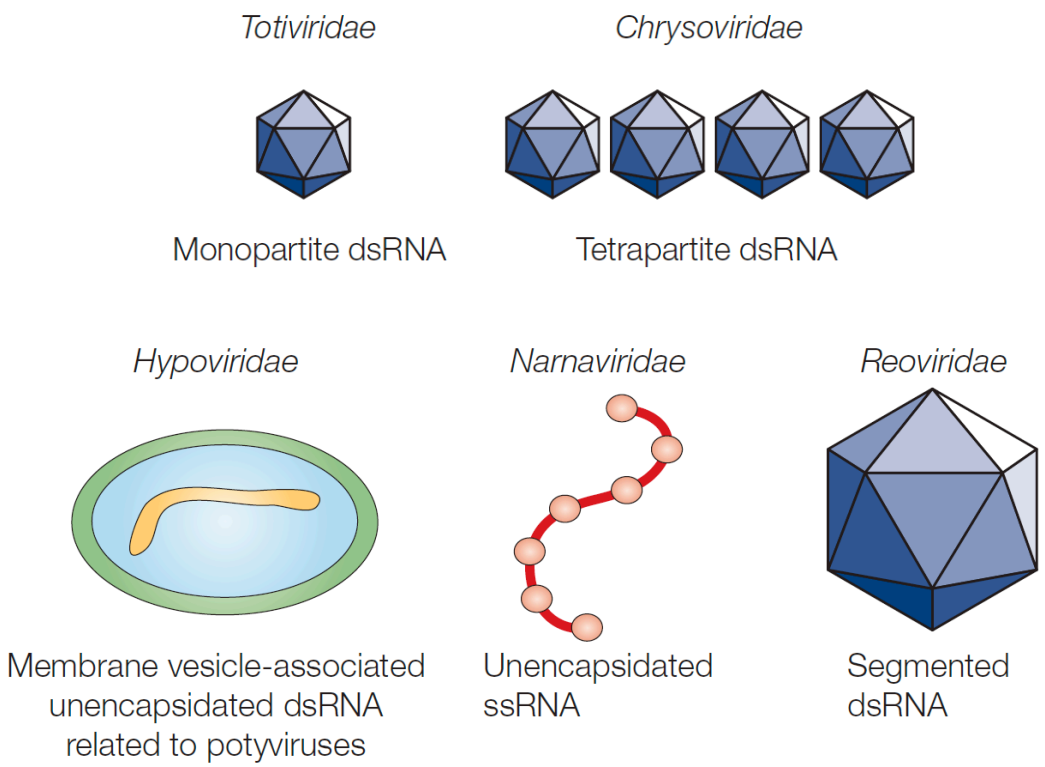

Figure 1.1 – Taxonomic families of select mycoviruses that are associated with hypovirulence of plant pathogenic fungi. The Internation Committee on Taxonomy of Viruses has recently reclassified the family *Hypoviridae* as a positive sense ssRNA virus in their 2013 report. Totiviruses, chrysoviruses and partitiviruses (not shown) form isometric particles 30-40 nm in diameter whereas reoviruses form isometric particles 80 nm in diamter. Hypoviruses, narnaviruses, and endornaviruses (not shown) do not encode structural proteins and do not form virions. (Adapted from Nuss, 2005).

Members of the family *Reoviridae* that infect fungi are organized within the genus *Mycoreovirus* (Mertens et al., 2005). Members of the mycoreovirus genus have a spherical double-shelled capsid, ~80 nm in diameter (Figure 1.1) and the genome consists of either 11 (group 1) or 12 (group 2) dsRNA segments ranging from 732 to 4127 base pairs (bp), that are numbered in order of decreasing bp size. Group 1 mycoreoviruses have been shown encode an RDRP (segment 1), a structural protein (segment 2), and a guanylyltransferase capping enzyme (segment 3) (Supyani et al., 2007; Attoui et al., 2012).

Members of the family *Endornaviridae* have a dsRNA genome ranging from 13.5- to 17.6-kbp, however, endornaviruses do not encode a coat protein and do not form true virions (Fukuhara and Gibbs, 2012). Although endornaviruses have a dsRNA genome, RDRP analysis indicates that they are phylogenetically related to viruses of the alpha-like super group (Gibbs et al., 2000).

Members of the families *Narnaviridae* and *Hypoviridae* have ssRNA genomes of positive polarity and do not encode structural proteins; consequently, infections by these viruses lack the presence of virions (Figure 1.1) (Ghabrial and Suzuki, 2009). The family *Narnaviridae* is comprised of the genus *Narnavirus* and the genus *Mitovirus*. The genomes of mitoviruses range from 2.3- to 2.7- kb and encode a single protein containing RDRP motifs, and it is believed that the viruses exist as an RNA-RDRP nucleoprotein complex (Ghabrial and Suzuki, 2009). Mitoviruses are associated with mitochondria of filamentous fungi, and the coding strand utilizes mitochondrial codons (Polashock and Hillman, 1994; Polashock et al., 1997; Hillman and Suzuki, 2004). The genomes of narnaviruses are approximately 2.5- to 2.8- kb in

size, lack a poly(A) tail at the 3' end and it is unknown whether the 5' end is capped. Narnaviruses encode a single protein of 91 kilodaltons (kDa) that is believed to be an RDRP and not to undergo proteolytic processing. Unlike mitoviruses, narnavirus replication is not associated with the mitochondria (Hillman and Esteban, 2012).

Members of the family *Hypoviridae* infect only the chestnut blight fungus *Cryphonectria parasitica* and are phylogenetically related to the plant potyviruses (Koonin et al., 1991; Nuss, 2005). Hypoviruses have a monopartite genome consisting of one (species CHV-3 and CHV-4) or two (species CHV-1 and CHV-2) open-reading frames (ORFs) of 9- to 12.7-kb in length (Paul and Fulbright, 1988; Shapira et al., 1991; Choi and Nuss, 1992; Hillman et al., 2000; Linder-Basso et al., 2005) and will be described in greater detail later in this chapter.

Origins of Mycoviruses

The limitations in mycovirus transmission and host range complicate our understanding of how viruses adapted to fungi as hosts, however two main hypotheses have been proposed. The first is the ancestral coevolution hypothesis, which proposes that mycoviruses are ancient RNAs from an unknown source and have co-evolved along with their hosts. The second is the plant virus hypothesis, which proposes that viruses have moved from a plant host to the fungal host, or that viruses have moved between fungi and plant hosts (Koonin et al., 1991; Pearson et al., 2009).

The ancestral co-evolution hypothesis is based on the theory that since mycovirus transmission is limited by an intracellular lifecycle, horizontal movement of the virus to other fungal hosts is expected to be rare, thus the association between

the fungal host and virus is believed to be ancient (Buck, 1998). This hypothesis is supported by the fact that some mycoviruses use mitochondrial genetic translation codes (Huang et al., 1997) and may account for why many mycovirus infections result in asymptomatic phenotypes (Pearson et al., 2009).

The plant virus hypothesis is mainly supported by sequence comparisons between mycoviruses and plant viruses. For example, members of the family *Hypoviridae*, CHV-1, CHV-2, CHV-3, and CHV-4 have been shown to have genome organization and sequence similarities with members of the plant-infecting *Potyviridae* (Koonin et al., 1991; Linder-Basso et al., 2005). Furthermore, viruses of the plant pathogenic fungi *Sclerotina sclerotorium* (Xie et al., 2006) and *Botrytis cinerea* (Howitt et al., 2006) are members of the family *Alphaflexiviridae* and are related to members of plant viruses belonging to the genus' *Potexvirus* and *Mandarivirus* (Adams et al., 2012).

The mostly likely explanation is that mycoviruses have emerged from a combination of both the ancient co-evolution and the plant virus hypotheses (Pearson et al., 2009).

Mycovirus-mediated modification of fungal-plant interactions

Much of the recent interest in mycoviruses stems from reports of their ability to modulate the interactions between fungi and plants. These reports primarily involve hypovirulence, or virulence attenuation, of plant pathogenic fungi, but the recent report of a mycovirus as one component of a three-way mutualistic symbiotic relationship suggests that mycoviruses may play a much greater role in modulating fungal-plant interactions. A panic grass, *Dichanthelium lanuginosum*, isolated from

geothermal soils in Yellowstone National Park, was shown to be colonized by an endophytic fungus, *Curvularia protuberata*, allowing both organisms to grow at high soil temperatures. *C. protuberata* was shown to harbor a dsRNA virus, termed *Curvularia* thermal tolerance virus (CThTV), and when the fungal host was cured of the virus, the fungus no longer conferred thermo-tolerance to the host plant. However, once the virus was reintroduced to *C. protuberata*, thermotolerance was restored. To confirm the ability of CThTV/*C. protuberata* to provide thermo-tolerance, *Solanum lycoperiscon* (tomato) was inoculated with CThTV-infected *C. protuberate* which resulted in *S. lycoperison* displaying thermo-tolerance (Márquez et al., 2007, Morsy et al., 2011; Roossinck 2011). Recent surveys suggest that mycovirus infections of endophytic fungi are a common occurrence (Herrero et al., 2009; Feldman et al., 2012).

Given that mycovirus infections are generally asymptomatic, it is notable that the overwhelming majority of reports of mycovirus-mediated symptom expression involve plant pathogenic fungi. It is unclear whether this apparent bias is (i) because viruses of plant pathogenic fungi are more apt to cause overt symptoms, (ii) plant pathogenic fungi are more intensively studied due to their economic importance, (iii) symptoms such as reduced virulence attract more attention due to potential for practical applications such as biological control; or a combination of the above. The list of examples of mycovirus-mediated virulence-attenuation continues to grow at a rapid pace and extends to a broad taxonomic range of pathogenic fungi including *Botrytis cinerea* (Grey mold disease), *Fusarium graminearum* (Scab disease of small grain), *Helminthosporium victoriae* (Victoria Blight of oats), *Magnaporthe oryzae*

(rice blast), *Ophiostoma ulmi* (Dutch Elm disease), *Rhizoctonia solain* (cosmopolitan soil pathogen), *Rosellinia necatrix* (White Root Rot), and *Sclerotinia honoeocarpa* (Dollar Spot disease) (Reviewed in Pearson et al., 2009; Suzuki and Ghabrial, 2009; Nuss, 2010).

Hypovirus-mediated virulence-attenuation of the chestnut blight fungus *Cryphonectria parasitica* is the best characterized example of mycovirus-mediated hypovirulence. This is partly due to the fact that *C. parasitica* was one of the first fungal pathogens for which the phenomenon of transmissible hypovirulence was described (Reviewed in Anagnostkis, 1982), but primarily due to the development of the first mycovirus reverse genetics system as well as genetic and genomic advances for the fungal host (Reviewed in Nuss, 2010; Dawe and Nuss, 2013).

1.3 Chestnut Blight and Hypovirulence

Cryphonectria parasitica, the causative agent of chestnut blight, is a filamentous fungus of the phylum *Ascomycota* and is responsible for the decimation of the American and European chestnut trees (*Castanea dentate* and *Castanea sativa* respectively). *C. parasitica* originated in Asia and was introduced separately into North America at the turn of the 20th century and Europe in the 1930s. By the 1950s, approximately 9 million acres of American chestnut trees in the United States had been destroyed (Anagnostakis, 1982). *C. parasitica* infects chestnut trees through open wounds in the bark of the tree or at broken branches. Through these wounds, the fungus penetrates into the cambium layer, growing out from its point of origin, eventually girdling the tree or limb resulting in loss of nutrient flow and dieback in the host tree (Figure 1.2) (Anagnostakis, 1982; Choi and Nuss, 1992). The *C.*

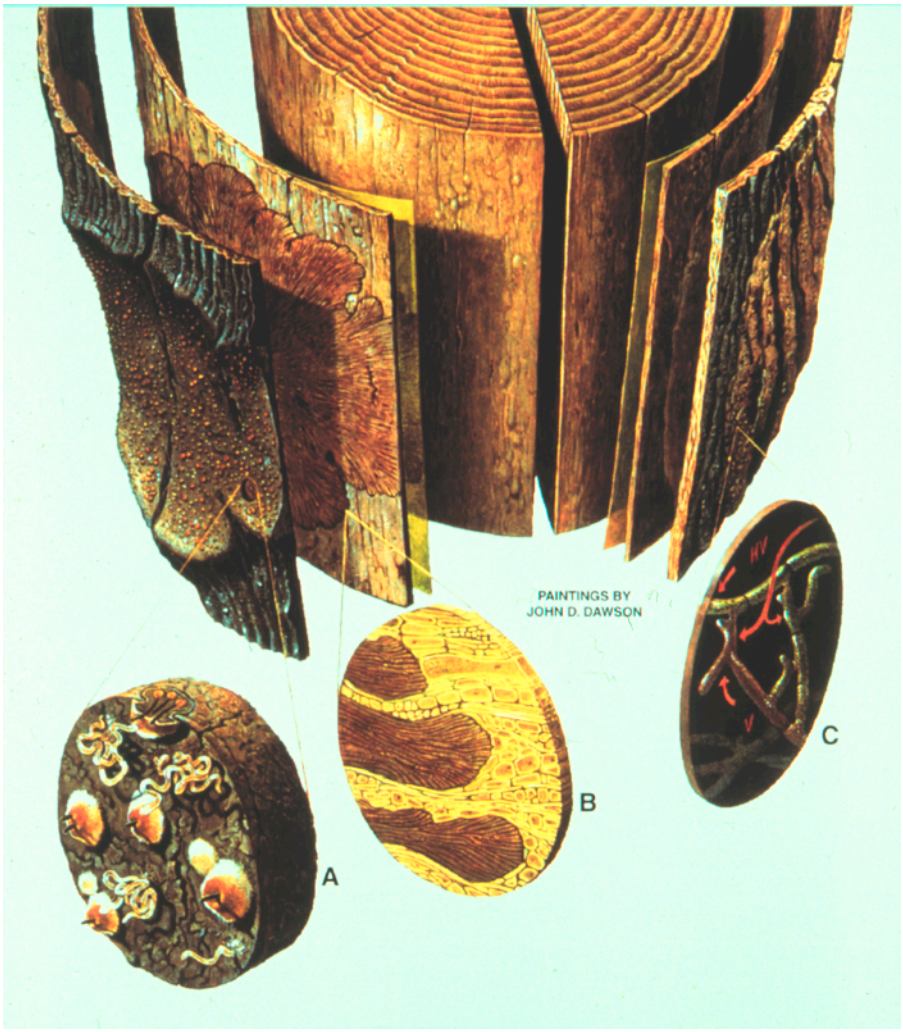

Figure 1.2 – Diagram of virulent and hypovirulent *C. parasitica* cankers. (A and B) Virulent *C. parasitica* penetrates into the cambium layer of the host chestnut tree, growing out from the point of origin, eventually girdling the tree or limb. Eventually water and nutrient flow are shutoff and the tree begins to die. (C) Hypovirulent *C. parasitica* is restricted to the outer layer of the bark, thus allowing the host tree to contain the invading fungi and survive. (Adapted from Cochran 1990, Image by John Dawson).

parasitica cankers appear as sunken, slightly orange, localized dead areas in the bark of the host chestnut tree (Anagnostakis, 1982). Neither the American nor the European chestnut has shown any type of genetic resistance to the fungus. The only identified line of defense that non-resistant chestnut trees possess is the ability to produce lignified zones consisting of wound periderm and callus tissue; however, *C. parasitica* can readily penetrate these tissues, resulting in the formation of a fungal canker (Anagnostakis, 1982).

Hypovirulence was discovered in Europe during the second half of the 20th century. In the 1950s, Antonio Biraghi, an Italian plant pathologist, first noticed that some European chestnut trees started to recover from blight, and that the expansion of *C. parasitica* on the tree was restricted to the outer layer of the bark (Anagnostakis, 1982). Then, in the early 1960s Jean Grente isolated *C. parasitica* from healing cankers on trees, and observed that the fungus displayed a reduced virulence phenotype. Grente also demonstrated that inoculating virulent cankers with the reduced-virulence fungal strain caused the virulent *C. parasitica* isolate in the canker to become less virulent and halted further expansion of the canker. Grente termed this phenomenon *transmissible hypovirulence* (Anagnostakis, 1982).

Moffit and Lister (1975) as well as Day et al. (1977), showed that hypovirulence was associated with the presence of dsRNA in the cytoplasm of *C. parasitica*, a general hallmark of RNA virus infection. However, attempts to isolate virus-like particles were unsuccessful. It was shown, though, that the dsRNA in hypovirulent strains was strictly associated with irregularly shaped pleiomorphic membrane vesicles that were present only in hypovirulent strains (Dodds, 1980).

These findings were further supported by studies of cellular ultrastructures (Newhouse et al., 1983; Newhouse et al., 1990; Newhouse and MacDonald, 1991) and biochemical studies that showed the pleiomorphic membrane vesicles were associated with dsRNA and contained RDRP activity (Hansen et al., 1985 and Fahima et al., 1993).

Despite the absence of identifiable virus-like particles, the dsRNA associated with the hypovirulence phenotype was thought to be of viral origin. In an effort to gain insight into the molecular features of the hypovirulence-associated dsRNA, the terminal ends were sequenced. The CHV-1 dsRNA 3′-terminus was found to contain a ~40 nucleotide stretch of polyadenylic acid (poly A) that was base paired to polyuridylic acid (poly U) at the 5′-terminus of the complementary strand (Hiremath et al., 1986; Tartaglia et al., 1986). Further analysis of the viral dsRNA determined that only the polyadenylated strand contained open reading frames. Furthermore, the 5' end of the plus-strand RNA was shown to contain a non-coding leader sequence of 495 nucleotides, followed by an open reading frame (Rae et al., 1989). These studies helped to elucidate the genome organization and expression strategy of the prototypic hypovirulence-associated CHV-1 isolate, designated CHV-1/EP713.

Hypovirus genome organization and basic expression strategy

Hypovirus CHV-1/EP713 was fully sequenced and the genome was determined to be 12.7- kb and encode two large contiguous open reading frames, designated ORF A and ORF B. The two ORFs were determined to be separated by an UAAUG stop/go pentanucleotide, in which the UAA was shown to serve as a stop codon for ORF A and the AUG was shown to serve as the start codon for ORF B

(Figure 1.3) (Shapira and Nuss, 1991; Shapira et al., 1991A). Processing of the CHV-1/EP713 ORF A and ORF B proteins was shown to involve autoproteolytic-processing events. ORF A encodes two polypeptides, p29 and p40, which are derived from an ORF A-encoded polyprotein, p69, as a result of autocatalytic cleavage by a papain-like protease domain located in p29. Through a series of *in vitro* studies, the essential catalytic residues of the p29 protease domain were mapped to amino acids (aa) Cys162 and His215, and the p29/p40 cleavage dipeptide was identified as Gly248 and Gly249 (Figure 1.4A) (Choi, Pawlyk, and Nuss, 1991; Choi, Shapira, and Nuss, 1991).

The N-terminus of ORF B also encodes a papain-like protease, p48, that is autocatalytically cleaved from the ORF B-encoded polyprotein (Shapira et al., 1991A). The essential catalytic p48 protease residues were also mapped by *in vitro* studies to include aa Cys341 and His388 and the p48/ORF B cleavage dipeptide was identified as aa Gly418 and Ala419 (Figure 1.4B) (Shapira and Nuss, 1991). It was predicted that p29 and p48 have evolved by an intragenomic duplication event, followed by subsequent divergence possibly due to the functional diversification of the two proteases (Koonin et al., 1991). The remainder of ORF B contains RDRP and helicase domains, although the processing pathway has not been fully elucidated.

Hypovirus reverse genetics.

In 1992, using a reverse genetics approach, Choi and Nuss demonstrated a causative relationship between the hypovirulent-associated dsRNAs and hypovirulence. A full-length cDNA clone copied from the largest viral RNA in the hypovirulent *C. parasitica* strain EP713 (the virus was later designated CHV-1/

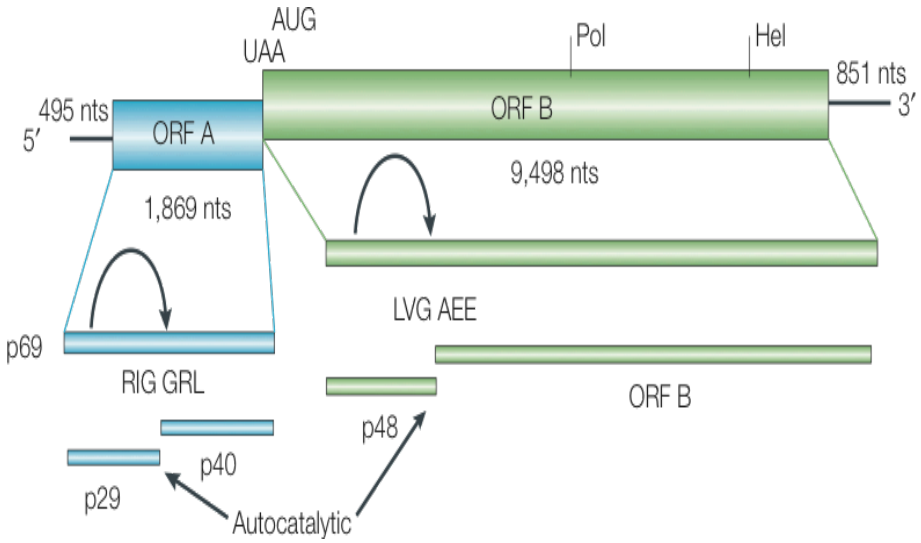

Figure 1.3 – The CHV-1/EP713 genome. CHV-1 viruses contain two open reading frames, ORF A and ORF B, separated by a stop/go frameshift where the pentanucleotide sequence UAA serves as the stop codon for ORF A and AUG serves as the start codon for ORF B. ORF A encodes two mature viral proteins, p29 and p40. The precursor, p69, is autocatalytically processed by p29. The only identified protein from ORF B is protease p48 that autocatalytically releases itself from the N terminal part of the ORF B encoded polypeptide. In addition, conserved RDRP and helicase domains have been identified (Adapted from Nuss, 2005).

A

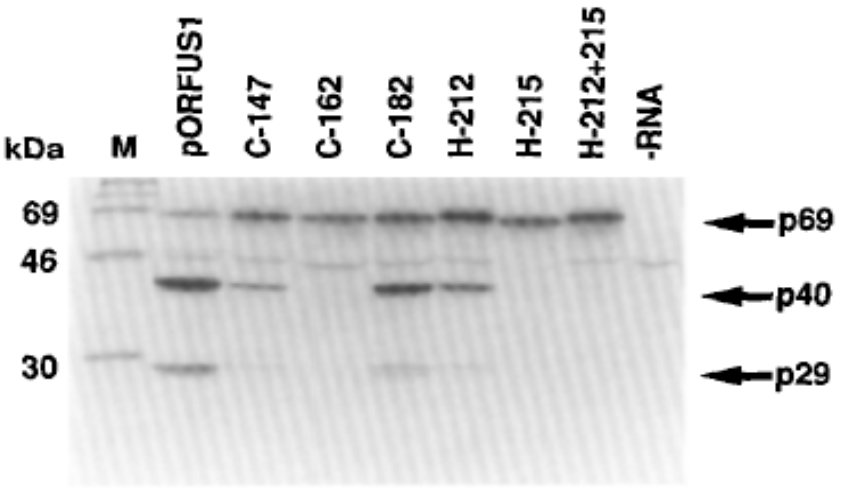

B

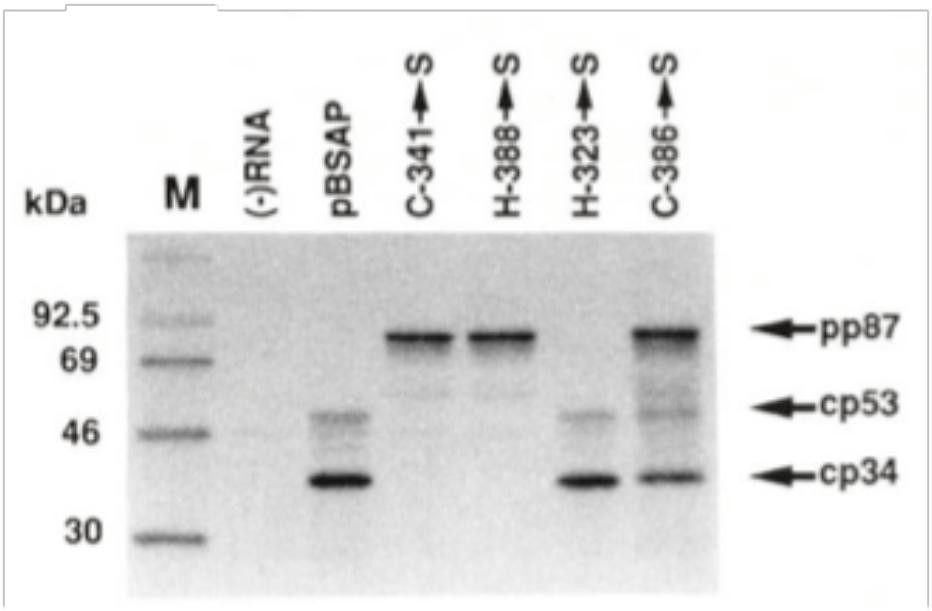

Figure 1.4 – Autoproteolytic activity of p29 and p48 proteins. (A) *In vitro* translation of CHV-1 ORF A p29 mutants. Mutation of Cys162 or His215 to serine resulted in the inability of protease p29 to autocatalytically process the p69 precursor into mature proteins p29 and p40 (Borrowed from Choi, Pawlyk, and Nuss, 1991). (B) *In vitro* translation of amino acids Met118 to Pro879 of CHV-1 ORF B. Mutation of Cys341 or His388 to serine resulted in the loss of p48 autocatalytic processing ability (Adapted from Shapira and Nuss, 1991).

1/EP713) was constructed and transformed into *C. parasitica* isolate EP155, a dsRNA-free strain with normal virulence (Figure 1.5). As shown by Choi and Nuss, integration of the virus-derived cDNA into the *C. parasitica* EP155 genome resulted in hypovirulence of the transformed fungi.

The fungal strains containing the integrated virus-derived cDNA produced viral RNA that was free of any sequences from the vector used in the transformation. The viral RNA replicated in the cytoplasm and the extracted dsRNA was determined to be the same size as that of the hypovirulence-associated dsRNAs (Chen, Craven, et al., 1994). These results demonstrated that the hypovirulence-associated dsRNA was the causative agent of *C. parasitica* hypovirulence. Furthermore, the strains transformed with viral cDNA displayed the novel ability to transfer fungal hypovirulence through ascospores. Ascospores, which result from a sexual cross, normally exclude hypovirus RNA; however, in the transformed strain, the chromosomally-integrated hypovirus cDNA was transmitted to ascospore progeny in which the hypoviral RNA was then expressed (Chen et al., 1993).

It was subsequently demonstrated that hypovirulence could be induced by transfecting *C. parasitica* spheroplasts with synthetic *in vitro*-generated RNA transcripts corresponding to the viral RNA coding strand (Figure 1.5) (Chen et al., 1994). This observation indicated that CHV-1/EP713 is a single-stranded positive-sense RNA virus and not a double-stranded RNA virus. The development of both the transformation and transfection protocols allowed for the completion of Koch's postulates, demonstrating that hypoviruses are responsible for hypovirulence (Dawe and Nuss, 2013).

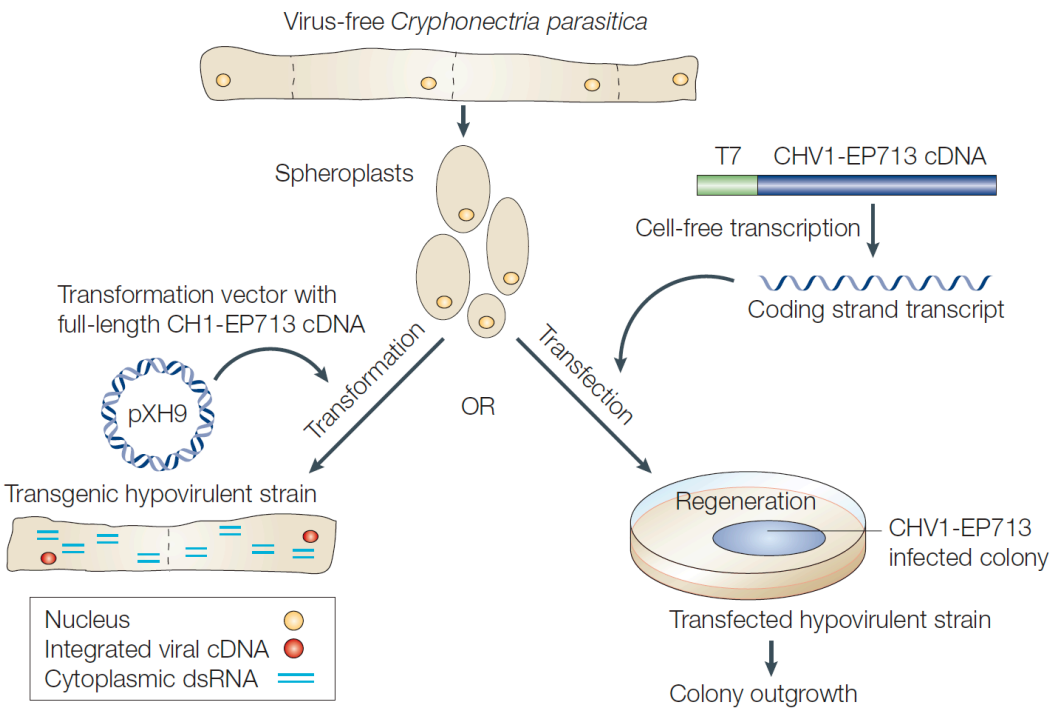

Figure 1.5 – *C. parasitica* hypovirus reverse genetics system. This figure highlights the basic transformation (left) and transfection (right) pathways of introducing the CHV-1 viral RNA into *C. parasitica*. For both protocols, the cell wall is removed from virus-free *C. parasitica* to produce spheroplasts. To generate a transformant strain, a plasmid containing a full-length hypovirus cDNA copy or a cDNA copy of a protein of interest, is introduced into the spheroplasts by DNA-mediated transformation. The cDNA transformation vector is fused downstream of the *C. parasitica* glyceraldehyde-3-phosphate dehydrogenase (GPD) promoter and upstream of the GPD terminator. The transformation plasmid also contains the *Escherichia coli* hygromycin B phosphotransferase gene as a selectable marker. The transformants containing a chromosomally integrated copy of the cDNA are selected following cell-wall regeneration and maintained on Potato Dextrose Agar (PDA) in the presence of 40 μg ml^{-1} hygromycin B. The transformants contain cDNA-derived

cytoplasmically-replicating ssRNA or express the protein of interest corresponding to the integrated cDNA. The hypovirus transfection system uses synthetic RNA transcripts derived from a plasmid containing a cDNA copy of the CHV-1/EP713 genome synthesized in a T7-polymerase-dependent cell-free transcription reaction. The synthetic RNA transcripts are introduced into spheroplasts through electroporation. As the *C. parasitica* hyphal structures are regenerated from the transfected spheroplasts, they fuse at a high frequency, resulting in a fungal colony connected through a cytoplasmic network. The replicating hypovirus RNA will then migrate throughout the colony, and a portion of the resulting infected mycelia is transferred to fresh PDA for future studies (Adapted from Nuss, 2005).

Hypovirus taxomony

The virus-like genome organization determined for hypovirus CHV-1/EP713 and development of the full length viral cDNA clone led the International Committee on Taxonomy of Viruses (ICTV) to establish a new family, *Hypoviridae*, the first for a group of viruses that does not encode a coat protein or form virions (Hillman et al., 1995). The *Hypovirdae* were initially grouped with the dsRNA virus families because of the early characterization of the replicative form dsRNAs isolated from hypovirulent *C. parasitica* strains. This has been rectified in the 9th ICTV report (Nuss and Hillman, 2012) where the *Hypoviridae* were grouped with the single-stranded positive-sense viruses consistent with the demonstration that the coding-strand transcript can initiate an infection when introduced into *C. parasitica* spheroplasts (Chen, Choi, and Nuss, 1994).

The family *Hypoviridae* currently contains a single genus consisting of four species, CHV-1, CHV-2, CHV-3, CHV-4, distinguished by differences in genome structure and sequence relatedness. The genome of each species contains one (CHV-3, CHV-4) or two (CHV-1, CHV-2) ORFs (Figure 1.6) (Nuss and Hillman, 2012). Complete nucleotide sequences have been reported for six members of the *Hypoviridae* family. Among the four species, CHV-1 is more closely related to CHV-2, and CHV-3 is more closely related to CHV-4, with isolates from these species sharing ~60% and ~50% amino acid sequence identity, respectively. The genome of CHV-1 is 12.7- kb in size and contains two ORFs separated by a UAAUG translation stop/go pentanucleotide (Shapira et al., 1991A; Chen and Nuss, 1999; Lin et al., 2007). The CHV-2-NB58 genome is 12.5- kb long and has similar organization

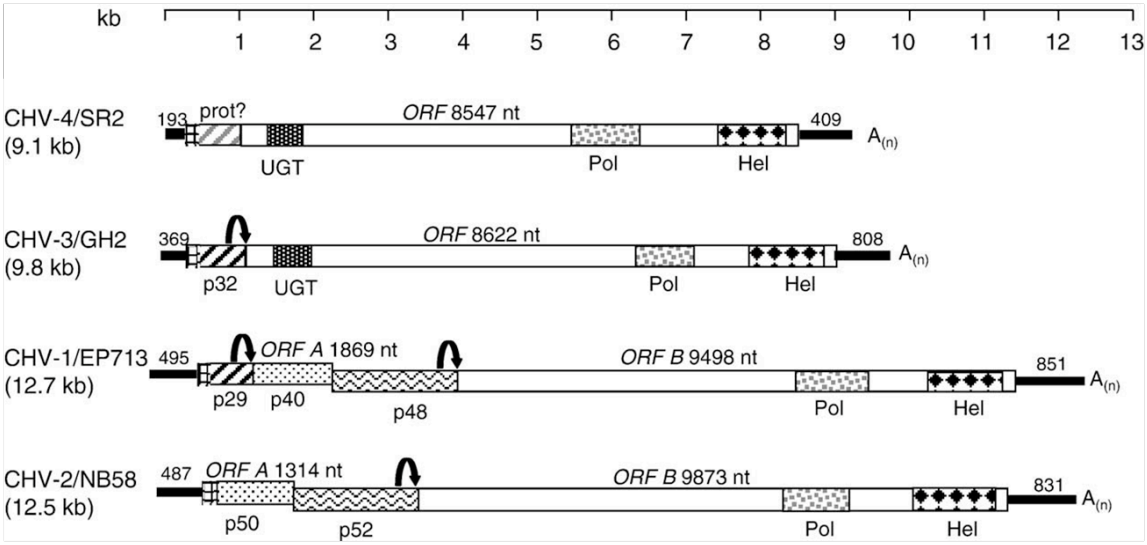

Figure 1.6 – Genome organization of *Cryphonectria parasitica* hypoviruses. Four CHV species have been isolated and identified. CHV-1 and CHV-2 contain two ORFs separated by a stop/go re-initiation frameshift pentanucleotide, while CHV-3 and CHV-4 viruses are monocistronic. Arrows indicate the cleavage sites of *cis*-acting viral proteases and abbreviations designate the following: UGT – UDP-glucose/sterol glucosyltransferase domain, Pol – RNA-dependent RNA polymerase domain, Hel – helicase domain (Adapted from Linder-Basso et al., 2005).

to that of the CHV-1 genome, except that CHV-2 ORF A encodes a single protein (p50) instead of two separate proteins (p29 and p40); p50 lacks sites for protease catalysis and cleavage that are present in p29 and p40 of CHV-1. ORF B in CHV-1 and CHV-2 is organized similarly, with CHV-1 and CHV-2 sharing a leader protease at the N-terminus and possessing conserved RDRP and helicase domains (Dawe and Nuss, 2013). CHV-1 infection results in a white colony phenotype, whereas CHV-2 infection results in an orange-brown phenotype, although both viruses reduce fungal virulence.

Members of CHV-3 and CHV-4 have genome sizes of 9.8 and 9.1 kb, respectively. Both CHV-3 and CHV-4 isolates contain a papain-like protease domain at the N-terminus that is similar to p29 of CHV-1; however, protease activity has only been confirmed for the CHV-3 protease (Smart et al., 1999; Linder-Basso et al., 2005). Unlike the CHV-1 and CHV-2 viruses, CHV-3 and CHV-4 contain a UDP-glucose/sterol glucosyltransferase (UGT) domain whose function is currently undefined (Linder-Basso et al., 2005). The CHV-3/GH2 viral isolate does induce hypovirulence, but does not reduce fungal sporulation, pigmentation, or laccase activity to the same extent as CHV-1 and CHV-2 (Smart et al., 1999); CHV-4 infection has little effect on fungal pigmentation and does not appear to reduce fungal virulence (Linder-Basso et al., 2005).

The RDRP domains of CHV-3 and CHV-4 are more closely related to the RDRP of a mycovirus isolated from *Fusarium graminicola* than to the RDRP of either CHV-1 or CHV-2. Comparison of genome size and the presence/absence of the UGT domain suggest that the divergence of the CHV-1 and CHV-2 lineage from

the CHV-3 and CHV-4 lineage was not a recent event (Linder-Basso et al., 2005). Interestingly, CHV-2, CHV-3, and CHV-4 were all originally isolated from North American *C. parasitica* strains, whereas CHV-1 is the predominant species in Europe and Asia. Despite multiple releases of European CHV-1 isolates throughout North America, it is rarely found circulating in this region.

Four viruses related to hypovirus species CHV-3 and CHV-4 were recently described. These include *Sclerotinia sclerotiorium* hypovirus 1 (SsHV1) (Xie et al., 2011); *Fusarium gramminearum* hypovirus 1 (FgHV1) (Wang et al., 2013); *Phomopsis longicolla* hypovirus 1 (PlHV1) (Koloniuk et al., 2014) and *Valsa ceratosperma* hypovirus 1 (VcHV1) (Yaegashi et al., 2012). In this regard, *Phomopsis longicolla*, *Valsa ceratosperma* and *C. parastica* are all classified within the order *Diaporthales*, but within three different genera. Sasaki et al., (2002) previously reported that *Valsa ceratosperma* and *Phomopsis* G-type can support replication of hypovirus CHV-1/EP713 introduced by biolistic delivery of the full-length viral cDNA. Based on the recent spate of reports of hypovirus-related mycoviruses, the current structure of the family *Hypoviridae* is likely to be revised in the near future.

Symptoms associated with hypovirus infections

Hypovirus infection results in a range of phenotypic changes in addition to reduced fungal virulence. These can include altered colony morphology, loss of pigment production, loss of female fertility and reduced asexual sporulation (Figure 1.7) (Reviewed by Dawe and Nuss, 2013). The association between these persistent phenotypic changes and hypovirus-mediated alterations of cellular signaling

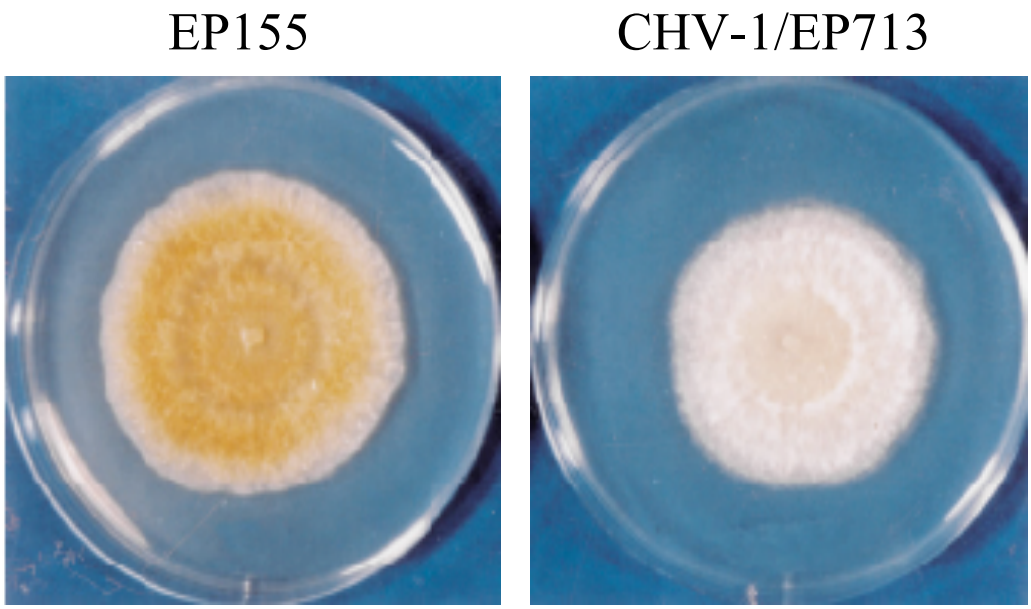

Figure 1.7 – Colony morphology of virus free and CHV-1 infected *C. parasitica*. Strain EP155 (left) is uninfected and displays a faster growth rate and orange pigmentation. EP155 isolates infected with hypovirus CHV-1/EP713 (right) display a decrease in growth rate, pigmentation and sporulation compared to uninfected isolates.

pathways has been reviewed extensively (Dawe and Nuss, 2001; Nuss, 2005; Nuss, 2010; Dawe and Nuss, 2013) and include G-protein signaling and the calcium/calmodulin/inositol triphosphate-dependent and the mitogen-activated protein kinase signaling cascades. The results of transcriptional profiling analyses indicated that hypovirus infection results in a persistent reprogramming of the *C. parasitica* transcriptome. Comparative studies have confirmed that a good portion of this reprogramming is due to virus-mediated alterations in G-protein signaling. It is anticipated that the completion of the *C. parasitica* draft genome sequence (http://genome.jgi-psf.org/Crypa2/Crypa2.home.html) combined with advances in deep sequencing technology will allow for more defined studies of the effect of hypovirus infection of host gene expression and the relation of those changes to virus-mediated symptom expression.

1.4 *C. parasitica* Anti-viral Defense Response

Fungi, like plants and animals, have evolved anti-viral defense mechanisms in response to viral infections. The innate immune response resulting in the production of interferon predominates in animals (Fensterl and Sen, 2009) and plants mainly rely on the RNA silencing response pathways as a viral defense mechanism (Ding, 2010). Two separate anti-viral defense mechanisms have been identified in *C. parasitica*: an RNA silencing response pathway and a non-self-recognition system, termed vegetative incompatibility.

Induction of the host RNA silencing pathway

RNA silencing, or RNA-mediated sequence-specific suppression of gene expression, has previously been described as post-transcriptional gene silencing in plants (Lindbo et al., 1993; Kumagai et al., 1995; English et al., 1996; Goodwin et al., 1996), RNA interference (RNAi) in animals (Fire et al., 1998), and quelling in fungi (Cogoni and Macino, 1997; Reviewed in Fulci and Macino, 2007). The mechanisms underlying RNA silencing in fungi have been identified primarily through studies with *Neurospora crassa* (Cogoni and Macino, 1997; Shiu and Metzenberg, 2002; Maiti et al., 2007). It is currently believed that RNA silencing in fungi evolved as an ancient defense mechanism against invasive nucleic acids and viruses, since microRNAs, which are involved in development and cellular regulation in plants and animals, have not been detected in fungi (Cerutti and Casas-Mollano, 2006; Nakayskiki et al., 2006). Further evidence that supports RNA silencing evolving as a defense mechanism in fungi is that transposon-silencing has been reported in *N. crassa* (Nolan et al., 2005) and viral RNA silencing has been reported in *C. parasitica* (Segers et al., 2007; Zhang and Nuss 2008).

Evidence supporting the role of RNA silencing in *C. parasitica* as an anti-viral defense response comes from studies in which components of the RNA silencing pathway, Dicer and Argonaute, were disrupted resulting in an increased susceptibility to mycovirus infection (Segers et al., 2007; Sun et al., 2009). The current view is that the roles of the components (i.e. Dicer and Argonaute) in RNA silencing are mostly conserved between fungi, plants, and animals. These include recognition of viral double-stranded or structured RNA and subsequent processing of the RNA into small

virus-derived RNAs of 21-24 nucleotides (vsRNAs) by Dicer, through an associated RNaseIII activity. The vsRNAs are subsequently transferred to the Argonaute protein and incorporated into an effector complex known as the RNA Induced Silencing Complex (RISC), where one strand of the vsRNA is removed. The remaining strand guides RISC to viral RNA that shares sequence identity to the vsRNA, which is then cleaved by the Argonaute associated RNase H-like activity (Reviewed in Ding, 2010).

C. parasitica encodes two Dicer genes and four Argonaute genes, but only Dicer gene *dcl2* and Argonaute gene *agl2* are required for the antiviral defense response (Segers et al., 2007; Sun et al., 2009). Disruption of Dicer genes, *dcl1* or *dcl2*, or Argonaute genes, *agl1*, *agl2*, *agl3*, or *agl4*, resulted in no observable phenotypic changes in the absence of virus infection. When hypovirus CHV-1/EP713 was introduced, the *dcl2* mutant strain (Δ*dcl2*) and the *agl2* mutant strain (Δ*agl2*) became severely debilitated. Additionally, viral RNA accumulation, specifically viral positive-sense single-strand RNA was significantly increased (Figure 1.8) and production of hypovirus-derived vsRNA was shown to be dependent on *dcl2* and independent of *dcl1* (Zhang et al., 2008).

Examination of transcript expression levels of *C. parasitica* strain EP155 infected with either CHV-1/EP713 or mycoreovirus MyRV1-9B21 indicates that both *dcl2* and *agl2* are induced during viral infection. During mycovirus infection, *dcl2* transcript accumulation is increased 10-15 fold and *agl2* transcript accumulation is increased 2-4 fold, however, *agl2* was found to be required for *dcl2* transcript induction in response to mycovirus infection (Zhang et al., 2008; Sun et al., 2009).

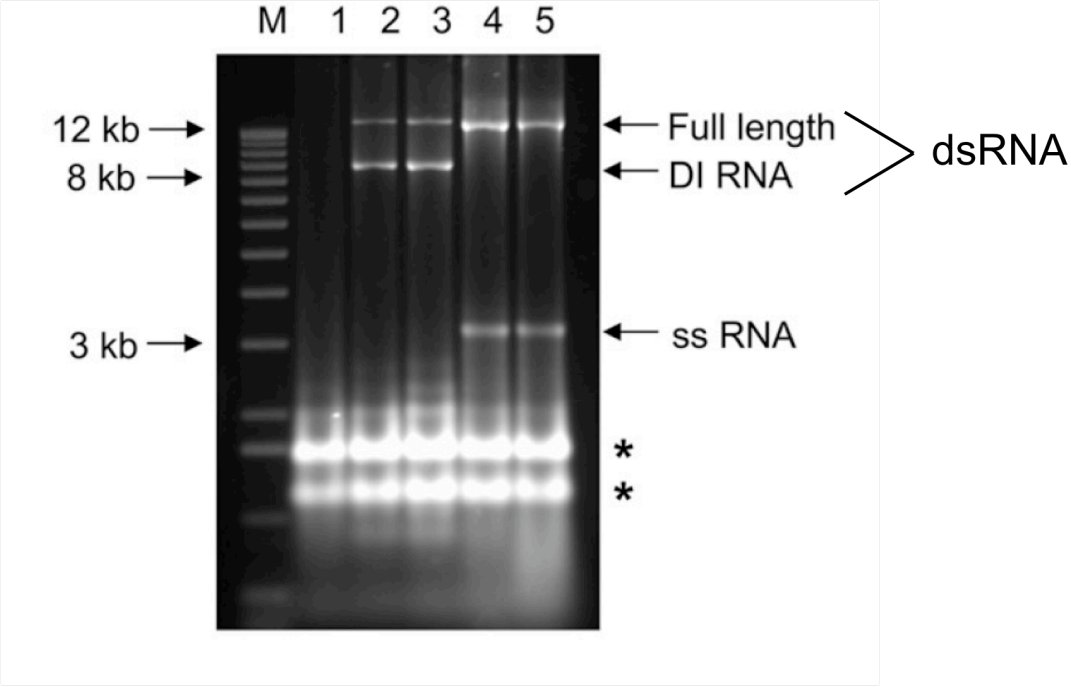

Figure 1.8 – Dicer gene *dcl2* and Argonaute gene *agl2* contributes to hypovirus recombination and reduction in positive-sense single-strand RNA accumulation. Disruption of the *C. parasitica* RNA silencing pathway results in an increase in positive-sense single-strand RNA and loss of viral recombination. Agarose (1%) gel analysis of total RNA isolated from virus-free WT strain EP155 (lane 1); CHV-1/EP713-infected strain EP155 (lane 2); CHV-1/EP713-infected Δ*agl1* mutant strain (lane 3); CHV-1/EP713-infected Δ*agl2* mutant strain (lane 4); CHV-1/EP713-infected Δ*dcl2* mutant strain (lane 5). DI RNA band in lanes 1 and 2 indicate defective interfering viral RNA generated as a result of internal deletions from full length CHV-1. The asterisks indicate the migration positions of *C. parasitica* ribosomal RNAs (Borrowed from Sun et al., 2009).

The RNA silencing pathway has also been shown to contribute to viral RNA recombination. During CHV-1 infection of wild-type (WT) *C. parasitica*, viral-derived defective interfering (DI) RNAs are generated at high frequencies. However, DI RNAs failed to form during CHV-1/EP713 infection of either Δ*dcl2* or Δ*agl2* strains, but reappeared when the virus was transferred to *C. parasitica* strain EP155 through anastomosis (Figure 1.7) (Zhang and Nuss, 2008; Sun et al., 2009). Further evidence that the RNA silencing pathway is involved in viral RNA recombination was demonstrated when testing the stability of non-viral nucleotide sequences inserted into the CHV-1 genome. It was previously observed that when strain EP155 was infected with CHV-1/EP713 –based vector viruses containing the enhanced green fluorescence protein (eGFP) coding domain, eGFP expression disappeared within two colony transfers (Suzuki et al., 2000). However, when the CHV-1/eGFP virus was introduced into either the Δ*dcl2* or Δ*agl2* mutant strains, eGFP expression and vector virus stability were retained for prolonged culturing and transfers (Zhang et al., 2008; Sun et al., 2009). The Δ*dcl2* strain has recently become an important experimental tool due to the discovery of decreased viral RNA recombination and increased accumulation of viral RNA and proteins as described in subsequent chapters.

Viral suppression of the host RNA silencing pathway

In response to the host anti-viral RNA silencing response, animal, plant and fungal viruses have evolved the ability to suppress the host response. Plant viruses have evolved many different mechanisms to suppress the host RNA silencing, including binding to vsRNAs, preventing RISC assembly, and degrading host Argonaute proteins (Reviewed in Díaz-Pendón and Ding, 2008).

The CHV-1 p29 protein has been demonstrated to suppress RNA silencing in *C. parasitica* and in *Nicotiana benthamiana* (Segers et al., 2006). During CHV-1 infection, *dcl2* transcript levels increase approximately 10- to 15-fold, however, *dcl2* transcript accumulation increased by 30- to 40-fold in response to infection by a CHV-1/EP713 virus lacking p29 (Δp29) (Sun et al., 2009). Accumulation of *agl2* transcript levels increased over 14-fold during Δp29 infection compared to approximately 2-fold increase observed during CHV-1/EP713 infection. The difference observed in *agl2* transcript accumulation levels was determined to be dependent on the *agl2* promoter region. Additionally, *agl2* was found to be required for *dcl2* transcript induction in response to virus infection. The current belief is that during CHV-1 infection, p29 suppresses the host RNA silencing pathway by suppressing transcriptional activation of the anti-viral defense response (Sun et al., 2009). Currently, no additional CHV-1 viral proteins have been shown to be suppressors of RNA silencing.

Host restriction of hypovirus transmission

In addition to the RNA silencing anti-viral response, fungi have the ability to restrict virus transmission at a population level through vegetative incompatibility (*vic*) non-self recognition systems (Caten, 1972; Anagnostakis, 1982B; Anagnostakis, 1982C). The ability of *C. parasitica* to restrict transmission of virulence-attenuating mycoviruses from one strain to another through anastomosis, fusion of the hyphae, when the two strains were vegetatively incompatible was first reported in 1982 (Anagnostakis, 1982). The incompatible reaction between fungal strains results in localized programmed cell death (PCD) of the interacting strains. This prevents

cytoplasmic mixing and restricts virus transmission. Studies of field isolates have shown that in *C. parasitica* populations in regions of Europe where *vic* diversity is generally low, hypovirulence spreads naturally; however, in North America, where *vic* diversity is high, hypovirulence spread is limited, and efforts to artificially introduce hypovirulence have been largely unsuccessful (Anagnostakis, 1982A; Milgroom and Cortesi, 2004).

Genetic analysis has revealed that the vegetative incompatibility interaction is triggered by allelic differences at *vic* genetic loci. Identified non-self recognition interactions that have been characterized in *N. crassa* and *Podospora anseria* involve proteins that share a common domain of approximately 150 aa, termed a HET domain. In most instances the HET domain gene products interact with a non-HET domain protein in non-allelic interactions that trigger PCD, leading to the formation of a line of dead cells (barrage) at the zone of fusion (Reviewed in Glass and Dementhon, 2006).

Currently 6 genetic loci, with two alleles at each locus, have been identified in *C. parasitica* (Anagnostakis, 1982b; Huber, 1996; Cortesi and Milgroom, 1998; Choi et al., 2012). Using *vic*-linked sequence markers (Kubisiak and Milgroom, 2006) combined with 454 and Illumina sequencing, candidate loci for *vic1*, *vic2*, *vic3*, *vic4*, *vic6*, and *vic7* were identified (Choi et al., 2012; Zhang et al., 2014) with observed polymorphism ranging from 39% aa identity for the *vic2* alleles to 82% aa identity for the *vic7* alleles. Analysis of alleles at four *vic* loci in 26 *C. parasitica* field isolates recovered from Europe and North America found no evidence of more than two alleles at each locus (Choi et al., 2012).

The *C. parasitica vic1*, *vic6*, and *vic7* loci have been shown to contain gene encoding HET domain proteins. The *vic6* locus was determined to contain two adjacent ORFs that include a HET domain-containing protein, *vic6*, and a non-HET domain protein designated *pix6*. PCD, barrage formation, and restriction of virus transmission were triggered by non-allelic interactions between the *vic6-1* and *pix6-,* and the *vic6-2* and *pix6-1* alleles. The identified *vic7* gene encodes a protein with a HET domain that is conserved in 9 of the 10 incompatibility genes previously characterized for *N. crassa* and *P. anseria.* The *vic7* alleles, designated *vic7-1* and *vic7-2* are 87% identical with significant polymorphism limited to a small portion of the C-terminal domain. Virus transmission for the *vic7* locus is naturally asymmetric; virus transmission is not inhibited when the recipient contains the *vic7-2* allele, but is restricted when the recipient contains the *vic7-1* allele (Cortesi et al., 2001).

The *C. parasitica vic2*, *vic3*, and *vic4* loci lack HET-domain proteins. *Vic2* contains two tightly linked polymorphic ORFs separated by a conserved helicase gene. The larger ORF, *vic2*, encodes a member of the patain-like phospholipase family, while the smaller ORF, *vic2a*, encodes a protein related to a fungal plasma membrane SNARE Sec9 protein. The allelic designations for the two genes are *vic2-2* and *vic2a-2* for fungal strain EP155 and *vic2-1* and *vic2a-1* for fungal strain EP146. Disruption of the *vic2-2* allele eliminated restrictions to virus transmission when the disrupted allele was present in the recipient strain, but not when the disrupted allele was in the donor strain.

When compared to the previously described *vic* genes, the *vic4* locus is atypical, in that the alleles are idiomorphic. The *vic4-1* allele encodes a 359 aa

protein that contains a protein kinase c-like domain while the *vic4-2* allele encodes a 1628 aa protein containing NACHT-NTPase and WD repeats found in several *P. anserine* HET genes (Choi et al., 2012; Paoletti et al., 2006). An allelic difference at the *vic4* locus triggers barrage formation, however it does not restrict virus transmission (Cortesi et al., 2001). These results have led Biella and colleagues (2002) to propose that allele-specific differences observed in the rate of *vic*-triggered PCD are responsible for differences in the frequency and symmetry of virus transmission, (i.e., delayed PCD results in greater frequency of virus transmission) (Huber and Fulbright, 1994).

Future studies are aimed at addressing the mechanisms underlying *vic*-mediated triggering of PCD and resistance to virus transmission by examining *vic* protein interactions, cellular distribution, and movement. Additionally, the ability to generate a universal donor to aid in hypovirus transmission in the field by disarming the *vic* genes is currently being investigated.

1.5 Hypovirus Replication and Function of Viral Proteins and RNA Structural Elements

Hypovirus replication

Despite many advances in hypovirus research, progress in characterizing mature CHV-1 proteins and elucidating viral replication mechanisms has remained elusive.

Although it has not been determined whether hypoviruses have a 5′ cap structure to facilitate translation or an internal ribosomal entry site (IRES) has not

been identified on the basis of secondary RNA structure (Baird et al., 2006), there is evidence that hypovirus replication proceeds in a 5′ cap–independent manner (Dawe and Nuss, 2013). It has also been demonstrated that uncapped RNA produced *in vitro* can initiate infection, which seems to support cap-independent translation (Chen, Choi, and Nuss, 1994).

Furthermore, the transcripts in CHV-1 viruses have a 5′ untranslated region (UTR) of ~495 nucleotides containing seven AUG triplets located upstream of the authentic start codon (Shapira et al., 1991), which is a feature similar to those found in other viruses that replicate in a cap-independent manner. For example, the RNA of poliovirus has a 5′ UTR of 750 nucleotides with seven or eight upstream AUGs (Pelletier et al., 1988), and the hepatitis C virus has a 5′ UTR of ~340 nucleotides with three or four upstream AUGs (Tsukiyama-Kohara et al., 1992).

Recently, Mu and colleagues (2011) used a coupled nuclease mapping/Mfold structure prediction approach (Zucker and Jacobson, 1998; Zucker, 2003) to examine the structural elements in the 5′ UTR of both the CHV-1/EP713 and CHV-1/Euro7 (Chen and Nuss, 1999) (494 nucleotides) viruses. This prediction analysis indicates that the secondary structures formed in the first 220 nucleotides of the 5′ UTRs are similar; however, the structures in the region between nucleotides 220 and the end of the 5′ UTRs are predicted to be significantly different, despite a high level of sequence similarity (>90%) (Figure 1.9) (Mu et al., 2011). The presence of secondary RNA structures in the 5′ UTR is also supported by the observation of vsRNAs that are generated by the *C. parasitica* RNA silencing pathway (Zhang et al., 2008). The vsRNAs generated from the CHV-1/EP713 5′ UTR can be mapped to

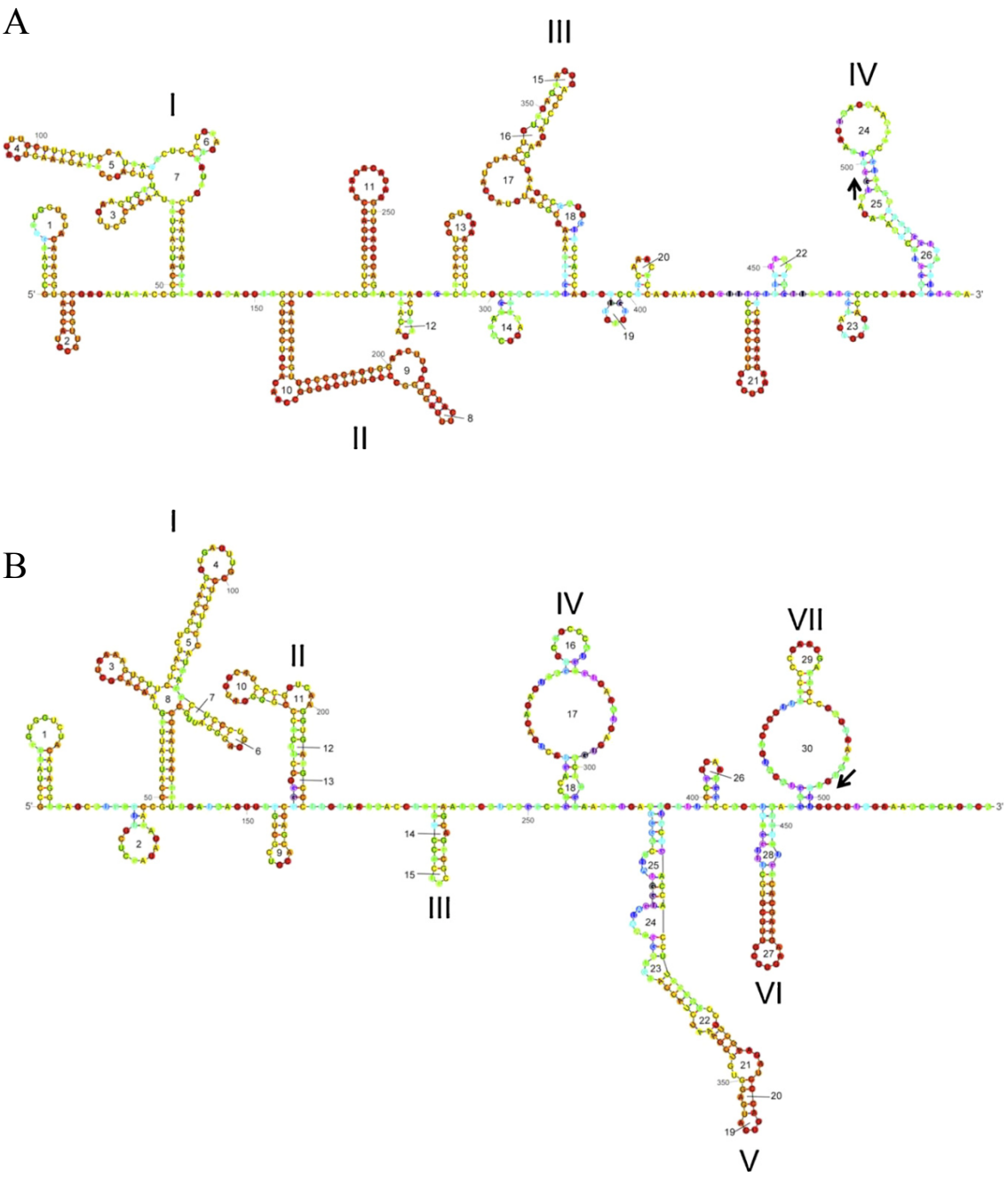

Figure 1.9 – Predicted structure of the 5' UTR of CHV-1/EP713 and CHV-1/Euro7. RNase digestion combined with M-fold prediction software were used to identify RNA structural elements within the 5' UTR of CHV-1 viruses. Depicted here is the predicted RNA structure for the first 675 nucleotides of CHV-1/EP713 (A) and CHV-1/Euro7 (B) (Borrowed from Mu et al., 2011).

regions that are predicted to form secondary RNA structures (Mu et al., 2011). The above evidence reported by Mu and colleagues supports the notion that CHV-1 viruses replicate in a cap-independent manner and that protein translation is mediated through an IRES (Dawe and Nuss, 2013).

The functional roles of the mature viral proteins in replication and translation of the viral genome are not completely understood. As previously noted, CHV-1 encodes two ORFs, ORF A and ORF B. ORF A encodes the polyprotein p69, which is autocatalytically cleaved into two viral proteins, papain like protease p29 and p40. In addition to ORF A processing, p29 appears to have multiple functions during CHV-1 infection. Suzuki et al. (2000), using engineered RNAs lacking various regions of p29, demonstrated that amino acids 1–24 are essential for viral replication. Subsequently, Suzuki and colleagues (2003) generated Δp29 and Δp69 CHV-1 viruses (in which p29 and p69 had been deleted), which accumulated to levels in fungal cells that were ~50% and ~15% lower than those of WT CHV-1/EP713. However, when p29 was expressed *in trans*, levels of RNA expressed from the Δp29 and Δp69 viruses were restored to either near WT levels or increased by three-fold, respectively. Furthermore, expression of p29 *in trans* in virus-free fungal mycelium resulted in several symptoms that were also observed in CHV-1/EP713-infected strains, including decreased orange pigment production, suppressed asexual spore production, and decreased extracellular laccase production. Although the specific mode of action of p29 is not fully understood, the host-symptom determinants have been mapped to the cysteine residues 70 and 72, which are conserved in the related potyvirus protein HC-Pro. Mutation of either Cys70 or Cys72 of p29 failed to induce

phenotypic changes or to restore viral RNA accumulation of the Δp29 mutant virus when supplied *in trans* (Craven et al., 1993; Suzuki et al., 1999; Suzuki et al., 2003). Moreover, as previously discussed, p29 has been shown to be a suppressor of RNA silencing, which is also an observed trait of the potyvirus protein HC-Pro (Segers et al., 2006; Segers et al., 2007).

The second protein of ORF A, p40, has also been shown to be dispensable for CHV-1/EP713 replication. Through a gain-of-function analysis, p40 has been shown to be involved in viral RNA accumulation and to contribute to suppression of sporulation and pigmentation (Suzuki and Nuss, 2002). However, when p40 was supplied *in trans*, fungal transformants showed no phenotypic changes when compared with untransformed EP155, and could not function *in trans* to enhance viral RNA accumulation (Suzuki et al., 2003).

The two ORFs of CHV-1, ORF A and ORF B, are separated by a stop/go region, containing the pentanucleotide UAAUG, where the UAA portion serves as the ORF A termination codon and the AUG portion serves as the ORF B initiation codon (Shapira et al., 1991A). The UAAUG pentamer is also found at the junction of ORFs in influenza B virus segment 7 (Horvath et al., 1990; Powell et al., 2008) and in *Bombyx mori* retrotransposon element SART1 (Kojima et al., 2005). Using a firefly luciferase reporter gene system, Guo and colleagues (2009) demonstrated that the re-initiation rate of ORF B is between 2.5–4.4%. In addition, Suzuki et al. (2000) demonstrated that the pentanucleotide sequence could be mutated to generate a monocistronic genome without negatively affecting viral replication or virus-mediated alterations to the phenotype of its fungal host.

Identification of the mature proteins and the processing pathway of ORF B has remained elusive. The only mature viral protein from ORF B that has been identified is p48, a 48 kDa papain-like protease located at the N-terminus of ORF B. Analysis of the p48 coding domain shows that p48 and p29 share conserved aa sequences surrounding the catalytic cysteine and histidine residues and the spacing of these residues relative to the cleavage sites (Shapira and Nuss, 1991). These similarities combined with the location of the two leader proteases at the N-termini of ORF A and ORF B, and sequence alignment studies indicate that p48 and p29 are products of a gene duplication event (Koonin et al., 1991; Shapira et al., 1991A).

Transformation of the fungal strain EP155 with the p48 coding region showed that p48 contributes to CHV-1/EP713-mediated suppression of host pigmentation and sporulation (Deng and Nuss, 2008). Moreover, p48 was shown to be required for viral replication. Generation of a mutant virus containing a deletion of the p48 coding domain (CHV-1/Δp48), resulted in a non-viable virus, however, transfection of a p48 transformant fungal strain with CHV-1/Δp48 synthetic RNA transcripts demonstrated that expression of p48 *in trans* could rescue the p48-deficient mutant virus (Figure 1.10 A and B) (Deng and Nuss, 2008). These results were confirmed by performing an anastomosis reaction between two EP155 transformant strains; one expressing p48 and the other expressing the CHV-1/Δp48 mutant virus. Upon fusion of the fungal hyphae and cytoplasmic mixing, the CHV-1/Δp48 mutant virus began to replicate. Once rescued, the CHV-1/Δp48 mutant virus could be transferred by anastomosis to a fungal strain not expressing p48, resulting in continued viral replication in the apparent absence of p48 (Figure 1.10C) (Deng and Nuss, 2008).

A

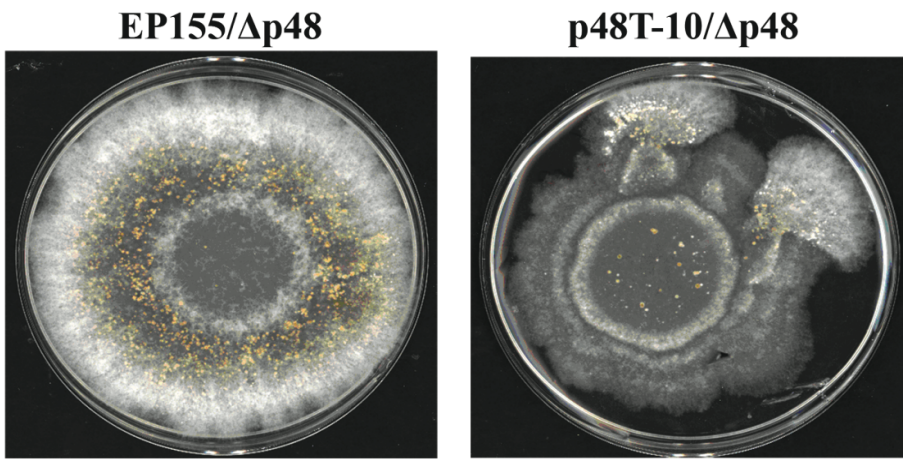
EP155/Δp48
p48T-10/Δp48

B

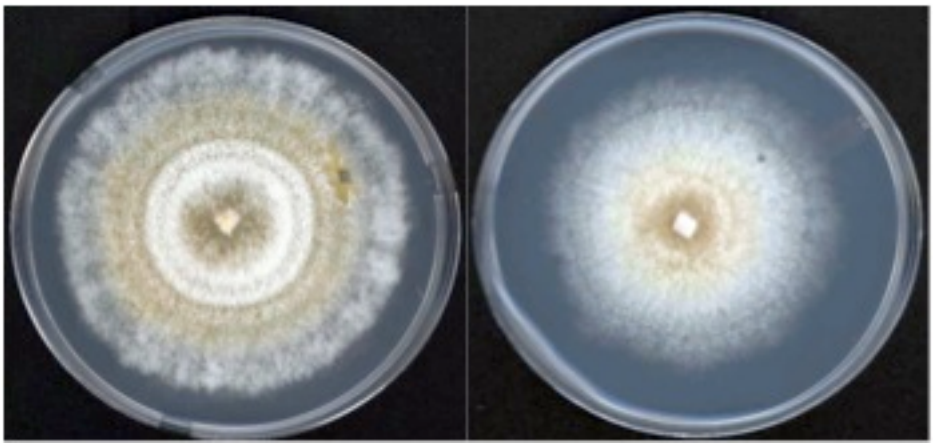
EP155/Δp48
p48T/Δp48

C

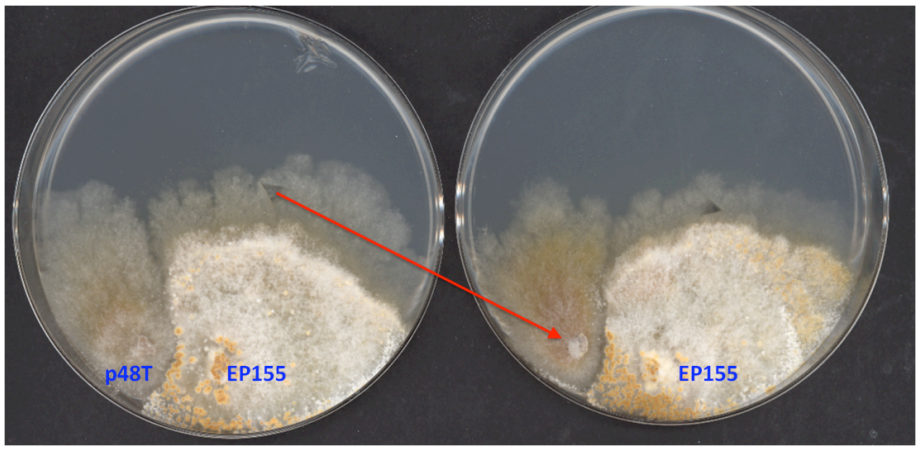
p48T
EP155
EP155

Figure 1.10 – Protease p48 complementation of the replication-defective Δp48 mutant virus. (A) Transfection of *C. parasitica* strain EP155 and the p48 transformant strain p48T-10, shown on regeneration media. Transfection of EP155 with the Δp48 mutant virus resulted in aerial hyphae and sporulation indicating that the p48 deficient virus is unable to replicate in WT *C. parasitica.* The transfected p48 transformant strain produced little aerial hyphae and reduced sporulation symptomatic of hypovirus infection, indicating that p48 is required for virus replication (Borrowed from Deng and Nuss, 2008). (B) Once transferred to PDA the rescued Δp48 mutant virus results in a reduction fungal pigmentation and aerial hyphae. (C) The rescued Δp48 mutant virus continues to replicate and cause symptoms after transmission to WT EP155 isolate and subsequent sub-culturing in the absence of p48.

Quantitative Real-time RT-PCR showed that viral RNA accumulation for the CHV-1/Δp48 mutant virus isolated from either the p48 transformant strain or EP155 was reduced approximately 80% when compared to CHV-1/EP713 (Deng and Nuss, 2008). These results indicated that p48 is essential for initiation of CHV-1 replication, but is not required for the maintenance of hypovirus RNA. In addition, recent analysis of vesicles isolated from a CHV-1-infected fungal host indicates that p48 associates with host vesicles during viral replication (Wang et al., 2013).

While mature proteins from the remaining region of ORF B have yet to be identified, the predicted amino acid sequence contains regions that correspond to RDRP and helicase domains. The N-terminal region has been implicated in contributing to changes in fungal colony morphology. Using chimeric CHV-1 viruses, Chen and Nuss (1999) and Chen et al. (2000) demonstrated that the region just downstream of p48 is responsible for virus-mediated alterations of fungal colony morphology, growth rate, and canker size. However, the proteins responsible for these differences have not been identified or isolated.

Despite the inability to identify processed RDRP, CHV-1 was shown to have RDRP activity. Fahima and colleagues (1993) isolated fungal vesicles from a CHV-1/EP713 infected isolate, shown to be associated with viral RNA and demonstrated that these vesicles possessed RDRP activity, while vesicles isolated from a virus-free fungal isolate lacked any noticeable RDRP activity. Furthermore, it was demonstrated that RDRP products, synthesized *in vitro*, hybridized specifically with *C. parasitica* genomic dsRNA, and over 80% of the synthesized RNA was of positive polarity (Fahima et al., 1993).

Fahima and colleagues (1994) subsequently identifed an 87 kDa protein, which associates with both the fungal vesicles that previously displayed RDRP activity and viral RNA. Furthermore, the 87 kDa protein was not detected in virus-free fungal isolates, leading Fahima and colleagues (1994) to hypothesize that this protein is the CHV-1 RDRP. Despite these results, complete mapping of the CHV-1 ORF B remains elusive and the 87 kDa protein, hypothesized to be the mature CHV-1 RDRP has yet to be independently isolated and confirmed.

1.6 The CHV-1/*C. parasitica* Experimental System

The ability to study mycoviruses has been limited due to difficulties in initiating infections by an extracellular route and by the inability to genetically manipulate the fungal host. To determine whether a specific virus is responsible for induced changes in the fungal host, the fungal strain has to be cured of the mycovirus, and then the mycovirus must be subsequently re-introduced into the cured strain. Additionally, since a majority of mycoviruses lack an extracellular lifecycle stage and some mycoviruses do not form infectious particles, re-introduction of mycoviruses is generally limited to anastomosis; however this is complicated by transmission of additional cytoplasmic elements (Nuss, 2010). These technical problems have been overcome for one select group of mycoviruses, CHV-1, with the development of an infectious cDNA clone and the ability to induce a viral infection through introduction of the corresponding synthetic RNA transcripts derived from the cDNA clone into fungal spheroplasts (Figure 1.2) (Choi and Nuss, 1992; Chen et al., 1994; Nuss, 2010). The CHV-1/*Cryphonectria parasitica* experimental system is currently the

only robust reverse genetics system available for studying mycoviruses and virus-host interactions in fungi.

Full-length infectious cDNAs are available for the prototypic sever hypovirus CHV-1/EP713, the mild hypovirus CHV-1/Euro7, and a low copy number hypovirus CHV-1/EP721. CHV-1/EP713 infected *C. parasitica* strains form small, superficial cankers with a low level of asexual spore-forming fruiting bodies. In contrast, CHV-1/Euro7 infected strains attain a canker size that is three- to four-fold larger than those produced by CHV-1/EP713 infected strains. CHV-1/Euro7 cankers are characterized by ridged margins and the formation of a high number of spore-forming fruiting bodies covering the canker (Chen and Nuss, 1999; Chen et al., 2000; and Parsley et al., 2002). Furthermore, CHV-1/EP721 infected strains display a phenotype similar to a CHV-1/Euro7 infected strain, however dsRNA isolated from CHV-1/EP721 infected strains is about 1/10 of the level observed in CHV-1/EP713 infected strains (Lin et al., 2007). These various isolates provide opportunities for comparative approaches to investigate mechanisms underlying hypovirus replication and specific viral and host factors that are important for viral pathogenesis.

In addition, complete sequences are available for all CHV isolates including CHV-1, CHV-2, CHV-3, and CHV-4 as well as two reoviruses that contain 11 segments of dsRNA, MyRV1-Cp9B21 and MyRV2-CpC18, narnavirus CMV1/NB631, partitivirus REN and chrysovirus OB5-11 (Hillman and Suzuki, 2004). These different viruses all have the ability to replicate within *C. parasitica* and infection results in a different sets of phenotypic changes, including reduced asexual sporulation and pigmentation, altered colony morphology, and reduced fungal

virulence. Thus, *C. parasitica* serves as an ample host for the study of a diverse set of mycovirus families.

The capability to genetically manipulate *C. parasitica* to further examine virus-host interactions has also benefited from several advances. Since *C. parasitica* is haploid and asexual spores are uninucleate, gene disruption is highly efficient. Recently, a mutant strain, DK80, has been engineered that increases the efficiency of homologous recombination from 5% to 85% (Lan et al., 2008). This strain contains a disruption of the KU80 gene, which encodes a key component of the non-homologous end joining DNA repair pathway. Moreover, a draft sequence of the *C. parasitica* genome has recently been completed and made available by the Joint Genome Institute at the DOE.

1.7 Research Objectives

Positive strand RNA viruses employ similar general replication strategies that include membrane restructuring, associated replication complex formation and polyprotein production, processing and multifunctionality. However, much remains to be determined about the precise functional and mechanistic contributions of individual viral proteins. The objectives of this project focused on the CHV-1 p48 papain-like protease and the requirements and mechanisms underlying its functional role in hypovirus replication.

Objective 1: Define the requirements for p48 proteolytic processing and the functional importance of autoproteolysis in the context of viral replication and *trans* complementation.

Objective 2: Identify and characterize the CHV-1 p48 functional domain(s).

Both objectives took full advantage of the CHV-1/EP713/*C. parasitica* experimental system that allows the construction of extensive site specific and deletion mutant viruses and enhanced detection and characterization of viral RNA and proteins. The completion of these objectives has significantly increased our knowledge of the requirements and role of p48 in hypovirus replications, moved us closer to understanding the underlying mechanisms and provided new insights into the diversity of replication strategies employed by positive strand RNA viruses.

Chapter 2: Mutagenesis of hypovirus papain-like protease p48 catalytic residues and cleavage site revealed requirements for *in trans* complementation, contribution to viral RNA accumulation, and alternative processing

2.1 ABSTRACT:

Viral proteases have been demonstrated to be responsible for polyprotein processing pathways that lead to mature viral proteins. *Cryphonectria parasitica* hypovirus 1 (CHV-1) contains two papain-like leader proteases, p29 and p48, located at the N-terminus of their respective ORF. Protease p48 has previously been shown to be essential for initiation but not maintenance of virus replication. In this study, mutation of the p48 protease residues eliminated the ability of p48 to complement a Δp48 mutant virus, in which the p48 coding region has been deleted. When the same mutations where introduced into the CHV-1/EP713 infectious cDNA clone, viral RNA accumulation was reduced by approximately 70-80%, but in contrast to *in vitro* results, p48 processing still occurred. Protease p29 was demonstrated not to be responsible for p48/ORF B processing and mutation of the p29 protease residues reduced viral RNA accumulation by 50%. However, in contrast to the results for p48, the mutant p29 precursor protein p69 was not processed. The results show that, while dispensable for hypovirus replication, the autocatalytic processing of the leader proteases p29 and p48 contributes to optimal virus RNA accumulation. The role of the predicted catalytic residues in

autoproteolytic processing of p29 was confirmed in the infected host, while p48 was found to also undergo alternative processing independent of the encoded papain-like protease activities.

In an attempt to gain insight into the p48 alternative-processing pathway, epitope tags were used to purify WT and mutant p48, which were subsequently subjected to either MS/MS and LC/MS fragmentation to identify differences in the location of p48/ORF B processing between WT and mutant viruses. MS/MS and LC/MS results were inconclusive due to the failure of the p48 C-terminal amino acids to ionize. In addition, a novel CHV-1 ORF B protein of approximately 60 kDa was identified and was isolated using a 6xHis tag that was inserted downstream of the p48/ORF B cleavage dipeptide. These results will guide future efforts into identification hypovirus polyprotein processing pathways and identification of mature CHV-1 ORF B encoded viral proteins.

2.2 INTRODUCTION:

Many single-stranded positive sense RNA viruses that infect hosts within all kingdoms comprising the Eukaryota have evolved gene expression strategies that employ proteolytic processing of encoded polyproteins (Barrett and Rawling, 2001; Dougherty and Semler, 1993; Koonin and Dolja, 1993). This includes members of the virus family *Hypoviridae* that infect and attenuate virulence of the fungal pathogen responsible for chestnut blight, *Cryphonectria parasitica*.

The genome of the prototypic hypovirus, CHV-1/EP713 consists of a 12.7- kb coding strand that contains two ORFs, ORF A (622 codons) and ORF B (3,165 codons), separated by a stop/go UAAUG pentanucleotide (Shapira et al., 1991A).

The two ORFs contain N-terminal leader papain-like proteases, p48 and p29. Protease p29 is cotranslationally released from the N-terminal portion of a 69 kDa precursor polypeptide, p69, encoded by ORF A to form mature proteins p29 and p40 (Choi, et al., 1991B; Shapira et al., 1991A). Cell-free translation studies identified the p69 cleavage dipeptide as Gly248 and Gly249, and showed that residues Cys162 and His215 were essential for autocatalytic cleavage (Figure 1.7A) (Choi et al., 1991A). Protease p48 is released from the N-terminal portion of the ORF B encoded polypeptide predicted to be in excess of 200 kDa and to contain the viral polmerase and helicase domains (Shapira et al., 1991). Using a combination of cell-free translation and *E. coli* expression studies, Shapira and Nuss (1991B) identified Cys341 and His388 (Figure 1.7B) as catalytic residues essential for autocatalytic cleavage between Gly418 and Ala419. Phylogenetic analysis (Koonin et al., 1991) underscored similarities between the hypovirus proteases and the papain-like plant potyvirus-encoded helper component proteases (HC-Pro) noted by Choi et al. (1991) and led to the proposal that p29 and p48 are the products of an intragenomic duplication event and subsequent divergence (Koonin et al., 1991; Shapira et al., 1991A).

Like many viral leader proteases, p29 and p48 also serve important functional roles. While the p29 protease is not essential for viral replication (Craven et al., 1993), it serves as a suppressor of the *C. parasitica* anti-viral RNA silencing response pathway (Segers et al., 2006; Zhang et al., 2008; Zhang and Nuss, 2008; Sun et al., 2009). Unlike p29, p48 is not dispensable for viral replication. However, when supplied *in trans*, p48 can rescue the Δp48 mutant virus (Deng and Nuss, 2008).

Surprisingly, once rescued, the Δp48 mutant virus continued to replicate in the absence of p48. Thus, p48 appears to have the unusual property of being required for the initiation but not the maintenance of viral RNA replication.

Given that p29 and p48 appear to share a common ancestor, it is interesting that p48 is required for viral replication, whether it is expressed *in cis* or *in trans*, whereas p29 is dispensable for virus replication. While both p29 and p48 have been detected in extracts of infected mycelium by immunological methods, processing has not been studied in the infected fungal host. In an attempt to examine the requirements for p48 *in trans* complementation of the Δp48 mutant virus, Cys341 and His388 were mutated to serine in *C. parasitica* p48 transformants. I now report that mutation of either or both of the catalytic residues eliminate the ability of p48 to complement the Δp48 mutant virus. Given the important functional roles played by the hypovirus leader proteases, I also describe the results of a mutational analysis of the p48 and p29 catalytic residues in the CHV-1/EP713 infectious cDNA and examine the contribution of the leader proteases to viral RNA accumulation. The results present here provide evidence of an ORF B alternative-processing pathway.

2.3 METHODS:

Fungal Strains and Growth Conditions:

The *C. parasitica* strains used in this study were maintained on potato dextrose agar (PDA; Difco) as previously described (Sun, et al., 2009). WT *C. parasitica* strain EP155 (ATCC 38755) and the isogenic strain EP713 (ATCC 52571) infected with hypovirus CHV-1/EP713 have been described by Chen and Nuss (1999). The RNA silencing mutant strain containing a disruption of the Dicer gene

*dcl*2 (Δ*dcl*2) was generated in the study described by Segers et al. (2007). Fungal cultures used for nucleic acid and protein preparations were grown for 7 or 10 days in potato dextrose broth (PDB; Difco) at 22-24^{o}C.

Cloning and Mutagenesis: (i) Construction of p48 and p29 Protease Domain and Cleavage Site Mutants

Point mutations were introduced into the p29 and p48 protease domains using the Quick Change II XL Site Directed mutagenesis (Stratagene) protocol, but employing the Phusion High-Fidelity polymerase (New England Bioloabs (NEB), Ipswich, Mass.) in place of *PfuUltra* High Fidelity polymerase. Point mutations were introduced into the p48 domain using a subclone containing the p48 coding domain. Nucleotides 392 to 4182 of plasmid pRFL4 (described in Zhang et al., 2013) were amplified using primers 391-ecoR1-FW (5'-GCATGAATTCCAGTGAAT TCGAGCTCGGTACC-3') and 4182-xbaI-RV (5'-CGCTCTAGAGGTATTA TCTTTGGCCCTTTGGC-3'), digested using *EcoRI* (NEB) and *XbaI* (NEB) restriction enzymes and ligated into pUC19 to yield plasmid pUC-p48. Using appropriate primer sets (Appendix 1) individual point mutations were introduced at Cys341, His388, and Gly418 in pUC-p48. The Cys341 mutant was used to subsequently generate the Cys341:His388 double mutant which was subsequently used to generate the Cys341:His388:Gly418 triple mutant. The mutated pUC-p48 plasmids were sequenced to confirm the mutations were present and digested with restriction enzymes *MreI* (Fermentas, Glen Burnie, MD) and *NheI* (NEB). The resulting fragments were used to replace the corresponding fragment in WT pRFL4 cDNA. The designations given to these plasmids were as follows: pRFL4-

p48(C341S); pRFL4-p48(H388S); pRFL4-p48(C341S:H388S); pRFL4-p48(G418R); pRFL4-p48(C341S:G418R); pRFL4-p48(H388S:G418R); pRFL4-p48 (C341S: H388S:G418R).

Mutagenesis of the p29 coding domain was performed using plasmid pRFL4 that contains the full-length CHV-1/EP713 cDNA proceeded by the T7 polymerase promoter and flanked at each end by NotI sites cloned into a modified pTZ19 vector (US Biochemicals, Cleveland OH). Using primer sets (Appendix 1) individual point mutations were introduced at either Cys162 or His215, to generate plasmids pRFL4-p29(C162S). The pRFL4-p29(C162S) construct then served as the template DNA for additional mutagenesis to generate a double mutant, pRFL4-p29(C162S:H215S).

(ii) Construction of Δp29-p48 Triple Mutant

The p29 coding domain was deleted from the p48 triple mutant plasmid pRFL4-p48(C341S:H388S:G418R) as follows. A primer set (AscI-F and 1836-R: Appendix 1) was designed to amplify nucleotides 1-1836 from plasmid pLDST-Δp29 (Suzuki et al. 1999) that contains the CHV-1/EP713 viral RNA sequence lacking 88% of the p29 coding domain. The resulting amplified fragment contained only the first 25 amino acids of p29, which were shown to be essential to viral replication, and as well as an introduced AscI site at the 5' terminus. Nucleotides 1836 to 4000 containing the p48 catalytic and cleavage site mutations were then amplified from pRFL4-p48(C341S:H388S:G418R). The two fragments were stitched together by a second round of PCR using primers AscI-F and 4KR to create the final Δp29-p48 triple mutant fragment, that was subsequently cloned into a PCR-blunt vector (Zero-Blunt PCR Cloning Kit; Invitrogen, Carlsbad, Cali.). Individual isolates were

sequenced to confirm that the point and deletion mutations were maintained and the resulting plasmid, Δp29-p48(C341S:H388S:G418R)-blunt was digested with restriction enzymes *AscI* (Fermentes) and *NheI* (NEB). The resulting fragment was used to replace the corresponding fragment in plasmid pRFL4. Individual isolates were sequenced to confirm that the desired deletion was still present and no additional point mutations were accidently generated. The resulting viral cDNA isolate was termed pRFL4/Δp29-p48(C341S:H388S:G418R).

(iii) Cloning and Epitope Tagging: Generation of Strep and 6xHis tagged viral proteins

Overlapping PCR was used to introduce a 6xHis or a strep-tag II, an eight amino acid tag (WSHPQFEK), was placed between amino acids 14-15 within the p48 coding region of WT pRFL4 and the triple mutant pRFL4-48(C341S:H388S:G418R) viral cDNAs. Using primer sets 1KF/p48-strep-R and p48-strep-F/5KR (Appendix 1), PCR was performed with plasmid pRFL4 as a template to generate two fragments, containing overlapping ends. The two fragments were stitched together by a second round of PCR using primers 1KF and 5KR to create the final fragment containing the strep-tag II and 6xHis sequence. The resulting fragment was ligated into a PCR-blunt vector and individual isolates were sequenced to confirm the correct mutation was generated. Plasmids containing either the 6xHis or the strep II tag [p48(His)blunt, p48(C341S:H388S:G418R)(His)blunt, p48(strep)blunt or p48 (C341S:H388S: G418R)(strep)blunt], were digested with restriction enzymes *MreI* and *NheI* and the resulting fragments were used to replace the corresponding fragment in plasmid pRFL4. Individual isolates were sequenced to confirm that the desired deletion was still present and no additional point mutations were accidently generated. The

resulting plasmids were termed pRFL4-p48(His), pRFL4-p48(C341S:H388S: G418R)(His), pRFL4-p48(strep), and pRFL4-p48(C341S:H388S:G418R)(strep). Additionally, a 6xHis tag was introduced into the pRFL4-p48(C341S), pRFL4-p48(388S) and pRFL4-p48(G418R) mutant viruses using the same methods as outlined above.

The insertion of a 6xHis-tag downstream of the p48/ORF B cleavage dipeptide at map position 3708 within the CHV-1/EP713 genome was facilitated through the use of unique restriction sites *NheI* and *KpnI* (NEB), spanning CHV1-EP713 map positions 3705 to 5289. The 6xHis-tag was introduced through PCR with a primer encoding for a 6xHis-tag with an GSG linker at the 5' and 3' ends of the His-tag (Appendix 1). pRFL4 was amplified, using primer set Nhe-HisF and 6KR with Phusion High Fidelity DNA polymerase to generate a 2-kb fragment containing the His-tag. The fragment was subsequently digested with *NheI* and *KpnI* and used to replace the WT *NheI-KpnI* Fragment in pRFL4.

Transfection of *C. parasitica* spheroplasts:

Infection of fungal strains with hypovirus CHV-1/EP713 or mutant CHV-1/EP713 was initiated by electroporation-mediated transfection of fungal spheroplasts with synthetic transcripts generated *in vitro* from *Spe*I (NEB) linearized viral cDNA clones using methods previously described by Suzuki and Nuss (2002) and Chen et al. (1994). Surviving spheroplasts were cultured on osmotic solid regeneration media for 7 to 10 days to allow cell wall regeneration, and then transferred to PDA plates for phenotypic characterization.

cDNA clones of the viral replicative form dsRNA recovered from mutant virus-infected strains were generated thorugh the use of the Monsterscript 1st strand cDNA synthesis kit (Epicentre Biotechnologies, Madison WI). Following manufacturers protocols, pimer 12.5KR was used to prime cDNA synthesis starting at the 3'-terminal end of the viral RNA. To confirm that no mutations to the p48 coding domain or flanking regions were generated during viral replication, PCR was subsequently performed on the cDNA using primer set 1KF-5KR to generate a 4kb product that was sequenced (Macrogen Inc, Rockville MD). Sequencing primers included 1KF, 2KF, 3KF, 4KF, 2KR, 3KR, 4KR, 5KR. Sequence analysis of the mutated viral p29 coding domain and flanking regions was performed on a 3KB fragment amplified with primer set NotI-F and 3KR (Appendix 1), using sequencing primers NotI-F, 1KF, 2KF, 1KR, 2KR, 3KR. Sequence analysis was performed using DNASTAR Lasergene 10 (Madison, WI).

Transformation and *in trans* Rescue:

Using primer set p48F and p48R (Appendix 1) [to map positions (2364) and (3618),] p48 from pRFL4-p48(C341S), pRFL4-p48(H388S), and pRFL4-p48(C341S:H388S) was amplified and digested with restriction enzyme *KpnI* and inserted into the transformation plasmid pCPXHY (Craven et al., 1993) to generate pCPXHY-p48(C341S), pCPXHY-p48(H388S), pCPXHY-p48 (C341S:H388S). The inserted DNA is flanked by the *C. parasticia* glyceraldehyde-3-phosphate dehydrogenase gene promoter and terminator to drive expression of p48 and contains the *E. coli* hygromycin B phosphotransferase gene as a selectable marker.

The transformation plasmids were introduced with the polyethylene glycol-mediated technique under the conditions previously described by Choi and Nuss (1992) into spheroplasts prepared from strain EP155 following methods outlined by Churchill et al. (1990). Single spore isolation was performed on initial transformant isolates to select for homokaryons.

Transfection of EP155 p48 transformant isolates was performed as previously outlined with synthetic RNA transcripts corresponding to viral cDNA clones pRFL4 and Δp48 (Deng and Nuss, 2008).

Total RNA and Protein Extraction:

Cultures used for viral RNA and protein analysis were grown in 200 ml of PDB for 7 days. Mycelium was harvested filtration through Miracloth (Calbiochem, La Jolla, Calif.), frozen in liquid nitrogen and ground to a fine powder with a mortar and pestle.

(i) Viral RNA isolation and quantification

Mycelial powder was resuspended in 4 ml of RNA extraction buffer (100 mM Tris-HCL (pH 8.0), 200 mM NaCl, 4 mM EDTA, 2% sodium dodecyl sulfate(SDS)) and total nucleic acid was extracted two times sequentially with phenol-chloroform and precipitated by the addition of 2 volumes of ethanol. The extracted nucleic acid samples were treated with RQ1 DNase I (Promega, Madison, Wis.) to eliminate fungal chromosomal DNA, followed by 2 rounds of extraction with phenol-chloroform, precipitated with ethanol and re-suspension in double-distilled water. Total RNA concentration was measured using a NanoDrop 1000 spectrophotometer (Thermo Scientific, Wilmington, Del.). The relative levels of viral RNA

accumulation for wild-type and mutant viruses were measured by semiquantitative real-time reverse transcriptase PCR (RT-PCR) as described by Suzuki and Nuss (2002).

(ii) Total protein extraction and western blot analysis

Total protein extracts for Western blot analysis were prepared by the method of Parsley et al. (2002) using the TEDS-C extraction buffer (100 mM Tris-HCl (pH 8.0), 1 mM EDTA, 10 mM DTT, 150 mM NaCl and 1% (w/v) CHAPS). Immunoblot analysis of relative p29 and p48 protein levels was performed as described previously (Shapira, et al., 1991A) using rabbit anti-sera raised against recombinant hypovirus CHV-1/EP713 proteins expressed from map position nt 496 to 898 (αp15) for p29 and nt 2364 to 4070 (αB1) for p48. The antigen used to generate antibody αB1 included all of the p48 coding region and extended 150 codons past the p48 cly418-Ala419 cleavage dipeptide.

(iii) Purification of epitope tagged proteins and 2D Gel analysis

The 6xHis epitope tagged protein was incubated in TEDS-C buffer containing 8M Urea, to denature tagged proteins allowing for accessibility of the 6xHis tag, at room temperature for 30 minutes. The 6xHis tagged protein was purified using cOmplete His-Tag Purification Resin (Roche) following manufacturer's protocols. The protein sample was eluted off the column in fractions using Buffer A (50 mM NaH_2PO_4, 300 mM NaCl, pH 8.0) supplemented with 20 mM, 30 mM, 40 mM, and 50 mM imidazole solutions. The His-tag purification resin was regenerated by washing the column with 10 column volumes of 1 M imidazole/HCl, pH 7.5 and 20

column volumes of 1 M imidazole/HCl, pH 7.5, 20% EtOH, 4% SDS, and stored in 20% EtOH at 4˚C.

The tagged viral protein containing the strep-tag II was purified according to manufacturers protocols. Briefly, extracted proteins were diluted 10x with Buffer A and purified using a Strep-Tactin Superflow Plus purification resin (Qiagen). The isolated protein was eluted off the column using Buffer A supplemented with 2.5 mM desthiobiotin. The Strep-Tactin resin was regenerated with 50 mM NaH_2PO_4, 300mM NaCl, 1 mM HABA, pH to 8.0 and stored in Buffer A at 4˚C.

Immunoblot quantification of purified protein was performed as described in Chapter 1 (Shapira et al., 1991A) using mouse monoclonal antibody that recognized either a 6xHis tag epitope (Thermo Scientific) or a strep-tag II epitope (Qiagen).

For 2D gel analysis, purified protein was concentrated with methanol: chloroform treatment. Briefly, proteins were washed in a chloroform methanol solution (4 volumes methanol, 1 volume chloroform, 3 volumes H_2O, 1 volume protein), centrifuged 20,000xg for 10 minutes. The top phase was removed without disturbing protein at the interface, and 4 volumes of methanol were added and centrifuged at 20,000xg for 10 minutes. The supernatant was discarded, the pellet was air dried and re-suspended with 125 µL 2 M thiourea, 7 M urea, 4% CHAPS, 0.5% Triton X-100, 50 mM DTT, 0.2% of (3-10) Biolytes, and Bromophenol Blue.

The first dimension of separation was performed on 7 cm strips with a 3-10 immobilized pH gradient using a PROTEAN Isoelectric Focusing (IEF) cell from Bio-Rad Laboratories (Hercules, CA). The strips were rehydrated with 125 µL of the protein solution. IEF was conducted at 250 V for 15 min, linearly increased over 2 h

to a maximum of 4,000 V, and then run to accumulate a total of 20,000 V/h. For the second dimension, the immobilized pH gradient strips were equilibrated for 15 minutes in 50 mM Tris-HCl (pH 8.8), 6 M urea, 30% glycerol, 2% SDS, and bromophenol blue. The strips were then embedded in 0.7% (w/v) agarose on the top of 10 % polyacrylamide gels and proteins were separated by 1-D PAGE.

Mass Spectrometry:

Staining of proteins in polyacrylamide gels was performed with a SilverSNAP kit from Pierce (Rockford, IL). Silver-stained gel pieces were excised and destained in accordance with the manufacturer's protocol. In-gel digestion was carried out with 1-4 µg/mL sequencing grade modified trypsin (Promega, Madison, WI, USA) in 25 mM ammonium bicarbonate (pH 7.9) for 15 h at 37˚C. After digestion, peptides were extracted with 50 % acetonitrile containing 0.1 % TFA and dried. Dry peptide samples were dissolved in 5 mg/mL α-cyano-4-hydroxycinnamic acid in 40 % acetonitrile containing 0.1 % TFA, and manually spotted onto an ABI 01-192-6-AB target plate.

MS analysis was performed using an AB4700 Proteomics Analyzer from Applied Biosystems (Framingham, MA). MS-mode acquisitions consisted of 1,000 laser shots averaged over 20 sample positions. For MS/MS-mode acquisitions, 3,000 laser shots were averaged over 30 sample positions for post-source decay fragments. Automated combined acquisition of MS and MS/MS data was controlled with 4000 Series Explorer software 3.0.

Liquid chromatography–mass spectrometry (LC–MS) analyses were performed in positive ion mode with a Finnigan LTQ Orbitrap Discovery ion trap

mass spectrometer (San Jose, CA) equipped with nanospray ionization (NSI) interface coupled with an Agilent 1100 HPLC (Palo Alto, CA). Chromatographic separations were achieved on in-house packed 50 μm i.d. silica capillary (Polymicro Technology, Phoenix, AZ) columns with 20 cm packed bed length with 3 μm Atlantis T3 C18 aqueous reversed-phase particles (Waters, Milford, MA). A flow rate of 80 nL/min was used to elute peptides with mobile phase A 0.1% formic acid in H2O and mobile phase B 0.1% formic acid in methanol. A 40 minute gradient was used to elute analytes: 100 min from 10% to 60% solvent B and 50 min from 60% to 95% solvent B. The temperature of the heated capillary was 200°C. Fragmentation was activated by collision-induced dissociation (CID). All peptides were analyzed using parent mass list-triggered datadependent analysis at a resolving power of 15,000.

MS/MS data analysis was performed with GPS Explorer software 3.5 utilizing Mascot 2.0 from MatrixScience (London, UK) as the search engine. During searching, the mass tolerance was 0.08 Da for the precursor ions and 0.2 Da for the fragment ions. A protein was listed as identified when the MOWSE score was higher than 63 or 64, the Mowse score at which statistical significance ($p<0.05$) occurred for that particular search. LC/MS data analysis was processed using MassMatrix (www.massmatrix.net) against a custom database file consisting of the sequence of the target protein.

2.4 RESULTS:

Ability of p48 protease mutants to rescue Δp48 mutant virus *in trans*:

It has been previously reported that the CHV-1 p48 protein has the ability to function *in trans* to rescue a CHV-1 Δp48 mutant virus, where the p48 coding domain has been deleted (Deng and Nuss, 2008). Furthermore, once the CHV-1 Δp48 mutant virus was replicating, p48 was no longer required, indicating that p48 is essential for initiation of viral replication. In an effort to better understand the role of p48 in the initiation of CHV-1 replication, and to determine how essential the protease domain is to virus replication, we asked if either or both of the ctalytic residues were necessary for *in trans* rescue of the CHV-1 Δp48 mutant virus. The CHV-1 p48 catalytic residues have previously been mapped *in vitro* to Cys341 and His388 (Shapira and Nuss, 1991)(Figure 2.1A). The ability of the protease mutant p48 to rescue the Δp48 mutant virus was examined by transfecting Δp48 RNA transcripts into transgenic *C. parasitica* strains expressing p48 with the following mutations; C341S, H388S, or C341S:H388S; these mutations have been previously shown to prevent p48/ORF B cleavage *in vitro* (Shapira and Nuss, 1991). In addition to the EP155 tranformants expressing mutant p48, an EP155 transformant expressing WT p48 containing a FLAG and strep-tag II domain at the N-terminus was generated in order to repeat the results previously obtained by Deng and Nuss (2008). The p48 transformants were screened for resistance to Hygromycin B, were single spore isolated and screened by PCR to confirm the presence of p48.

The results obtained using epitope tagged WT p48 were consistent with the previous p48 complementation results; the WT p48 was able to complement the Δp48

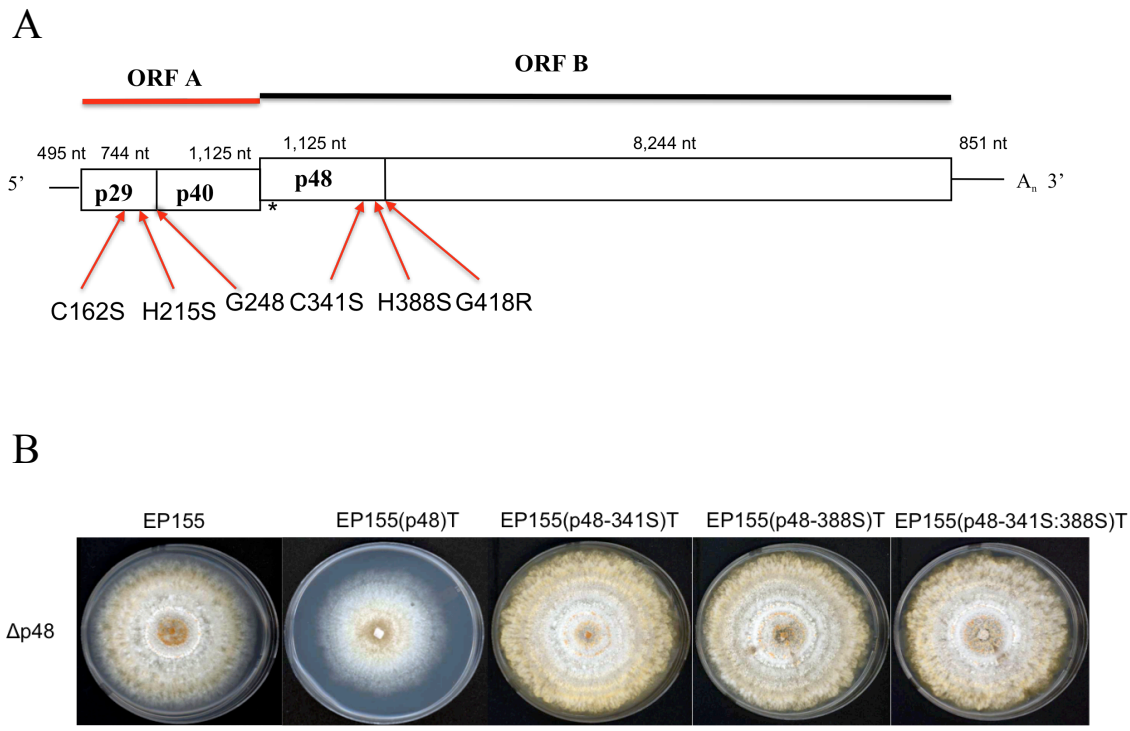

Figure 2.1 – Mutation of p29 and p48 catalytic and cleavage site residues and *in trans* complementation. (A) Diagram of the CHV-1/EP713 viral genome. The p29 catalytic residues have been mapped *in vitro* to Cys162 and His215. The p48 catalytic residues have been mapped to Cys341 and His388 of ORF B, additionally, the cleavage has been identified as occurring between Gly418/Ala419. The * denotes the location of either a 6xHis or strep-tag II, placed after amino acid Thr14. The catalytic residues of both p29 and p48 were mutated to serine thereby disrupting the protease domains. Additionally, the p48/ORF B cleavage site residue Gly418 was mutated to Arg, which has previously been shown to prevent cleavage *in vitro*.

(B) *In trans* complementation of the Δp48 mutant virus with WT and mutant p48 protein. Fungal strain EP155 was transformed with WT epitope tagged p48, as well as with p48 containing mutations to protease residues Cys341Ser and His388Ser,

individually and in combination and transfected with RNA transcripts corresponding to the Δp48 mutant virus. *C. parasitica* transformant strains expressing mutant p48 were unable to rescue the Δp48 mutant virus and showed uninfected phenotypes.

mutant virus (EP155(p48)T isolate, Figure 2.1B), and once replicating, the Δp48 mutant virus could continue to replicate in the absence of p48. In contrast to the ability of WT p48 to rescue the Δp48 mutant virus, Δp48 RNA transcripts failed to show any CHV-1 associated phenotypic changes upon introduction into spheroplasts expressing the mutant p48 protein. Transfected isolates were similar to uninfected EP155 in their growth rate, pigmentation, and sporulation (Figure 2.1B). Furthermore, no viral RNA could be detected by RT-PCR from nucleic acid extracts. Additionally, RNA transcripts corresponding to WT CHV-1/EP713 readily established infections when elecroporated into spheroplasts expressing the mutant p48 protein. Thus the protease mutant p48 proteins was unable to complement the Δp48 mutant virus *in trans*, resulting in the Δp48 virus being unable to establish an infection under conditions that supported CHV-1/EP713 replication.

CHV-1 p48 protease catalytic residues are not required for viral replication:

The inability of the mutant p48 to complement the Δp48 mutant virus combined with the report by Shapira and Nuss (1991) that demonstrates p48/ORF B cleavage does not occur *in vitro*, when either of the catalytic residues or the cleavage site was mutated, indicates that the p48 catalytic residues are essential CHV-1 ORF B processing and may be required for viral replication. To test this prediction, C341S and H388S mutations were introduced into the p48 coding domain of the CHV-1/EP713 infectious cDNA clone individually and in combination. The full-length viral cDNA containing the mutations was used to generate RNA transcripts, which were electroporated into *C. parasitica* strain EP155 and Δ*dcl*2 spheroplasts. The Δ*dcl*2 strain is a dicer knockout strain in which the *C. parasitica* RNA silencing anti-

viral response has been disabled, resulting in a severely debilitated phenotype and an increase in viral RNA and protein accumulation (Segers et al., 2007; Sun et al., 2009). Thus the Δ*dcl*2 strain was used due to the ability to quickly identify transfected fungal isolates based on CHV-1 symptoms being more pronounced and increased protein accumulation facilitating analysis of viral proteins.

Colonies transfected with full-length viral transcripts exhibited the typical set of phenotypic changes associated with CHV-1/EP713 infection and viral dsRNAs were detected. In contrast, transfection of EP155 with the CHV-1 p48 protease mutant viruses resulted in less severe infection symptoms when compared to CHV-1/EP713. However, infection of Δ*dcl2* spheroplasts displayed similar colony morphologies despite the mutations to p48 (Figure 2.2). Thus, transcripts derived from the p48 protease mutant plasmids were able to establish an infection when introduced into *C. parasitica* spheroplasts, indicating that the catalytic residues are not essential for virus replication.

In an effort to understand the functional importance of p48 protease activity has on viral RNA accumulation, semi-quantitative real-time PCR (RT-PCR) was performed to examine RNA levels of the protease mutant viruses compared to WT CHV-1/EP713. As quantified by qRT-PCR, the protease mutant viral RNAs accumulation was shown to be reduced by approximately 67% (CHV-1/p48(341S), 78% (CHV-1/p48(388S), and 82% (CHV-1/p48(341S:388S), indicating that mutations to either or both catalytic residues, Cys341 and His388, has a negative effect on viral RNA accumulation (Figure 2.3). Additionally, viral RNA was screened by RT-PCR and sequenced to confirm that the protease mutations, C341S

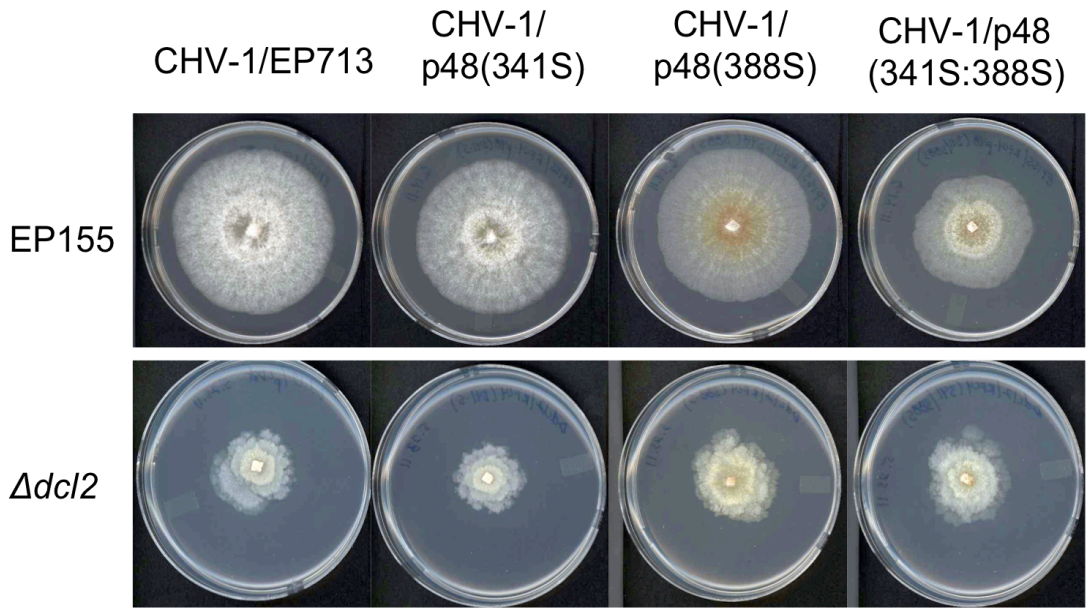

Figure 2.2 – Colony morphology of strains EP155 and Δ*dcl2* transfected with RNA transcripts corresponding to WT CHV-1/EP713 and p48 protease mutant viruses CHV-1/p48(341S), CHV-1/p48(388S), and CHV-1/p48(341S:388S). Infection of strain EP155 with CHV-1/p48(341S) produced a fungal phenotype similar to CHV-1/EP713, including a white phenotype and reduction in sporulation. Infection of EP155 with CHV-1/p48(388S) and CHV-1/p48(341S:388S) resulted in further reduction of ariel hypae however, there was increased fungal pigmentation when compared to CHV-1/EP713 infection. Infection of strain Δ*dcl2* with the p48 protease mutant viruses produced a phenotype similar to that of CHV-1/EP713 infected colonies.

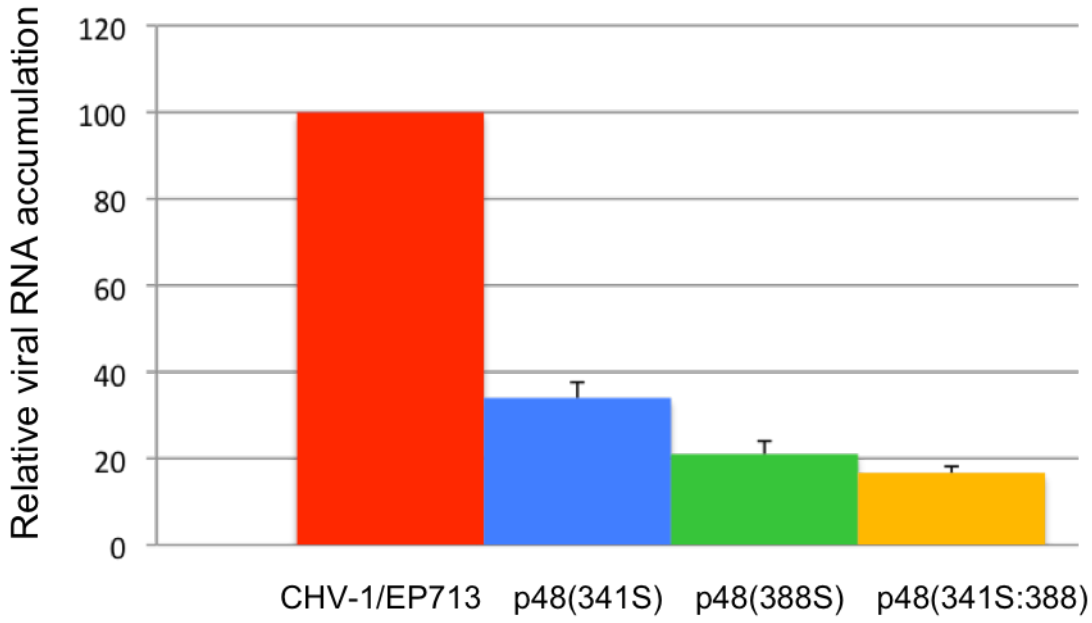

Figure 2.3 – Real time RT-PCR quantification of viral RNA accumulation for p48 catalytic residue mutant viruses. Viral RNA accumulation levels were measured as described in Materials and Methods and are reported as percentages of the value obtained for CHV-1/EP713 infected EP155 fungal colonies, with standard deviations indicated by the error bars based on three independent measurements.

and H388S, were still present and that the virus had not reverted or generated a compensatory mutation to allow for virus replication.

The ability of the mutant p48 CHV-1 viruses to replicate was an unexpected result. To determine if there was a difference in p48/ORF B processing, viral proteins were extracted from EP155 and Δ*dcl2* infected colonies and analyzed by Western blot. Due to the low levels viral RNA accumulation in EP155 colonies infected with the p48 protease mutant viruses, no viral proteins could be detected. Surprisingly, using protein extracted from Δ*dcl2* infected colonies, Western blot results showed that p48/ORF B processing was still occurring (Figure 2.4).

Mutation of the p48/ORF B cleavage site does not prevent processing:

Since the *in vivo* results were in contrast with the previously reported *in vitro* results obtained by Shapira and Nuss (1991), it was of interest to determine if mutation of the p48/ORF B cleavage site would abolish cleavage *in vivo* as it was previously shown to do *in vitro*. To examine this, a cleavage site mutation, G418R, which was previously shown to abolish p48/ORF B processing (Shapira and Nuss, 1991) was introduced into CHV-1/EP713. The G418R mutation was introduced individually and in combination with either one or both of the p48 catalytic residue mutations. Upon transfection of RNA transcripts into EP155 and Δ*dcl2* spheroplasts through electroporation, all mutant viruses displayed the ability to replicate, and resulted in a decrease in fungal pigmentation and sporulation. Fungal isolates harboring mutant CHV-1/ EP713 viruses (C341S:G418R), (H388S:G418R), and (C341S:H388S: G418R) displayed more pigmentation than WT CHV-1/EP713 (Figure 2.5); believed to be the result of a decrease in viral RNA accumulation in the

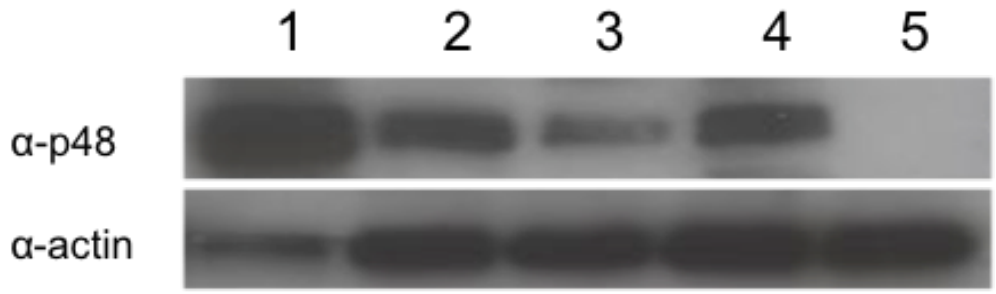

Figure 2.4 – Western blot analysis of CHV-1 mutant p48. Despite mutation of the p48 protease residues, p48/ORF B cleavage still occurs. Proteins were detected with a polyclonal antibody directed against p48 (αB1) in protein extracts isolated from Δ*dcl*2 fungal isolates infected with full-length CHV-1/EP713 (lane 1) or one of the p48 protease mutant viruses (lane 2: CHV-1/p48(341S), lane 3: CHV-1/p48(388S), lane 4: CHV-1/p48(341S:388S). The WT p48 protein was diluted 10x compared to mutant p48 before loading the gel. The p48 protein was not detected in protein extracts from an uninfected Δ*dcl*2 isolate (lane 5).

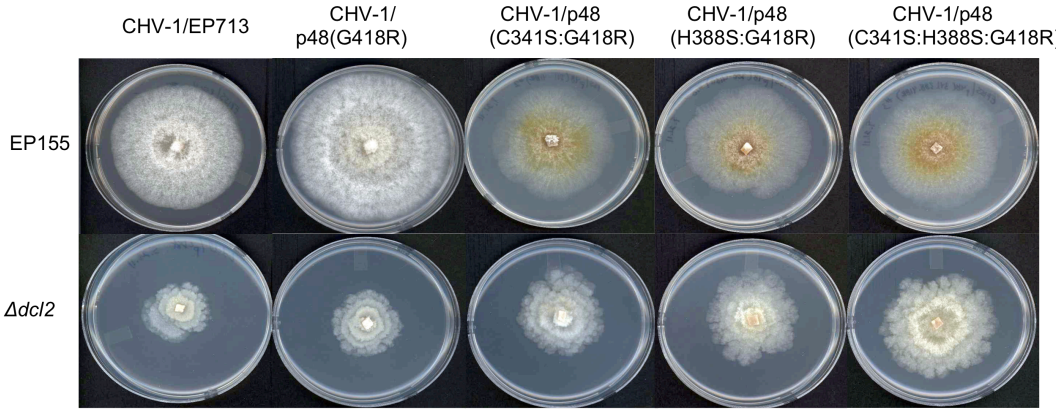

Figure 2.5 – Colony morphology of EP155 and Δ*dcl2* isolates infected with p48 cleavage site mutant viruses. Fungal strains EP155 and Δ*dcl2* were transfected with RNA transcripts derived from p48/ORF B cleavage site mutant virus cDNA plasmids. Fungal colonies were photographed after culturing on PDA plates for 7 days. Infection of EP155 with the CHV-1/p48(418R) mutant virus resulted in a hypovirulent phenotype similar to wild-type CHV-1/EP713. Infection of EP155 with a CHV-1 virus containing a mutation to the protease residues and the cleavage site residue results in an increase in fungal pigmentation. When the p48 mutant viruses were introduced into Δ*dcl*2 spheroplasts, the infected fungal isolates displayed a faster growth rate and increased pigmentation when compared to CHV-1/EP713 infection.

mutants. Once again, due to low levels of virus replication in EP155, Western blot analysis was performed on total protein extracts from infected Δ*dcl2*. Despite mutation of the protease residues and the cleavage site, Western blot results indicate that the p48/ORF B processing still occurred (Data not shown).

In addition, due to the lack of a monoclonal antibody against p48, and because antibody αB1 has the ability to recognize epitopes of a downstream protein, a 6xHis epitope tag was inserted after amino acid Thr14 of p48 in the following mutant viruses; CHV-1/p48(C341S), CHV-1/p48(388S), CHV-1/p48(418R) and CHV-1/p48(C341S:H388S:G418R), as well as in WT CHV-1/EP713. A monoclonal anti-6xHis antibody (Pierce Scientific) was used to detect the p48 protein and eliminated background bands due to antibody αB1 recognizing additional CHV-1 proteins thereby allowing for a better comparison of WT and mutant p48. Western blot analysis against protein extracted from CHV-1/p48(C341S)6xHis, CHV-1/p48(388S)6xHis, CHV-1/p48(418R)6xHis and CHV-1/p48(C341S:H388S:G418R)6xHis showed that p48/ORF B processing still occurs however the p48 protein accumulates to lower levels then during CHV-1/EP713 infection (Figure 2.6).

Protease p29 is not responsible for p48/ORF B processing:

One possible explanation for why p48/ORF B processing is still occurring, despite mutation of the protease and cleavage site residues, is that protease p29 has the ability to process ORF B, and is responsible for the low level of viral replication that is observed. It has been previously proposed that p29 and p48 arose from a gene duplication event, and then subsequently evolved (Koonin et al., 1991). To investigate this possibility, the p29 coding domain, with the exception of the first 25

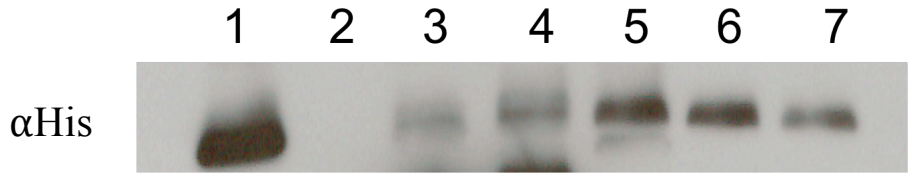

Figure 2.6 – Western blot analysis of 6xHis tagged WT and mutant p48 viruses. Results indicate that despite mutation of the p48 catalytic or cleavage site residues demonstrated to be essential for p48 processing in vitro are not required for processing in vivo. Lane 1: CHV-1/p48(His); Lane 2: EP155; lane 3: CHV-1/p48(341S)(His); lane 4: CHV-1/p48(388S)(His); lane 5: CHV-1/p48 (418R)(His); lane 6: CHV-1/p48(341S:388S:418R)(His) extraction #1; lane 7: CHV-1/p48 (341S:388S:418R)(His) extraction #2

amino acids which are essential for viral replication, were deleted from the plasmid encoding the CHV-1/p48(C341S:H388S:G418R) mutant virus, to generate a CHV-1/ Δp29-p48(C341S:H388S:G418R) mutant virus. Corresponding synthetic RNA transcripts were generated and electroporated into Δ*dcl2* spheroplasts. The CHV-1/ Δp29-p48(C341S:H388S:G418R) mutant virus was replication competent and p48/ORF B processing still occurred (Figure 2.7). These results suggest that either mutant p48 maintains a low rate of proteolytic activity or a host protein(s) is involved in p48/ORF B processing.

Mutation of the p29 protease residues:

In view of the previous results demonstrating that p48/ORF B processing still occurs despite mutations to the catalytic and cleavage site residues, it was of interest to determine whether mutation of the protease p29 catalytic residues had any effect on virus replication and ORF A processing. It has been previously demonstrated that strain EP155 transformed with the CHV-1 ORF A coding domain, that contained a mutation to the p29/p40 cleavage site residue resulted in an inactive p29. EP155 transformant strains expressing WT ORF A were shown to have decreased pigmentation and sporulation, however, an EP155 transformant expressing mutant ORF A, containing a mutation at the p69 cleavage residue resulted in a fungal phenotype similar to WT EP155 (Craven et al., 1993). The authors concluded that the release of p29 from the p69 precursor was required for p29 activity. However, it was never determined if mutation of the p29 catalytic residues, Cys162 and His215, would result in an inactive p29 and prevent processing of ORF A *in vivo*. In an effort to determine if p69 cleavage can occur despite mutations to the catalytic residues,

A

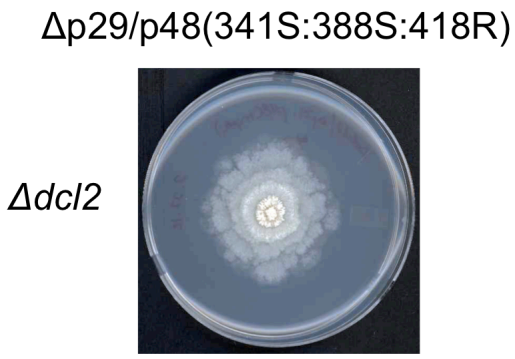

B

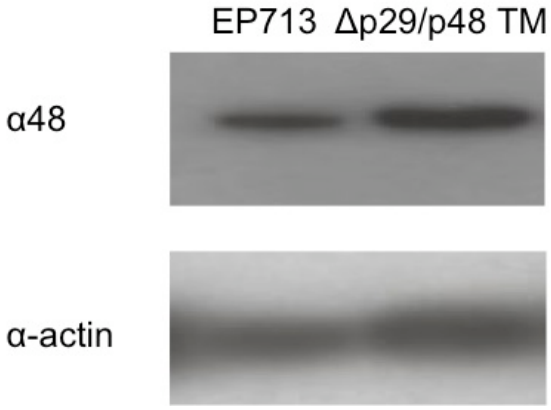

Figure 2.7 – Protease p29 is not responsible for p48 cleavage. (A) Phenotype of a Δ*dcl2* fungal isolate transfected with RNA transcripts derived from a Δp29/ p48(341S:388S:418R) mutant virus cDNA plasmid. The infected fungal phenotype is similar to one exhibited by CHV-1/EP713 infection (Figure 2.2). (B) Western blot analysis of proteins extracted from a Δ*dcl2* fungal isolate infected with CHV-1/EP713 (lane 1) and the Δp29/p48(341S:388S:418R) mutant virus (lane 2). Protein p48 was detected using a polyclonal antibody against p48 (αB1).

much in the way p48/ORF B cleavage occurs, CHV-1/p29(C162S) and CHV-1/p29(C162S:H215S) mutant viruses were generated.

Transfection of strains EP155 and Δ*dcl*2 with either mutant virus resulted in an infectious phenotype (Figure 2.8). These results indicate that the p29 catalytic residues are not essential for virus replication. To assess whether either of the p29 protease mutant virus RNA levels accumulate to the same levels as CHV-1/EP713, RNA levels were quantified by real-time RT-PCR. Viral RNA levels for both p29 catalytic mutant viruses, CHV-1/p29 (C162S) and CHV-1/p29(C162S:H215S), were determined to be reduced by 43% and 47% respectively when compared to wild-type CHV-1 respectively (Figure 2.9).

We next examined whether p69 processing was occurring despite mutation to the catalytic residues, as was observed in the p48 protease mutant viruses. As determined by Western blot, p69 processing does not occur, and there appears to be a significant decrease in p69 accumulation during CHV-1/p29(162S) or CHV-1/p29(162S:215S) infection, when compared to p29 levels in CHV-1/EP713 infected Δ*dcl*2. Moreover, no mature p29 was detected (Figure 2.10).

Efforts to identify the p48/ORF B cleavage site:

As previously demonstrated, mutation of the p48 protease catalytic residues and Gly418 of the predicted cleavage dipeptide did not disrupt p48/ORF B processing in infected cells. One possibility is that p48 is released through an alternative cleavage event that is occurring at a nearby residue. In an effort to (1) confirm the previous *in vitro* results mapping the p48 cleavage dipeptide to Gly418 and Ala419 and (2) determine if p48/ORF B is being processed by an alternative cleavage event,

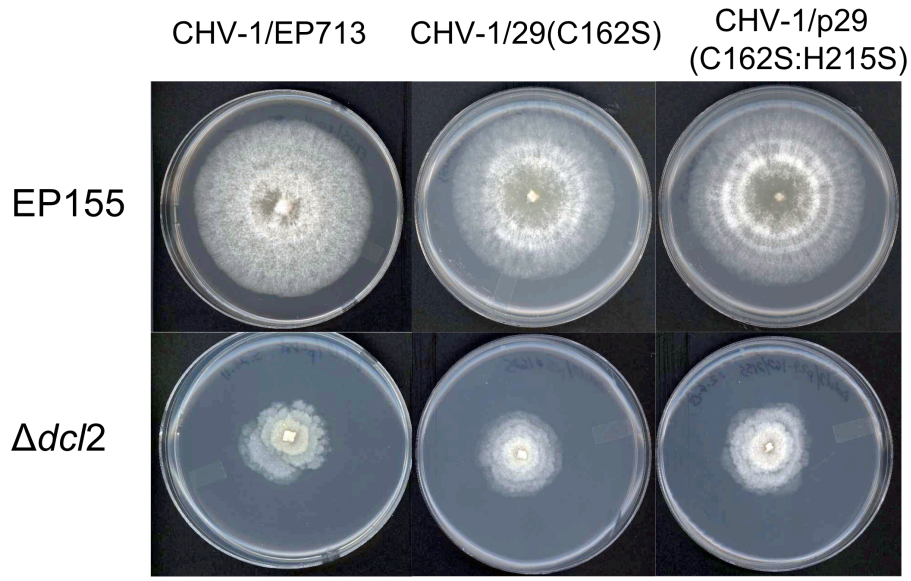

Figure 2.8 – Colony morphology of *C. parasitica* infected with CHV-1/EP713 p29 mutants. Synthetic RNA transcripts derived from cDNA plasmids containing mutations to p29 catalytic residues Cys162 and His215 were transfected into EP155 and Δ*dcl2* spheroplasts. Mutation of the p29 catalytic residues does not significantly alter EP155 or Δ*dcl2* colony morphology or pigmentation when compared CHV-1/EP713 infected isolates.

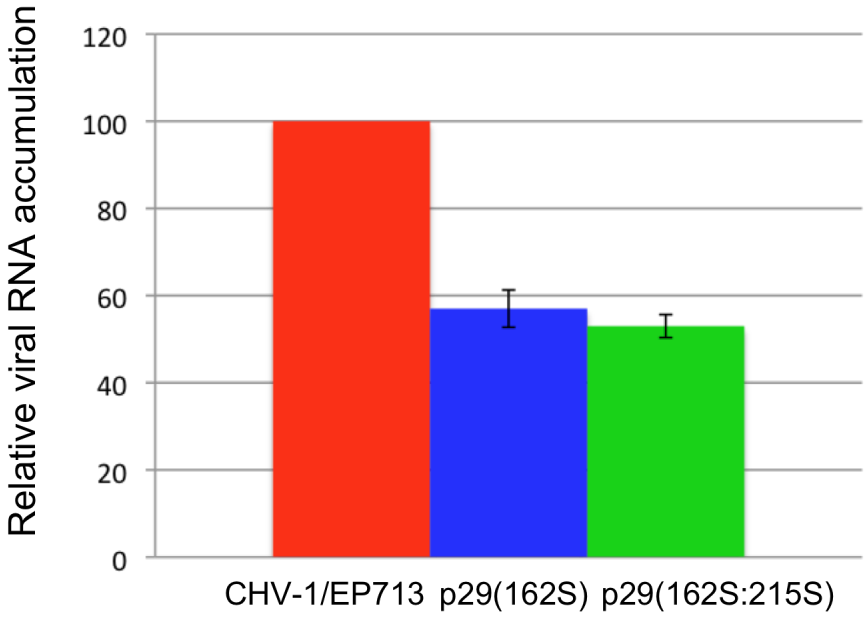

Figure 2.9 – Real time RT-PCR of viral RNA. Accumulation of p29 mutant viral RNA in fungal strain EP155 was measured as described in the Materials and Methods. Viral RNA levels are reported as percentages of the value for CHV-1/EP713 infected colonies, with standard deviations indicated by the error bars based on three independent measurements.

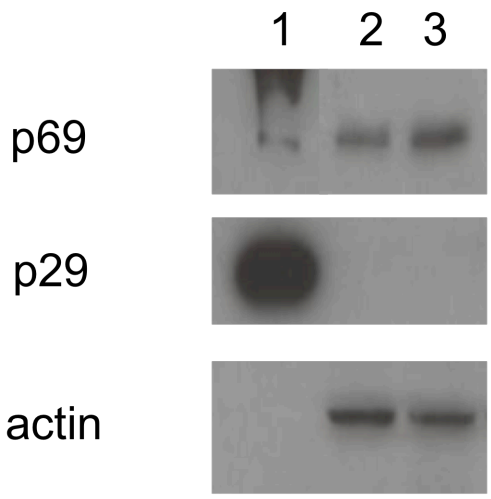

Figure 2.10 – Western blot analysis of ORF A processing. Protein extracted from Δ*dcl2* infected isolates were analyzed by Western blot using a polyclonal antibody to detect p29 (αp15). CHV-1/EP713 (lane 1) infected isolates displayed a large accumulation of viral protease p29, and a very small amount of ORF A polyprotein, p69. Mutation of either a single p29 catalytic residue Cys162 (lane 2) or both catlytic residues, Cys162 and His215 (lane 3) result in an apparent absence of p69 processing and mature p29 was not detectable. Additionally, mutation of the catalytic residues results in a large decrease in total viral protein levels. To avoid overloading p29 isolated from CHV-1/EP713 infected isolates, total protein levels were diluted 50x compared to protein extracted from isolates infected with the p29 protease mutant viruses (actin control lanes).

CHV-1/EP713 constructs containing either a strep-tag II or a 6xHis epitope tag within the p48 coding region were constructed in CHV-1/EP713 and CHV-1/p48 (341S:388S:418R) cDNA plasmids (Figure 2.11A). Synthetic viral RNAs corresponding to the cDNAs containing the strep-tag II and 6xHis were transfected into Δ*dcl*2 spheroplasts. The Δ*dcl*2 strain was used in these experiments because as previously discussed, the loss of host RNA silencing leads to a reduction in viral RNA recombination and allows for stable expression of foreign DNA elements within the CHV-1 genome (Zhang and Nuss, 2008) and an increase in protein accumulation. The strep-tag II and the 6xHis tag were placed in the p48 coding region after amino acid Thr14, with and without a Gly/Ser/Gly linker region before and after the epitope tags. To determine the stability of the tags within the CHV-1 genome, an infected Δ*dcl*2 isolate was transferred 4 times, with proteins being extracted after each transfer. A Western blot was performed on the extracted proteins using anti-p48 and anti-strep antibodies. Western blot results show that the strep-tag II was stable for at least 4 transfers after transfection (Figure 2.11B).

Once the tag was determined to be stable, the p48(strep) and p48(6xHis) tagged proteins were purified through either a streptactin resin column or cOmplete His-tag resin column, respectively. To confirm the presence of the purified p48 in the protein elution buffer, a Western blot was performed using antibodies directed against p48 as well as against the epitope tag. These results confirmed that the epitope tagged p48 protein could be purified (Data not shown). After confirmation of the presence of the epitope tagged protein in the eluted fraction, the proteins were separated through a 2D gel (Figure 2.12) and extracted for MS/MS analysis. MS/MS

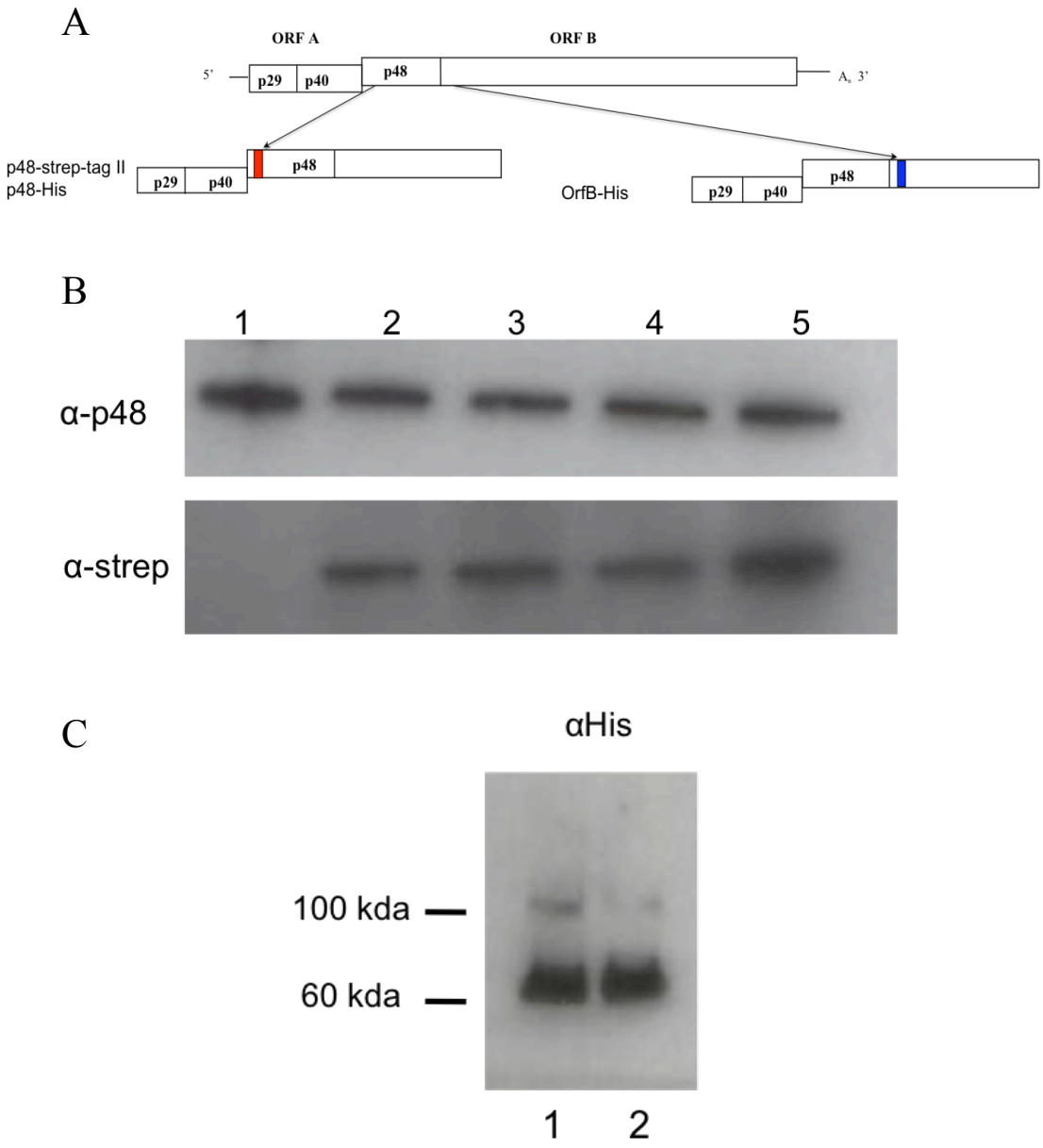

Figure 2.11 –Epitope tagging and purification of CHV-1/EP713 viral proteins. (A) A strep-tag II or 6xHis tag were placed within the p48 coding region after amino acid Thr14, with and without a GlySerGly linker region before and after the tag. Additionally, a 6xHis molecular tag was placed after amino acid Lys447 of ORF B, with a GlySerGly linker region. (B) Stability of epitope tags within the CHV-1

genome. A transfected Δ*dcl*2 isolate containing the replicating CHV-1/p48(strep) virus was transferred 4 times and total protein extracts from each transfer were examined by Western blot to determine the stability of a strep-tag II placed within the p48 coding region. Two gels were run simultaneously containing 1 µg of total protein extract per lane. Antibody αB1 was used to detect p48 in top gel and an αstrep antibody (Qiagen) was used to detect the strep epitope tag in the bottom band. Lane 1 – wild-type p48; Lane 2 – p48(strep) transfer 1; Lane 3 – p48(strep) transfer2; Lane 4 – p48(strep) transfer 3; Lane 5 – p48(strep) transfer 4. (C) Western blot analysis of a novel ORF B protein containing a 6xHis tag 28 amino acids downstream of the Gly418/Ala419 cleavage dipeptide. The protein was purified using a cOmplete His tag resin column (Roche) and eluted using 50 mM Imidazole. An anti-6xHis antibody was used to detect a protein band of approximately 60 kDa and 100 kDa. Lane 1 – CHV-1/EP713; Lane 2 – CHV-1/p48(341S:388S:418R).

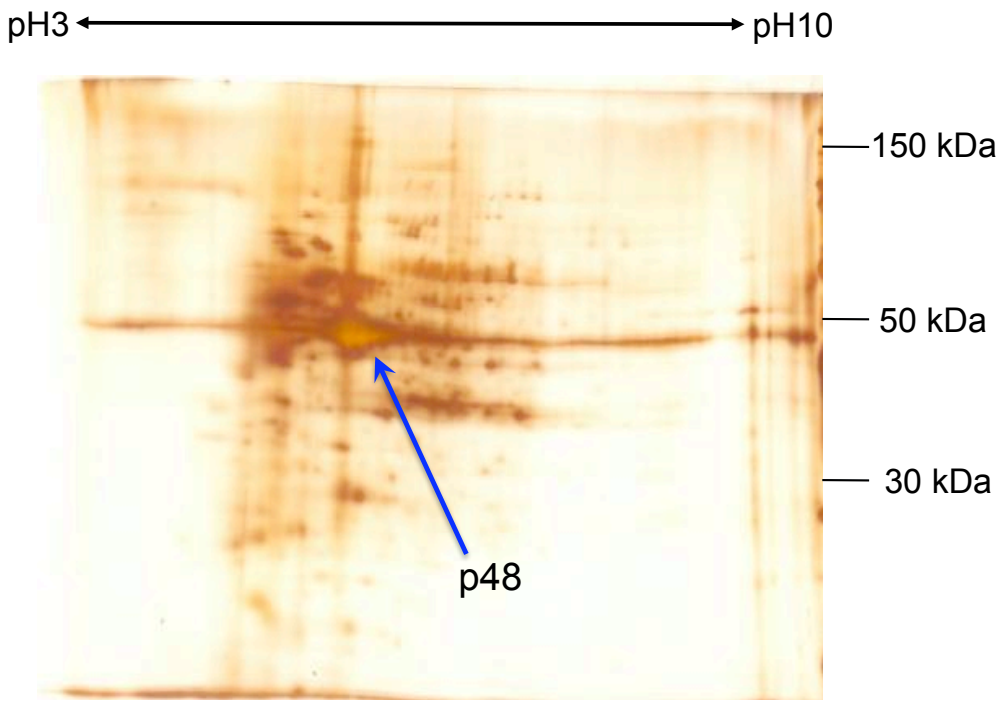

Figure 2.12 – 2D gel of purified p48(strep). Protein extracts containing the p48(strep) protein was purified through a streptactin column. Purified protein was separated through a 2D gel (10% polyacrylamide), silver stained and spots were picked and subjected to MS/MS and LC/MS. The p48(strep) spot is indicated by the arrow.

fragmentation results were inconclusive due to the inability to detect C-terminus region were constructed in CHV-1/EP713 and CHV-1/p48(341S:388S:418R) cDNA plasmids (Figure 2.11A). Synthetic viral RNAs corresponding to the cDNAs containing the strep-tag II and 6xHis were transfected into Δ*dcl*2 spheroplasts. The Δ*dcl*2 strain was used in these residues. These results were consistent with the MS/MS results obtained by Wang and colleagues (2013, who also could not detect the C-terminus residues of p48.

Identification of Novel ORF B Protein:

In response to the inability to detect the C-terminus of p48 through MS/MS, a 6xHis tag was placed 28 amino acids downstream of the predicted Gly418 and Ala419 cleavage dipeptide in WT CHV-1/EP713 and in the CHV-1/p48(341S:388S:418R) mutant virus, in an attempt to isolate the downstream viral protein for N-terminal sequencing. Synthetic RNAs corresponding to cDNAs of the WT and p48 triple mutant 6xHis tagged viruses was introduced into Δ*dcl*2 spheroplasts; both the WT and p48 triple mutant virus were replication competent.

To confirm the presence of the 6xHis tag within both viruses, a Western blot was performed on protein extracted from the infected fungal isolates (Figure 2.10C). In both protein extracts a protein band of approximately 60 kDa was detected, as well as a protein band at approximately 110 kDa. In an effort to molecularly characterize these novel CHV-1 proteins, the 6xHis tagged proteins were purified using cOmplete His tag resin and isolated through a 2D gel (Figure 2.13). Identified spots include CHV-1 protein p29, histone proteins, glyceraldehyde-3-phosphate dehydrogenase

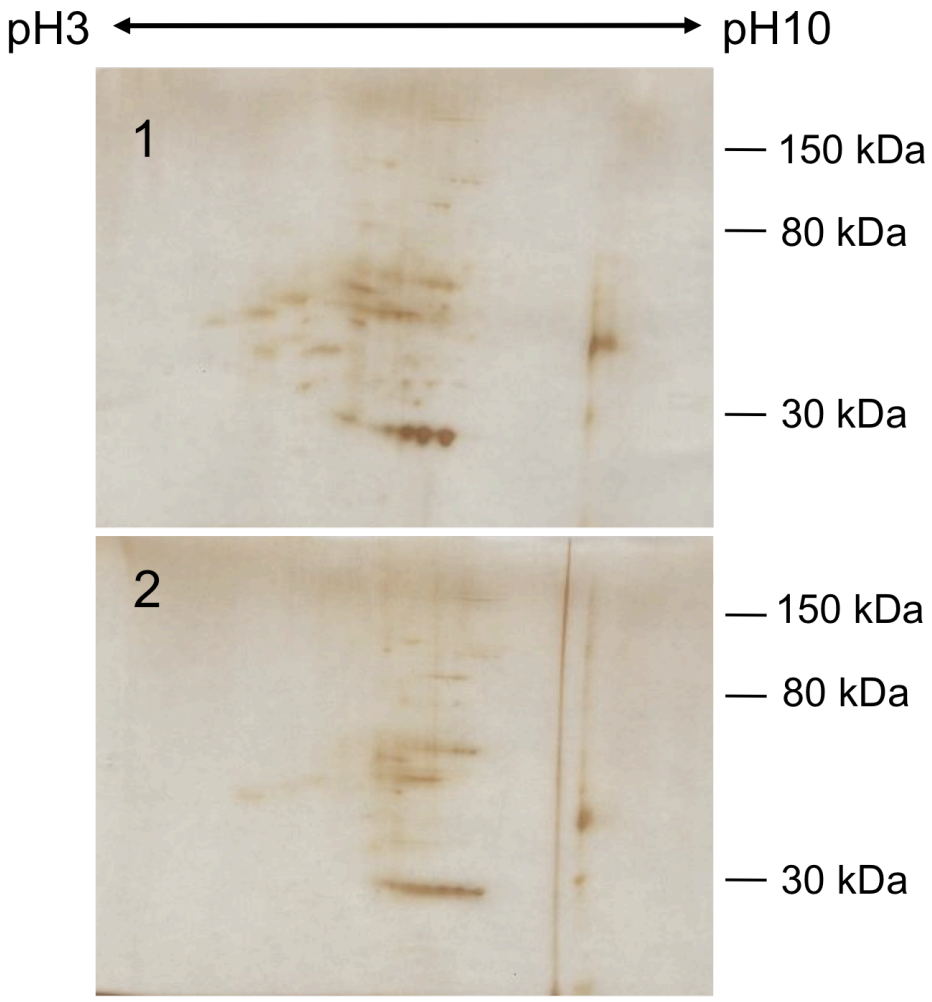

Figure 2.13 – Analysis of novel ORF B protein. 2D gel analysis of purified (1) ORF B-6xHis and (2) p48(341S:388S:418R)/ORF B-6xHis. Purified protein was separated through a 2D gel (10% polyacrylamide), silver stained and spots were picked and subjected to MS/MS and LC/MS. No spots were identified as corresponding to the region directly downstream of p48.

(GAPDH), elongation factor 1-alpha (eEF1a), and pyruvate kinase, as well as additional hypothetical proteins that have been isolated in *Neurospora crassa*.

Due to the lack of detection of viral proteins corresponding to the anticipated region, a monocystronic CHV-1 virus was generated in an attempt to increase protein accumulation. ORF A of CHV-1/EP713 has previously been shown to be dispensable for virus replication (Suzuki and Nuss, 2002), as along as the first 24 amino acids are present. Using this approach, CHV-1/EP713 WT and p48 triple mutant viruses containing a deletion of ORF A were generated Δp69/ORFB-His and Δp69/p48(341S:388S:418R)-ORFB-His) and synthetic RNAs were transfected into Δ*dcl*2 spheroplasts. Extracted protein was examined by Western blot to confirm the presence of the 6xHis tag; a band of ~60 kDa was visible. The ORF-B-6xHis protein was purified using His tag resin and purified through a 2D gel and silver stained, however, no new spots or spots with increased intensity were identified.

In addition to performing MS/MS and LC/MS, purified protein run through a 2D gel was transferred to a PVDF membrane for N-terminal sequencing. However, due to low levels of protein recovery, there was no detectable protein after staining the membrane with Coomassie Blue (0.1% Coomassie Blue, 40% Methanol, 1% Acetic acid).

2.5 DISCUSSION:

In an effort to determine if the p48 protease activity is required for *in trans* complementation of the CHV-1/Δp48 mutant virus, *in trans* rescue was attempted with p48 containing mutations to the catalytic residues. The results of this study

showed that mutation to either catalytic residue, Cys341 or His388, of the hypovirus-encoded p48 protein eliminated the ability to rescue the CHV-1/Δp48 mutant virus. I also demonstrate that when the catalytic residues are mutated *in cis*, neither residue is required for viral replication. Additionally, the p48/ORF B cleavage site could be mutated individually and in combination with either or both of the p48 catalytic residues without preventing processing. Mutation of these residues does result in a decrease in the efficiency of viral replication, and both viral RNA and protein accumulation in strain EP155 are significantly decreased. These results were surprising and unexpected since it was previously demonstrated *in vitro* that mutation of any of the three sites would prevent the cleavage event from occurring.

The observation that the p48 catalytic residues are required for *in trans* complementation, whereas the same residues are not required for *in cis* replication, raises some interesting points. Either the p48 protein, when supplied *in trans*, is responsible for the cleavage or recruitment of a specific host protein or the mutation of the catalytic residues disrupts the ability of p48 to localize to the site of viral replication. In the former scenario, the mutation of the catalytic residues would not disrupt p48 protein structure, however, would prevent cleavage of a host protein and possibly affect subsequent dissociation between p48 and the substrate protein. If p48 cannot cleave and dissociate from the target host protein, then p48 would not be able to initiate viral replication. In the latter scenario, disruption of the p48 catalytic residues may result in either a faster turnover of mutant p48 compared to WT or p48 may lose the ability to localize to the site of viral replication through either host sequestration or may result in the loss of a function that allows p48 to localize to a

specific site. It would be of interest to place an eGFP or similar fluorescent maker at the N-terminus of WT and mutant p48, expressed *in trans*, and determine if there are any differences in the localization pattern of the two proteins.

The difference in protein accumulation compared to RNA accumulation during infection of the p48 and p29 mutant viruses was quite startling. While RNA levels were reduced approximately 70-80% for the p48 catalytic mutants, protein accumulation was reduced to undetectable levels in strain EP155. In addition, protein accumulation for both mutant p48 and p29 was reduced in the Δ*dcl*2 strain, despite dsRNA levels being comparable to CHV-1/EP713 levels. One possible explanation is that the mutant virus proteins are not as stable as WT proteins and leading to them being targeted for degradation by the host cell. It is also possible that either translation of the viral RNA or maturation of the viral polyprotein is the rate limiting step during replication of the p48 and p29 catalytic mutant viruses. The mutant viruses may not be able to recruit host factors that are required for translation of viral RNA in an efficient manner, leading to a greater decrease in viral protein accumulation.

One intriguing aspect of this study is that and p48/ORF B processing still occurs in the absence of p29, the only other identified viral protease. These results would appear to rule out the possibility that p29 has a role in ORF B processing. One possible explanation is that since hypoviruses do not encode structural proteins and their lifecycle is completely intracellular, these viruses may have initially relied upon a host protease for processing of the CHV-1 ORF B polyprotein and the p48 protease domain evolved as a mechanism to increase viral RNA concentration. Protease p29

may have subsequently arose as the result of a duplication and subsequent divergence from protease p48. This is supported by the observation that p48 cleavage appears to be essential for virus replication, while p69 cleavage is not. While no known host proteases have previously been identified as having a role in viral polyprotein processing, several enveloped viruses use the host protease furin for viral maturation (Löving et al., 2012; Volchkov et al., 1998; Zimmer et al., 2001; Zybert et al., 2008), indicating that viruses have the ability to use a host protease for their own advantage.

It has been previously demonstrated that the Murine Hepatitis Virus (MHV) papain-like proteinase 1 (PLP1) is dispensable for virus replication (Denison et al., 2004) and PLP1 directed cleavage of nonstructural protein 1, nonstructural protein 2, and nonstructural protein 3 is not required for virus replication (Graham and Denison, 2006). Mutation of the catalytic cysteine residue of PLP1 and at the respective PLP1 cleavage sites prevents processing of the viral polyprotein, however, as is observed with the CHV-1 protease mutant viruses, the mutant MHV is still capable of replication, but at much lower levels when compared to WT MHV. Recently, deletion analysis of the two leader papain-like proteases of the Grapevine leafroll-associated virus-2 (GLRaV-2), L1 and L2, indicated that neither protease is required for viral replication. Examination of the GLRaV-2 catalytic residues indicates that L1, but not L2, autocatalytic cleavage is not required for virus replication (Liu et al., 2009). In contrast to these results, the papain-like protease HC-Pro catalytic residues, of Tobacco Etch virus (TEV), are required for viral replication in plant protoplasts (Kasschau and Carrington 1995). Taken together, these results indicate different requirements for viral papain-like proteases of different positive sense RNA viruses.

While it is apparent that not all viruses require a functionally active protease for replication, it is not clear why viruses have evolved different requirements for polyprotein processing. One possible explanation is that some viral proteases evolved as a way for viruses to maximize replication efficiency. This can be further explored by examining the activity of papain-like proteases of other plant and animal ssRNA viruses.

While attempts to identify the p48/ORF B cleavage site *in vivo* were not successful, it was possible to show that specific viral proteins can be isolated through the use of epitope tags and the infected Δ*dcl*2 fungal strain. These results have the ability to allow for future advances in identifying both mature and immature CHV proteins, as well as advancing the current understanding of CHV polyprotein processing.

Despite being able to purify the tagged p48 protein, I was unable to confirm the *in vitro* results (Shapira et al., 1992) that previously mapped the cleavage dipeptide to amino acids Gly418 and Ala419. Purified epitope tagged p48 isolated from the Δ*dcl2* strain, infected with either WT CHV-1/EP713 or CHV-1/p48(C341S:H388S:G418R) was analyzed by MS/MS and LC/MS fragmentation, however the C-terminus of p48 could not be detected which was consistent with the results obtained by Wang and colleagues (2013). Wang and colleagues performed MS/MS on p48 extracted from CHV-1 infected EP155 as well as from *in vitro* expressed p48 and obtained similar results. These results led them to conclude that because regions of the C-terminus of p48 are predicted to be hydrophobic, they may have been lost during the extraction process prior to MS/MS identification.

Moreover, identification of the p48/ORF B cleavage site was attempted by isolating the protein that is directly downstream of p48. Although the novel 60 kDa ORF B protein accumulated to levels that were detectable by Western blot, large enough amount of protein could not be purified to allow for subsequent N-terminal sequencing or mass spectrometry. While the purified protein spotting pattern on the silver stained 2D gel from the CHV-1/ORFB-6xHis and the p48(341S:388S:418R) /ORFB-6xHis viruses are similar, the protein accumulation for the mutant CHV-1 was reduced compared to WT, consistent with the results observed when the tag was placed in WT and mutant p48. MS/MS fragmentation identified several spots around 60 kDa in size, however all proteins were host proteins. One potential explanation is that the viral protein does not accumulate or is quickly turned over during viral replication so that the protein is not detectable by silver stain.

The identification of eEF1a in possible association with the novel 60 kDa CHV-1 protein is quite interesting. eEF1a has been identified as having several functions in addition to binding and delivering aminoacylated tRNAs to the ribosome during translation, including being involved in: protein degradation (Gonen et al., 1994; Hotokezaka et al., 2002), anti-apoptotic response pathways (Ruest et al., 2002; Chang and Wang, 2007), and cytoskeletal regulation (Kim and Coulombe, 2010). Several groups of viruses including members of the families *Tombusviridae*, *Flaviviridae*, *Potyviridae*, *Rhabdoviridae*, and *Picornaviridae* have been shown to interact with eEF1a in a variety of ways (Reviewed in Li et al., 2013). The possible interaction of the novel CHV-1 protein identified in this study with eEF1a could indicate that this protein is involved numerous aspects of virus infection. It would be

of interest to further explore the functions and localization of this novel protein during CHV-1 infection.

Future studies will be directed at identifying differences in the p48/ORF B cleavage dipepetide of WT CHV-1 and the p48 catalytic mutant viruses. Identification of the p48/ORF B cleavage dipeptide in the catalytic mutant viruses will aid identification of the host protease involved in the alternative cleavage event responsible for liberating p48. Further characterization of the p48 catalytic mutant viruses will provide new insight on host contributions to virus replication.

Chapter 3: Mapping of the CHV-1/EP713 p48 Functional Domains

3.1 ABSTRACT:

The papain like protease p48, derived from the N-terminus of the CHV-1/EP713 ORF B was previously shown to be essential for viral replication and can be detected in association with host membranes. In an effort to identify the p48 functional domain(s) that are essential for virus replication and *in trans* complementation, a series of progressive deletions were generated to the N- and C-termini of the p48 coding domain. The results indicate that p48 contains two separate functional domains, where only one domain is sufficient for CHV-1 replication. One domain has been mapped to the last 87 aa of p48, 331-418, the predicted papain-like protease domain. The second functional domain was determined to be in the region between aa 169-302. However, expression of mutant p48, containing only one of the predicted functional domains, was unable to complement the Δp48 mutant virus when provided *in trans*, indicating that both functional domains may be required for rescue of the mutant virus. In addition, the ability of the p48Δ1 virus to become viable when a threoinine was substituted for serine at position 14 suggests that there may be a requirement for threonine at aa position 14 of ORF B. The ability of the CHV-1/EP713 virus to maintain replication competency with only one of the identified domains indicates that there may be a built in redundancy between the two domains.

3.2 INTRODUCTION:

Members of the RNA virus family *Hypoviridae* infect the plant pathogenic fungus *Cryphonectria parasitica*, the causative agent of chestnut blight disease. Hypovirus infection of *C. parasitica* is persistent and results in a stable set of phenotypic modifications, such as a reduction of fungal virulence and sexual and asexual sporulation, but does not cause any observable cytopathic effects or cell death (Nuss, 1992; Nuss 2005; Dawe and Nuss, 2013). The ability of hypoviruses to reduce fungal virulence coupled with the development of a reverse genetics system for several different hypovirus isolates allows for the potential to engineer hypoviruses for enhanced biological control of *C. parasitica*.

Cryphonectria parasitica hypovirus-1/EP713 (CHV-1/EP713), the prototypic hypovirus, has a single strand positive sense 12.7-kb RNA genome that encodes two contiguous open reading frames (ORFs) designated ORF A and ORF B, which contain N-terminal leader proteases p29 and p48, respectively (Choi et al., 1991 and Shapira et al., 1991A, and Shapira and Nuss, 1991). CHV-1 infection results in the rearrangement of intracellular membranes, which have been shown to support viral replication and are in close association with viral dsRNA (Fahima et al., 1993; Suzuki and Nuss 2002). Moreover, both p29 and p48 have been isolated from vesicles that support CHV-1/EP713 replication (Jacob-Wilk et al., 2006; Wang et al., 2013).

CHV-1 protease p48 is believed to be a multifunctional protein, responsible for the cotranslational autocatalytic cleavage of ORF B at Gly418 and Ala419 (Shapira and Nuss, 1991) and has been shown to contribute to suppression of host pigmentation and conidiation (Deng and Nuss, 2008). It has recently been

demonstrated that p48 has a central role in initiation of hypovirus replication. Deletion of p48 from the CHV-1/EP713 infectious cDNA clones, Δp48, resulted in mutant viruses that were unable to establish infection in *C. parasitica* when introduced as DNA form by transformation or as synthetic coding strand transcripts by electroporation. The Δp48 mutant virus could be rescued when p48 was supplied *in trans*, however viral RNA accumulation was reduced by 60% when compared to WT CHV-1/EP713. Once replicating, the Δp48 mutant virus retained replication competence in the apparent absence of p48 following transmission to an untransformed *C. parasitica* isolate and successive subculturing.

The functional domains of the CHV-1/EP713 p29 and p40 proteins have been previously identified through a loss of function/gain of function analysis (Suzuki et al., 1999 and Suzuki and Nuss, 2002). In an effort to gain additional insights into the role of p48 during virus replication, a similar approach was used to map the functional domains of p48. I now report that large regions of the p48 coding domain corresponding to both the N- and C-termini are not required for hypovirus replication. In addition, two potential functional domains were identified; the first located between aa Thr169-Glu302 and the second between aa Thr331-Gly418.

3.3 METHODS:

Fungal Strains and Growth Conditions:

C. parasitica strains EP155 (ATCC 38755) and Δ*dcl*2 (Segers et al., 2007) were used in this study. All fungal strains were maintained on potato dextrose agar (PDA; Difco, Detroit, Mich.) at 22 to 24^{o}C under ambient light.

Cloning and Mutagenesis: (i) Generation of N-terminal and C-terminal Deletions

The construction of specific deletions to the p48 protein within the context of the CHV-1/EP713 infectious cDNA clone, plasmid pRFL4 (Zhang et al., 2013), was facilitated by the use of overlapping Polymerase Chain Reaction (PCR). Using primer sets 1KF/p48Δ1-R and p48Δ1-F/5KR (Appendix 2), PCR was performed to generate two fragments, containing overlapping ends. The two fragments were stitched together by a second round of PCR using primers 1KF and 5KR to create the final deletion fragment. The resulting fragment was ligated into a PCR-blunt vector (Zero-Blunt PCR Cloning Kit; Invitrogen, Carlsbad, Cali.) and individual isolates were sequenced to confirm that the correct mutation was generated. The resulting plasmid, p48Δ1-blunt and plasmid pRFL4, containing a WT cDNA clone of CHV-1/EP713 virus, were digested with restriction enzymes *MreI* (Fermentes, Glen Burnie, MD.) and *NheI* (New England Biolabs (NEB), Ipswich, Mass.) and the resulting p48Δ1-blunt fragment was used to replace the corresponding fragment in WT pRFL4. Individual isolates were sequenced to confirm that the desired deletion was still present and no additional point mutations were accidently generated. The resulting viral cDNA isolate was termed pRFL4(p48Δ1). The previous cloning steps were followed to generate additional pRFL4 cDNA clones containing deletions to either the N-terminus or C-terminus of p48 using primer sets p48Δ2 through p48Δ20 (Appendix 2).

(ii) Generation of p48 Ser-14-Thr Point Mutations

Individual point mutations were introduced at Ser14 in p48 of the cDNA clones pRFL4(p48Δ1), pRFL4(p48Δ2), and pRFL4(p48Δ5). An adapted Quick Change II XL Site Directed mutagenesis (Stratagene, La Jolla, Cali.) protocol, with Phusion High-Fidelity polymerase (NEB) being used in place of *PfuUltra* High-Fidelity polymerase, was used to introduce the S14T mutation into each cDNA clone. Briefly, primer sets p48Δ1(T), p48Δ2(T) and p48Δ5(T) were used to perform PCR on plasmids pRFL4(p48Δ1), pRFL4(p48Δ2), and pRFL4(p48Δ5). The PCR product was digested with *DpnI*, ligated and transformed into Top10 cells (Invitrogen). The resulting plasmids pRFL4(p48Δ1T), pRFL4(p48Δ2T), and pRFL4(p48Δ5T) were sequenced to confirm that the desired mutation was present.

(iii) Generation of Gain of Function Mutants

To construct pRFL4 cDNA clones containing deletions to both the N-terminus and C-terminus of p48, primer set p48Δ4 or p48Δ6 was used with plasmids pRFL4(Δ12), pRFL4(Δ13), pRFL4(Δ14), pRFL4(Δ15) and primer set p48Δ15 was used with plasmids pRFL4(p48Δ1T), pRFL4(p48Δ2T), pRFL4(p48Δ3), and pRFL4(p48Δ4). Using the procedures previously described, overlapping PCR was used to generate plasmids pRFL4(p48Δ1T/Δ15), pRFL4(p48Δ2T/Δ15), pRFL4(p48Δ3/Δ15), pRFL4(p48Δ4/Δ15), pRFL4 (p48Δ6/Δ15), pRFL4(p48Δ4/Δ12), pRFL4(p48Δ4/Δ13), pRFL4(p4846/Δ14), pRFL4(p48Δ6/Δ12), pRFL4(p48Δ6/Δ13), pRFL4(p48Δ6/Δ14).

(iv) Mutagenesis of Potential Functional Domains

Point mutations were introduced at amino acid position Glu302Ala, Glu303Ala, Glu337Ala, and Glu338Ala of protease p48 using the adapted Quick Change II XL protocol previously described. Briefly, using primers p48EE302/303AA-F and p48EE302/303AA-R (Appendix 2) PCR was performed on plasmids pRFL4 and pRFL4(p48Δ3/Δ15), digested with *DpnI* (NEB), ligated and transformed into Top10 cells. The resulting plasmids were sequenced to confirm the presence of the mutations, and then subjected to a second round of mutagenesis using primer set p48EE337/338AA-F and p48EE337/338AA-R. The resulting plasmids were sequenced to confirm the presence alanine at positions 302, 303, 337, and 338.

Transfection of Δ*dcl*2 Spheroplasts:

Mutant virus pRFL4 plasmids, all of which have the T7 RNA polymerase promoter upstream of the CHV-1/EP713 5'-noncoding sequence, were utilized as a template for *in vitro* RNA synthesis with the T7 RNA polymerase after linearization with restriction enzyme *SpeI* (NEB). Reaction conditions followed manufacturer's recommendations (Ambion, Life Technologies, Carlsbad, Calif.). The synthetic plus-sense transcripts were extracted with phenol, precipitated with ethanol, transfected by electroporation (Chen, Choi, and Nuss, 1994) into *C. parasitica* Δ*dcl*2 spheroplasts, using a Gene Pulser II system electroporator (Bio-Rad Laboratories, Hercules, Calif.). Surviving spheroplasts were cultured on high osmotic solid regeneration media for 10 days to allow cell wall formation and movement of replicating viral RNA through the regenerated mycelia and then transferred to PDA (Difco) plates for phenotypic

measurements and to potato dextrose broth (PDB; Difco) for nucleic acid and protein isolation.

Total RNA Extraction:

C. parasitica strains were grown in 200 ml of PDB for 7 days and harvested by filtration through Miracloth (Calbiochem, La Jolla, Calif.), and homogenized with a mortar and pestle in the presence of liquid nitrogen.

Nucleic acids were isolated by two rounds of phenol-chloroform extraction in 4 ml of 100 mM Tris-HCL (pH 8.0), 200 mM NaCl, 4 mM EDTA, 4% sodium dodecyl sulfate and then precipitated by the addition of 2 volumes of ethanol. The extracted nucleic acid samples were treated with RQ1 DNase I (Promega, Madison, Wis.) to elimate fungal chromosomal DNA, followed by 2 rounds of phenol-chloroform extractions and precipitation with ethanol. Total RNA concentration was measured using a NanoDrop 1000 spectrophotometer (Thermo Scientific, Wilmington, Del.).

3.4 RESULTS:

N-terminus Deletion Mutants:

The objective of these studies was to identify the functional domain(s) of the CHV-1 p48 protein. It has been previously shown that the p48 protein can act *in trans* to rescue a CHV-1 Δp48 mutant virus, suggesting that p48 is involved in a critical stage of viral replication (Deng and Nuss, 2008). Furthermore, once rescued the Δp48 mutant virus can continue to replicate in the absence of p48. To better understand the role of p48 in CHV-1/EP713 replication and in an effort to

identify the functional domain(s) of p48 that contribute to viral replication, we made a series of deletions starting at aa Arg13. The first 13 codons were not involved in the deletion analysis due to the potential requirement for secondary RNA structure involvement in the ORF A/ORF B stop/go translation mechanism. The initial p48 deletion was generated from Arg13 to Ser73, and additional deletions were generated approximately every 50 aa. In WT CHV-1/EP713, the codon corresponding to aa 14 encodes threonine, so all CHV-1 p48 deletion mutants were designed to maintain the presence of a threonine at this position; when that was not possible, a serine was exchanged for threonine at aa 14 (Figure 3.1). A total of nine CHV-1 p48 deletion mutant viruses were constructed (CHV-1/p48Δ1 thru CHV-1/p48Δ9). To determine the ability of each p48 deletion mutant virus to establish an infection, synthetic transcripts were electroporated into virus-free *C. parasitica* strain Δ*dcl*2 spheroplasts (Segers et al. 2007). Transfection results indicate that the CHV-1/p48Δ2, CHV-1/p48Δ3, CHV-1/p48Δ4, and CHV-1/p48Δ6 deletion mutant viruses were able to replicate (Figure 3.2A). However, it was apparent that the p48 mutant viruses that contained a serine at position 14 either did not replicate, CHV-1/p48Δ1 and CHV-1/p48Δ5, or viral dsRNA did not accumulate to levels consistent with p48 mutant viruses with threonine in position 14, CHV-1/p48Δ2 versus CHV-1/p48Δ3, CHV-1/p48Δ4, and CHV-1/p48Δ6 (Figure 3.2B). This was of particular interest because these results were independent of and did not correlate with the size of the deletion within p48.

The presence of a serine at aa position 14 appeared to correspond with a decrease in viral RNA accumulation or lack of ability to replicate when compared to

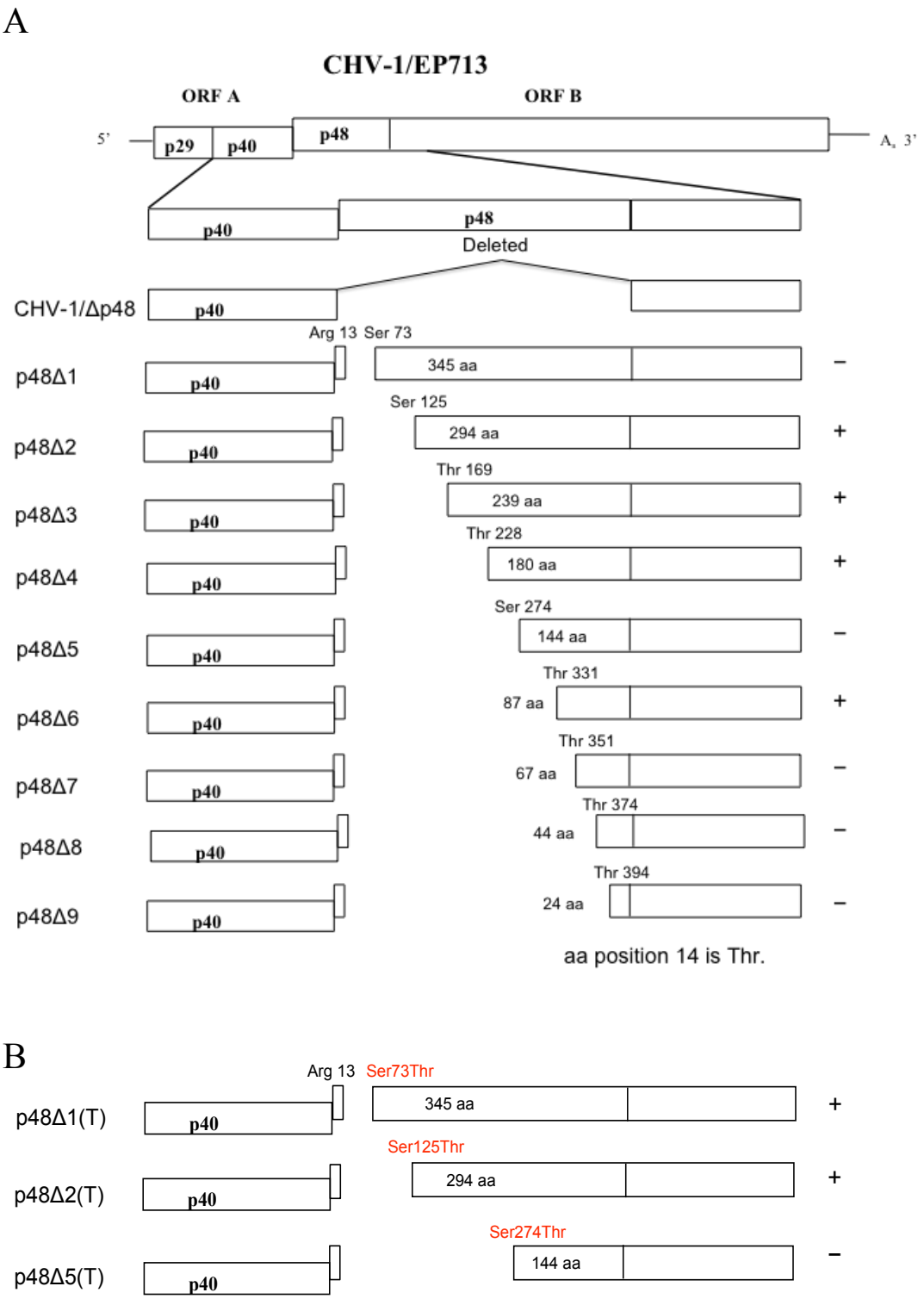

Figure 3.1 – Diagram showing the organization of p48 mutant viruses. (A) The genetic organization of the CHV-1/EP713 virus is shown at the top. The p48 deletion

mutant viruses are shown below the wild-type virus. All mutant viruses were generated through overlapping PCR, digested with *MreI* and *NheI* restriction enzymes and the resulting fragment was used to replace the corresponding region within the CHV-1/EP713 infectious cDNA clone, pRFL4. A series of nine mutant viruses, containing deletions extending from Arg13 through Thr394 were generated. These mutant viruses were transfected into Δ*dcl*2 spheroplasts to map the functional region of p48. (B) Mutant viruses p48Δ1(T), p48Δ2(T), and p48Δ5(T) included the same deletion fragment as the p48Δ1, p48Δ2, p48Δ5 viruses, however, the serine at aa 14 was replaced with threonine, which is present in WT CHV-1/EP713. The + indicates that the virus was replication competent and the − indicates that the virus was not able to initiate replication.

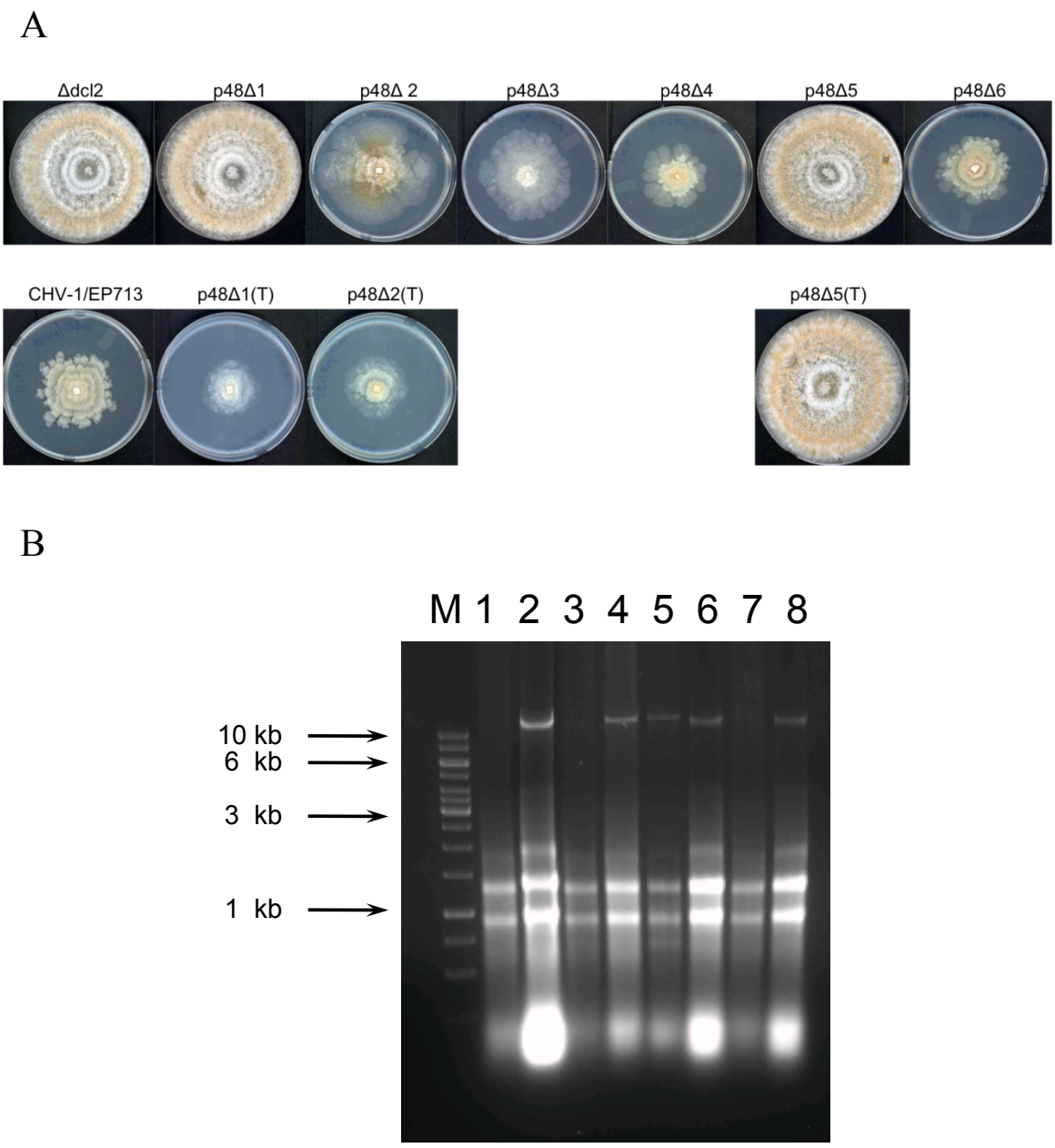

Figure 3.2 – Transfection of Δ*dcl*2 with p48 deletion mutant viruses. (A) Phenotype of Δ*dcl*2 *C. parasitica* colonies infected with p48 deletion mutant viruses. Spheroplasts of *C. parasitica* strain Δ*dcl*2 were transfected with synthetic transcripts derived from WT virus (CHV-1/EP713) and each of the mutant virus cDNA plasmids. Note that the virus-infected colonies had a slower growth rate and irregular

margins when compared to uninfected colonies. Fungal colonies were photographed after culturing on PDA plates for 7 days.

(B) Agarose gel electrophoretic analysis of total RNA isolated from *C. parasitica* colonies, transfected with p48 deletion mutant viruses. Equal amounts of total RNA extracted from Δ*dcl*2 isolates were loaded into each lane (3µg); uninfected (lane 1), CHV-1/EP713 (lane 2), p48Δ1 (lane 3), p48Δ2 (lane 4), p48Δ3 (lane 5), p48Δ4 (lane 6), p48Δ5 (lane 7), and p48Δ6 (lane 8).

the other p48 deletion mutant viruses. In the three mutant viruses that contained serine at aa position 14, p48Δ1, p48Δ2, and p48Δ5, a threonine was substituted for serine in an effort to restore viral replication. Transfection results indicate that the CHV-1/p48Δ1(T) virus was replication competent, and the CHV-1/p48Δ2(T)replicated to levels comparable to the other deletion viruses (CHV-1/p48Δ3, CHV-1/p48Δ4, and CHV-1/p48Δ6). However, replication was not restored for the CHV-1/p48Δ5(T) mutant virus.

In order to determine if threonine at aa position 14 is important for phosphorylation of the p48 protein, an aspartic acid or glutamic acid was substituted for threonine at position 14 within the p48Δ1 mutant virus. The substitution of aspartic acid or glutamic acid supply a negative charge, simulating a phosphorylated residue. Introduction of synthetic RNAs corresponding to cDNAs encoding the p48Δ1(14D) and p48Δ1(14E) mutant viruses into Δ*dcl*2 spheroplasts failed to initiate viral replication (Data not shown), indicating that the importance of threonine at aa position 14, may not be related to phosphorylation of p48 at this position.

The p48 deletion analysis results indicate that the region between aa 13-330 can be deleted without abolishing viral replication. Efforts to generate further deletions past aa 331, into the protease region of the protein were attempted. Three additional deletion viruses were constructed, CHV-1/p48Δ7 (deletion of aa 14-350), CHV-1/p48Δ8 (deletion of aa 14-373), and CHV-1/p48Δ9 (deletion of aa 14-393) and transfected into EP155 and Δ*dcl*2 spheroplasts (Figure 3.1). Transfection results indicate that these viruses did not replicate and no viral RNA was detected.

C-terminus Deletion Mutants:

The ability to delete aa 14-330 of p48 without disrupting viral replication indicates that the region containing the p48 protease domain is necessary for viral replication, despite that fact that the protease catalytic residues themselves are not essential for replication (Chapter 2). In an effort to determine the location of the functional domain at the C-terminus of p48, a series of deletion mutants were generated starting with the region corresponding to aa 399-414, and progressively moving towards the N-terminus (Figure 3.3A). In total 11 deletion mutants were generated covering the region from aa ASP52 to ASP414.

C. parasitica Δ*dcl*2 spheroplasts were transfected with synthetic RNA transcripts corresponding to the 11 C-terminal CHV-1 deletion mutant viruses. Transfection of CHV-1 p48 deletion viruses p48Δ11 thru p48Δ16 resulted in a phenotypic change indicating viral replication and was accompanied by the presence of viral RNA (Figure 3.3B). Reverse transcription-PCR (RT-PCR) and nucleotide sequencing confirmed the deletion of the specified regions. These results indicate that residues 306-414 are also dispensable for CHV-1/EP713 replication. These results appear to be in contradiction to the p48 N-terminal deletion mutants, which suggested that aa 330-418 are essential CHV-1 replication. Taken together, the N- and C-terminal deletion results indicate that p48 has two functional domains, where only one domain is necessary for viral replication.

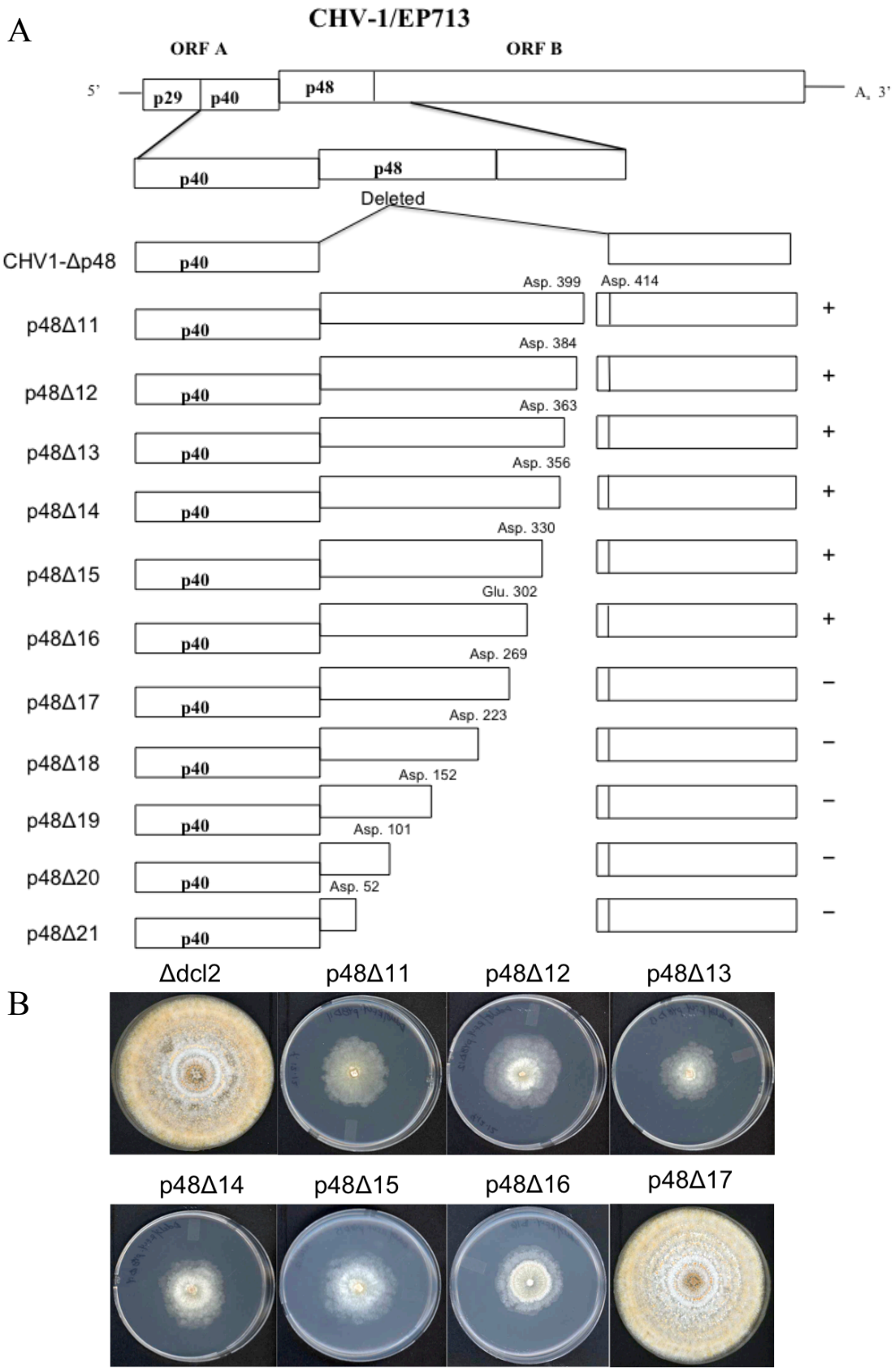
A
CHV-1/EP713
ORF A
ORF B
5'
p29
p40
p48
A, 3'
p40
p48
Deleted
CHV1-Δp48
p40
Asp. 399
Asp. 414
p48Δ11
p40
+
Asp. 384
p48Δ12
p40
+
Asp. 363
p48Δ13
p40
+
Asp. 356
p48Δ14
p40
+
Asp. 330
p48Δ15
p40
+
Glu. 302
p48Δ16
p40
+
Asp. 269
p48Δ17
p40
−
Asp. 223
p48Δ18
p40
−
Asp. 152
p48Δ19
p40
−
Asp. 101
p48Δ20
p40
−
Asp. 52
p48Δ21
p40
−
B
Δdcl2
p48Δ11
p48Δ12
p48Δ13
p48Δ14
p48Δ15
p48Δ16
p48Δ17

Figure 3.3 – Replication competency of p48 C-terminus deletion mutants. (A) Diagram showing the organization of p48 C-terminus deletion mutant viruses. The last 5 aa of the C-terminus of p48 were left intact so as not to disrupt any potential p48/ORF B cleavage events from occurring. (B) Colony morphology of Δ*dcl*2 *C. parasitica* colonies infected with C-terminus p48 mutant viruses. Fungal colonies were photographed after culturing on PDA plates for 7 days. The p48Δ17 fungal isolate is representative of the p48Δ18, p48Δ19, p48Δ20, and p48Δ21 fungal isolates, indicating that these viruses did not replicate. These results provide evidence that aa 303-414 of p48 are not essential for virus replication. The + indicates that the virus was replication competent and the − indicates that the virus was not able to initiate replication.

Fine mapping of the p48 functional domains

The ability of the CHV-1 mutant viruses to replicate with deletions to either the N-terminus or the C-terminus of p48, suggests the possibility that p48 contains two independent but redundant functional domains. To further investigate this possibility, a CHV-1 mutant virus was constructed containing deletions to both the N- and C-termini of p48 (CHV-1/EP713 (p48Δ6Δ15) (Figure 3.4A). Transfection of the corresponding RNA transcripts into Δ*dcl*2 spheroplasts failed to initiate virus replication and no phenotypic changes were observable, and no viral dsRNA was detected, providing further evidence that there are functional domains at the N-terminus and C-terminus of p48 (Figure 3.4C).

In order to confirm these results, a gain of function strategy, which was used to successfully map the p29 (Suzuki et al. 1999) and p40 (Suzuki et al et al. 2002) functional domains, was employed. The p48Δ6Δ15 mutant protein was progressively repaired toward the N-terminus and RNA transcripts corresponding to the resulting 4 constructs were transfected into Δ*dcl*2 spheroplasts (Figure 3.4A). Transfection of p48Δ3Δ15 and p48Δ2Δ15 mutant viral synthetic RNA transcripts into Δ*dcl*2 spheroplasts resulted in colonies with a delayed growth rate, reduction in pigmentation, and irregular margins, indicating that these two mutant viruses were capable of replication and viral replication was confirmed by the recovery of viral RNA and RT-PCR. These results demonstrate that extension of the p48 coding domain from Thr228 to Thr169 restored viral replication, leading to the conclusion that one of the p48

A

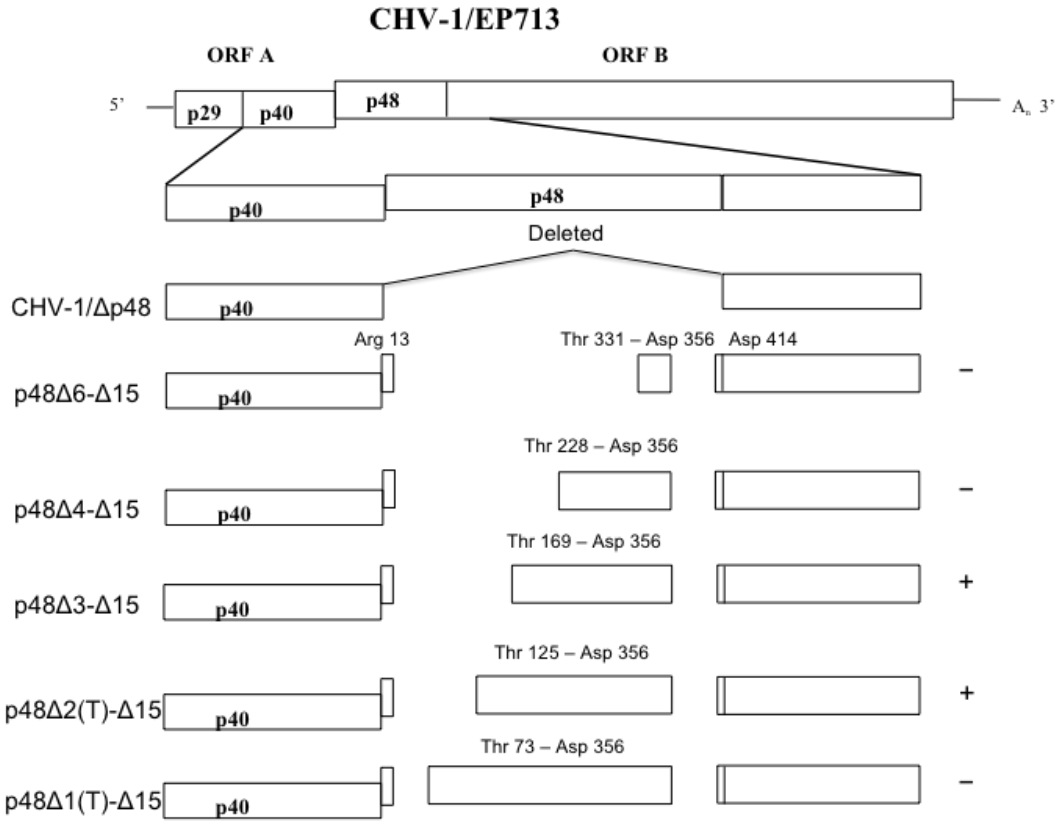
CHV-1/EP713
ORF A
ORF B
5'
p29
p40
p48
A$_n$ 3'
p40
p48
Deleted
CHV-1/Δp48
p40
Arg 13
Thr 331 – Asp 356
Asp 414
p48Δ6-Δ15
p40
−
Thr 228 – Asp 356
p48Δ4-Δ15
p40
−
Thr 169 – Asp 356
p48Δ3-Δ15
p40
+
Thr 125 – Asp 356
p48Δ2(T)-Δ15
p40
+
Thr 73 – Asp 356
p48Δ1(T)-Δ15
p40
−

B

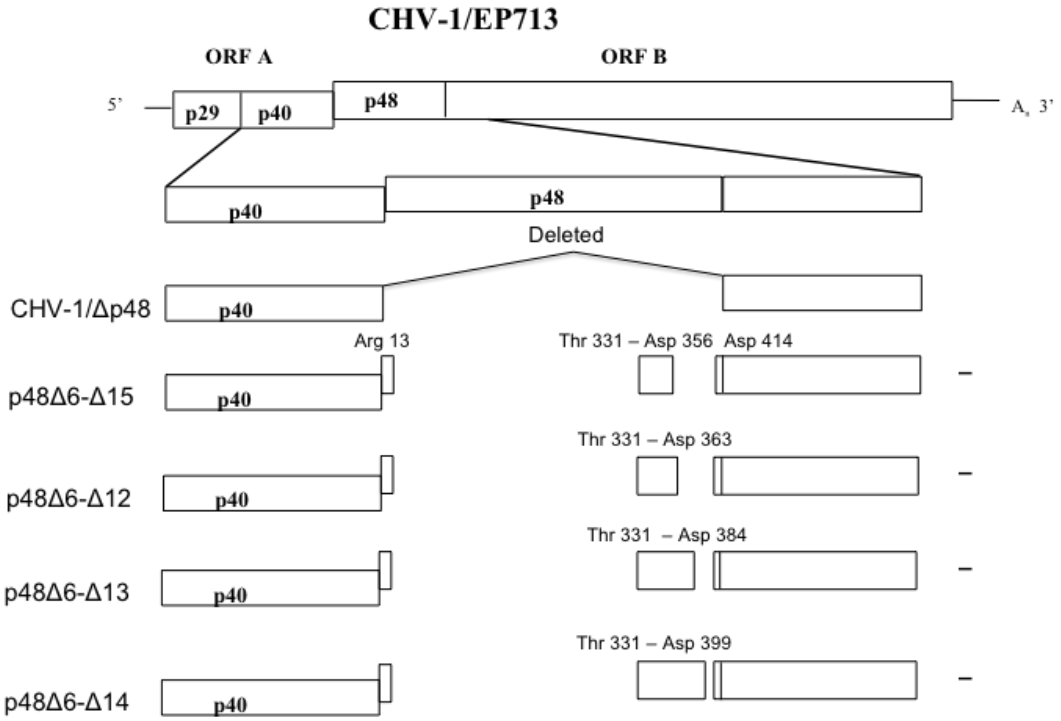
CHV-1/EP713
ORF A
ORF B
5'
p29
p40
p48
A$_n$ 3'
p40
p48
Deleted
CHV-1/Δp48
p40
Arg 13
Thr 331 – Asp 356
Asp 414
p48Δ6-Δ15
p40
−
Thr 331 – Asp 363
p48Δ6-Δ12
p40
−
Thr 331 – Asp 384
p48Δ6-Δ13
p40
−
Thr 331 – Asp 399
p48Δ6-Δ14
p40
−

C

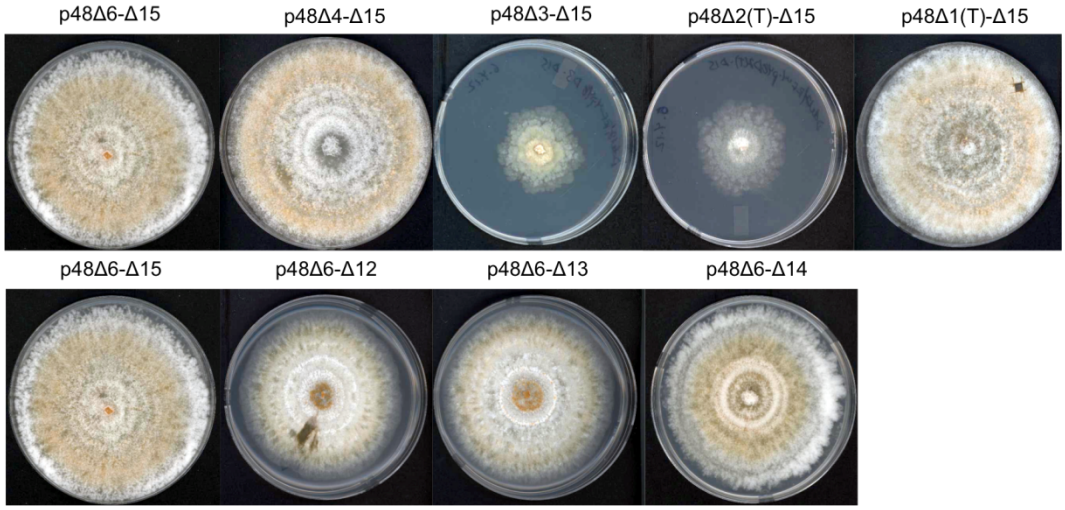

Figure 3.4 – CHV-1 p48 gain of function mutants. (A) CHV-1 p48 N-terminus gain of function mutants. The N-terminus of the non-viable CHV-1/p48Δ6-Δ15 mutant virus was progressively repaired. Spheroplasts of *C. parasitica* strain Δ*dcl*2 were transfected with synthetic RNA transcripts derived from the p48 mutant cDNA plasmids. (B) CHV-1 p48 C-terminus gain of function mutants. The C-terminus of the non-viable CHV-1/p48Δ6-Δ15 was progressively repaired. Spheroplasts of *C. parasitica* strain Δ*dcl*2 were transfected with synthetic RNA transcripts derived from the p48 mutant cDNA plasmids. (C) Phenotype of Δ*dcl*2 *C. parasitica* colonies infected with CHV-1 p48 N-terminus and C-terminus gain of function mutant viruses. Isolates transfected with p48Δ3-Δ15 and p48Δ2(T)-Δ15 mutant viruses produced a phenotype similar to that of CHV-1/EP713. Fungal colonies were photographed after culturing on PDA plates for 7 days. For figures A and B, the + indicates that the virus was replication competent and the − indicates that the virus was not able to initiate replication.

functional domains can be defined within the region extending from Thr169 to Glu302.

To map the C-terminal functional domain, the CHV-1/EP713(p48Δ6Δ15) mutant virus was progressively repaired toward the C-terminus (Figure 3.4B). Synthetic transcripts of the resulting 3 constructs (p48Δ6Δ12), (p48Δ6Δ13), and (p48Δ6Δ14) were transfected into Δ*dcl*2 spheroplasts. All 3 of the mutant viruses failed to replicate, indicating that in the absence of the N-terminal region (aa 14-330), the whole C-terminal region (331-418) is essential for viral replication (Figure 3.4C).

Mutagenesis of Short-Repeated Amino Acid Domains

In an effort to further map potential functional domains essential for virus replication, we identified two regions within p48 that have a similar repeated sequence, from aa 299 to 305 and from 334 to 340 (VPMEEAK and VPVEEGR respectively) (Figure 3.5A). To further investigate these regions glutamic acid at positions 302, 303 and 337, 338 were mutated to alanine within context of the WT CHV-1/EP713 virus and the CHV-1/p48Δ3Δ15 mutant virus (Figure 3.5B). Synthetic RNA transcripts derived from CHV-1/EP713 (EE302/337AA) and CHV-1/p48Δ3Δ15(EE302/337) cDNA plasmids were introduced into Δ*dcl*2 spheroplasts through electroporation.

Recovered isolates displayed a phenotype similar to CHV-1/EP713, including reduced growth rate, loss of pigmentation, and irregular margins (Figure 3.5C). Isolated viral RNA was subjected to RT-PCR and sequenced and the presence of the Glu → Ala mutations was confirmed. These results indicate,

A


169
TAQVSVAKLEWPPLPIIQAQ
PTILAGIIDNFKICFPVNGKW
IYGQGLSWTRYDGDASVPT
SLLSNRQHARFWNEKDIPT
GLKLSKEGFIKLWAQKSRK
WQDHMARSIGLSHEAAVEL
VRATRVNEAKPHLVPMEEA
KEAPRQQLVPRRSTFVDNH
EEEVEIDTLRVPVEEGRCFE
L L F N N Q V T P A I F D
356

B

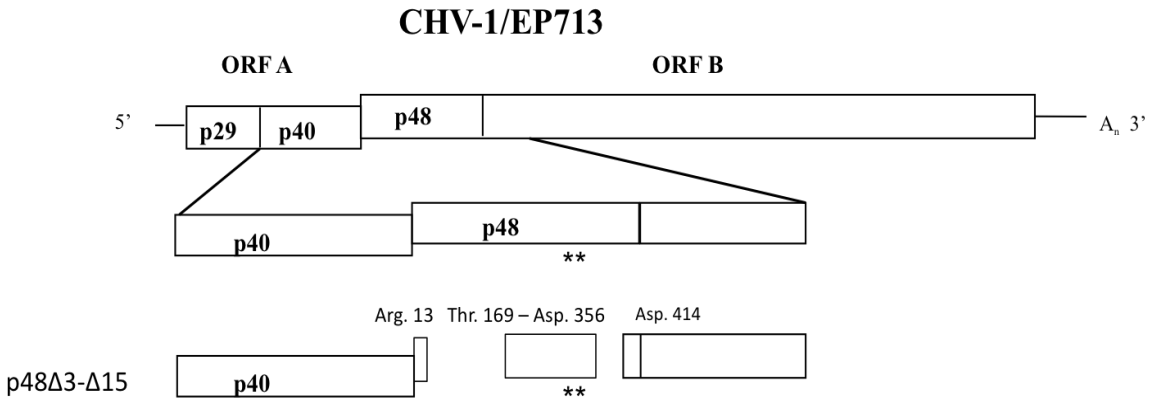
CHV-1/EP713
ORF A
ORF B
5'
p29
p40
p48
A$_n$ 3'
p40
p48
**
Arg. 13
Thr. 169 – Asp. 356
Asp. 414
p48Δ3-Δ15
p40
**

C

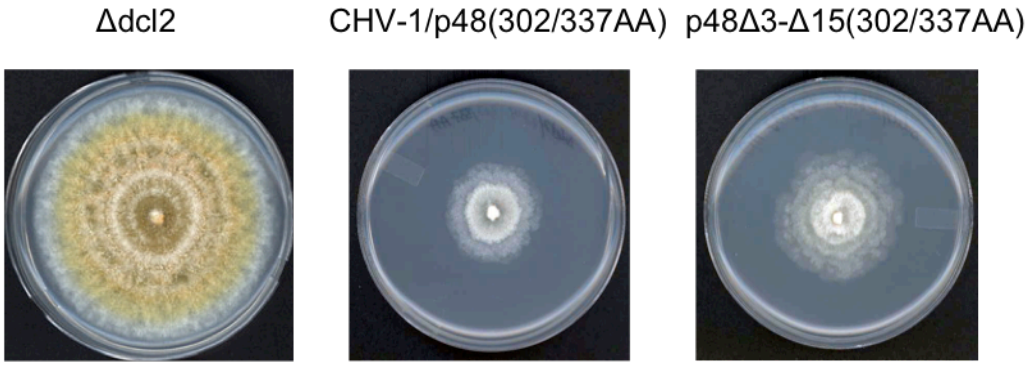

Figure 3.5 – Disruption of repeated sequences within potential p48 functional domains. (A) Analysis of p48 amino acids between Thr169 and Asp356. Two specific sequences, amino acids 299-305 and 334-340 (red sequences), were identified that appear to be repeats. Amino acids Glu302, Glu303, Glu337, Glu338 (underlined) were mutated to Ala in CHV-1/EP713 and mutant virus p48Δ3-Δ15. The p48 protease catalytic residue Cys341 is marked in blue and underlined (B) Diagram of the two potential repeated sequence functional domains within WT CHV-1 p48 coding domain and within mutant virus p48Δ3-Δ15. The domains are indicated by the astrick (*). (C) Synthetic RNA transcripts of the CHV-1/p48(302/337AA) and p48Δ3-Δ15(302/337AA) mutant cDNA plasmids were transfected into Δ*dcl*2 spheroplasts. Fungal colonies transfected with mutant viruses displayed a slower growth rate, loss of pigmentation, and irregular margins when compared to uninfected colonies

that despite the presence of these unique repeated sequences, they are not essential for viral replication.

Rescue of the CHV-1/Δp48 Mutant Virus

It has been previously reported that when supplied *in trans*, p48 has the ability to rescue a p48 deficient virus, CHV-1/Δp48 (Deng and Nuss, 2008). In an effort to better understand the role of p48 in CHV-1 replication, and to determine if either functional domain was involved in the rescue of the CHV-1/Δp48 virus, it was of interest to attempt to compliment the replication deficient Δp48 mutant virus *in trans* with p48Δ6, p48Δ15, and p48Δ3Δ15. Putative mutant p48 transformants were screened by RT-PCR in place of Western blot analysis due to a lack of epitopes on the mutant p48 and an expression level that is expected to be approximately 400-fold less than observed in CHV-1 infection (Deng and Nuss, 2008). Introduction of RNA transcripts of the Δp48 mutant virus into the p48 transformants failed to establish an infection. Mycelia formed by the transfected p48 transformant spheroplasts on transfection regeneration medium exhibited morphology typical of uninfected WT *C. parasitica* (Figure 3.6) and no viral dsRNA was detected. These results suggest that only one of the two functional domains is insufficient for *in trans* rescue of the Δp48 mutant virus. Future studies will examine the ability of a mutant p48 protein, containing a deletion of aa 14-168, but preserving both predicted functional domains, to complement the CHV-1/Δp48 mutant virus.

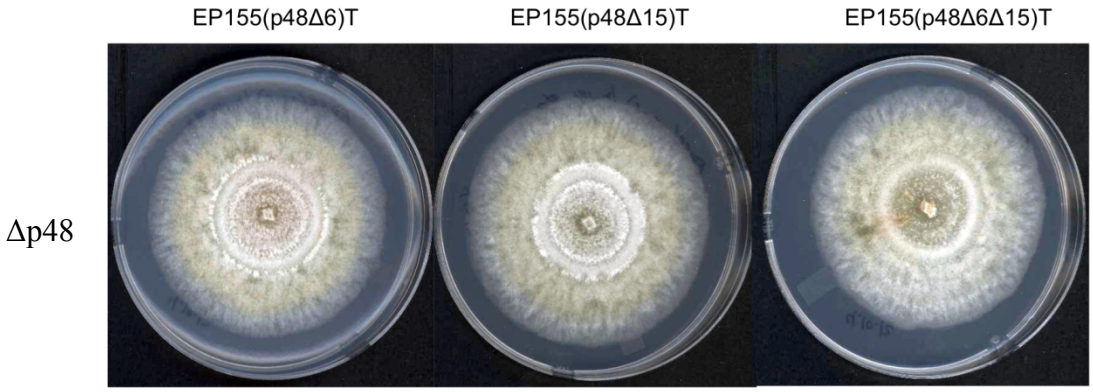

Figure 3.6 – *In trans* complementation of the Δp48 mutant virus with mutant p48. Fungal strain EP155 was transformed with wild-type p48, as well as with p48 containing deletions to aa 14-330 (p48Δ6-T), aa 331-413 (p48Δ15) and aa 14-168 and 357-413 (p48Δ3Δ15). Spheroplasts were transfected with RNA transcripts corresponding to the Δp48 mutant virus. *C. parasitica* transformant strains expressing mutant p48 were unable to rescue the Δp48 mutant virus and displayed phenotypes similar to uninfected EP155 (Figure 2.1B).

DISCUSSION:

As previously discussed in Chapter 1, the CHV-1 p48 protein, unlike p29 and p40, is required for initiation of CHV-1 replication, however the underlying mechanisms by which p48 contributes to replication are not understood. In an effort to map the p48 functional domains, a series of deletion mutant viruses were generated and transfected into Δ*dcl*2 spheroplasts. The results indicate that large portions of the N-terminus and C-terminus can be deleted independently of each other as well as in combination, from the CHV-1 p48 coding domain, while still allowing viral replication to occur. It was determined that the last 87 aa of the p48 coding domain are essential for CHV-1 replication in the absence of the N-terminus, and the first 302 aa are essential in the absence of the C-terminus (Figure 3.7). Moreover, smaller sections of the N-terminus and C-terminus, aa 14-168 and 357-413, could be deleted from within the p48 coding domain of the same virus.

These results support a hypothesis that p48 contains 2 separate functional domains where either of these domains have a redundant function and only one domain is essential for virus replication. The first identified functional domain appears to between residues 330-418, named Domain 2 (D2). Attempts to generate mutant viruses containing a deletion to different regions within the 330-418, in the absence of residues 14-330, resulted in all viruses being non-viable, indicating that this whole region contains a functional domain (Figures 3.4B, 3.4C, and 3.7). The second identified functional domain can be

A

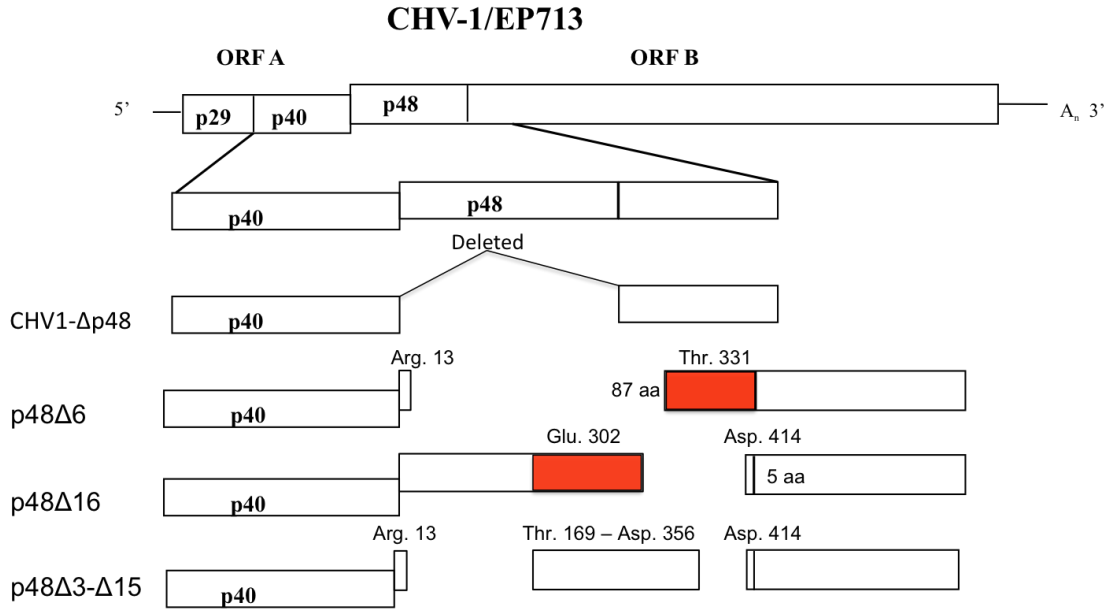

B

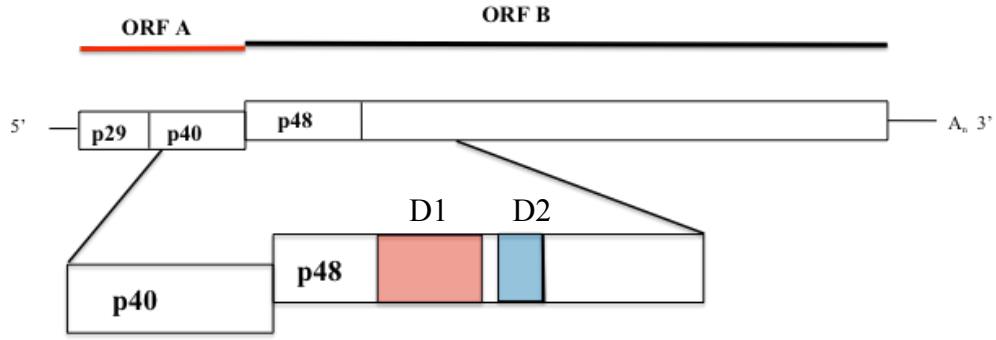

MYKEAERPIE VWRTQVMDGP TWTALSESCRDRLFFASGEGGEHMTLDIIQPDSYTKIRLF
RSGRFEVSVD GKSFGQGGNRYRFVFRYDSLLSTPFGYPAEDKEIALQDYNHKQLLGEMFL
KLPDSYVDGR PIAEAFFRYV DDLKWDVGVFRDRRSLTELHLPASSGLTTAQVSVAKLEWP
PLPIIQAQPT ILAGIIDNFK ICFPVNGKWI YGQGLSW TRYDGDASVPTSL LSNRQHARFW
NEKDIPTGLK LSKEGFIKLWAQKSRKWQDHMARSIGLSHEAAVELVRATR VNEAKPHLVP
MEEAKEAPRQ QLVPRRSTFVDNHEEEVEIDTLRVPVEEGR CFELLFNNQV TPAIFDKKPL
LKDVLGVFEE NVCTMDSLEI SHSDQCVHIV AGETFRNYDE IKAVLEVILE NEPDILVG

Figure 3.7 – Map of potential p48 functional domains. Deletion analysis demonstrated that in the absence of the N-terminus, the last 87 aa are essential

for virus replication. Any attempt to alter the C-terminus resulted in non-viable virus, indicating that one functional domain resides between aa Thr331 and Gly418, the p48/ORF B cleavage residue. Moreover, the second functional domain appears to be located between aa Thr169 and Glu302. Deletion past Glu302 resulted in nonviable virus, and virus replication in the double deletion mutant was restored once the internal aa fragment was extended to Thr162. (B) The p48 aa sequence with the predicted functional domains highlighted. Domain 1 (D1) is highlighted in red and Domain 2 (D2) is highlighted in blue.

mapped to the region between aa Thr169 and Glu302, termed Domain 1 (D1) (Figure 3.7). The approximate carboxy terminus of D1 was determined by generating deletions to the C-terminal region of p48. Attempts to generated deletions into the region upstream of Glu302 resulted in non-viable virus (Figure 3.3) indicating that this region is necessary for virus replication in the absence of residues 331-418. The N-terminus of the functional domain was mapped through a gain of function assay, in which the C-terminal functional domain was disrupted and the N-terminus was progressively repaired and examined to determine if the mutant viruses gained the ability to replicate. The deletion virus gained the ability to replicate once the p48 N-terminal region was extended to amino acid Thr169, indicating that one of the functional domains had been repaired.

Recently, the streptococcal C1 phage lysine PlyC X-ray crystal structure was solved and shown to contain separate catalytic domains, where only one domain was required for bacterial cell lysis. Crystal structure of the PlyC subunit, PlyCA, was determined to have two functional domains, a cysteine, histidine-dependent amidohydrolase/peptidase (CHAP) domain, where a catalytic cysteine and histidine are responsible for amidase catalytic activity, at the C-terminus and a glycosyl hydrolase (GyH) domain located at the N-terminus (McGowan et al., 2012). McGowan and colleagues (2012) demonstrated that while mutation of the CHAP domain or the GyH domain reduced lytic activity, the lysine remained functional. It is currently unclear if the two domains work in a synergistic manner, where both cleave the respective substrate at the same time

or if they work cooperatively, where one domain is active while the other is silent, and vice versa.

The requirement for only one domain to remain functionally intact for p48 and PlyCA to remain active is not completely understood. While both of the PlyCA domains were demonstrated to be catalytic domains, there is no evidence that the p48 D1 has a catalytic function, indicating that the redundancy between D1 and D2 may be restricted to another aspect of viral replication, such as interaction with host membranes or recruitment of host proteins essential for replication. One possible explanation for the presence of the redundant domains within p48, is that they provide an evolutionary advantage. During hypovirus replication DI RNAs are generated due the host RNA silencing response. One possible explanation is that the DI RNAs have the ability to express proteins during viral infection. While this has not been formally demonstrated, the DI RNAs are derived from the CHV-1 genome and are generated by internal deletion events (Shapira et al., 1991B) therefore, any proteins generated from DI RNAs would be expected to be truncated forms of the WT protein. Recently, Wang and colleagues (2013) identified 30 kDa and 28 kDa proteins isolated from EP155, by MS/MS, and determined that these proteins were isoforms of p48, however they were missing the first 219 amino acids from the N-terminus. While it is not known if these truncated proteins are functional or to the extent that they accumulate in the infected cell, it would not be surprising if CHV-1 viruses evolve protein domains that can function independently of each other;

thereby, if one domain, such as D1, is deleted or disrupted in a truncated protein, the other domain, D2, remains functional.

The apparent requirement of a threonine at amino acid 14 and the inability to substitute serine at this position is quite puzzling. Threonine and serine are both polar amino acids and are the only amino acids containing a hydroxyl side group. The requirement for threonine at this position could indicate that amino acid 14 is a site of post-translational modification, either phosphorylation or glycosylation. Wang and colleagues (2013) have recently demonstrated that different isoforms of p48 isolated from CHV-1 infected EP155, and have predicted that p48 is phosphorylated during CHV-1 infection. However, attempts to mutate Thr14 to negatively charged residues, either aspartic acid and glutamic acid in the p48Δ1 mutant virus, to mimic a phosphorylated residue resulted in non-viable virus. These results indicate that Thr14 is not a phosphorylated residue and the significance of threonine at position 14 is not completely understood.

Surprisingly, the mutant virus CHV-1/p48Δ1(T)Δ15 did not replicate where as the p48Δ2(T)Δ15 and p48Δ3Δ15 deletion viruses were able to replicate. It is not completely clear why the p48Δ1(T)Δ15 virus would not be able to replicate while the p48Δ3Δ15 mutant virus, which contains a larger deletion, could replicate. As previously discussed, Thr14 appears to be an essential aa and the p48Δ1(T)Δ15 protein may fold in a manner that does not allow for modification or correct presentation of the threonine, resulting in a protein that is unable to contribute to viral replication, ultimately resulting in a

non-viable virus. Another possible explanation is that the location of the specific deletions at the N- and C-terminus result in the disruption or misfolding of the p48 protein producing an unstable or non-functional protein, thereby resulting in a non-viable virus.

Two potential regions of similar amino acid sequence were noticed to fall within C-terminus region of p48 between aa 299 and 340 (Figure 3.5A). At least one of these domains is present within each deletion virus that maintained the ability to replicate, with the exception being the p48Δ16 mutant virus in which the first amino acid domain (aa 299-305) is mutated to VPMEDIL from VPMEEAK. The aspartic acids (aa 302, 303 and 337, 338) were mutated to alanine in both CHV-1/EP713 and the p48Δ3Δ15 mutant virus. Mutations of these residues did not noticeably impact the ability of either virus to replicate, indicating that those domains are not essential to the larger p48 function domains.

Although not directly examined, there is a possibility that the presence of RNA secondary structures located in the p48 coding domain may be involved with or responsible for the ability of the deletion viruses to replicate. While several viruses contain cis-acting replication elements (CRE) at the 5' and 3' ends, as well as internal CRE elements to aid in viral replication and switching between negative- and positive-strand RNA synethesis, this does not appear to be the responsible for effects that are observed with p48. As was previously demonstrated, the p48 coding domain can be deleted from the CHV-1 virus and replication can still occur as long as p48 is supplied *in trans*. Additionally, since

the p48 deletion mutants discussed within this chapter are spread over the whole p48 coding domain, any potential CRE domain would be absent in at least one replication competent deletion virus. The Δp48 rescue experiments taken together with the deletion results discussed here, indicate that any RNA structural elements within the p48 coding domain are not essential for virus replication. The possibility of a CRE element within p48 can be confirmed or disproved in the future studies by introducing a frameshift mutation at the beginning and the end of the p48 coding domain, thereby changing the protein coding sequence without disrupting nucleotide sequence.

While the mechanism underlying the role of p48 during *in trans* rescue is still unclear, it appears as though one functional domain is insufficient for initiation of viral replication. Disruption of either functional domain may result in the inability of p48 to bind or recruit a host protein or factor to the site of CHV-1 replication. To examine the requirement of both functional domains for *in trans* complementation, an EP155 p48 transformant strain can be generated, where amino acids 14-168 have been deleted, leaving the two predicted functional domains intact. Synthetic RNA transcripts corresponding to the Δp48 mutant virus can then be introduced into mutant p48 EP155 transformant and the presence of viral RNA accumulation can be examined to determine if the Δp48 mutant virus is replicating.

Future studies will be directed at further characterizing the p48 functional domains. Determining the structure of D1 and D2 will aid in the identification of potential RNA binding domains and protein-interacting

domains. Structural analysis results can also be used to identify residues for additional mutagenesis to examine *in trans* complementation and potential recruitment of host proteins. Characterization of domains D1 and D2, will provide new insights into how p48 contributes to CHV-1 replication.

Chapter 4: Conclusions and Perspectives

Positive sense single strand RNA viruses are the largest group of RNA viruses and have been isolated from animal, plant, and fungal hosts. Although these viruses share a common genome polarity, they employ cobinations of several different replication and protein expression strategies, ranging from the ability to catalytically process an immature viral polyprotein into mature viral proteins (picornaviruses, potyviruses), production of sub-genomic RNAs (bromoviruses, tumbusviruses), and frameshift events (hypoviruses, coronaviruses). Despite advances in elucidating the numerous mechanisms employed by positive sense RNA viruses to amplify their genome, several aspects of viral replication remain unclear. The initial goal of this project was to investigate the underlying 'hit and run' mechanism displayed by the CHV-1 p48 protein and gain additional insight into how p48 contributes to viral replication.

CHV-1 infection and subsequent viral replication is similar to other positive sense RNA viruses, and results in rearrangement of host intracellular membranes into vesicles that support viral RNA replication; however, the mechanism driving membrane rearrangement or the proteins involved are not clearly understood. Unfortunately, with the exception of the identification of the p48 papain-like protease, the processing pathway and the mature viral protein products derived from the CHV-1 ORF B polyprotein have not been identified. While p48 is known to be essential for the initiation of virus replication, not much else is known about how p48 contributes to viral RNA accumulation or CHV-1 infection. Analysis of fungal vesicles that support viral RNA replication have been shown to associate with p48

(Wang et al., 2013) and p48 expressed *in trans* has been demonstrated to be able to rescue mutant CHV-1 virus in which the p48 coding domain has been deleted (Deng and Nuss, 2008). Taken together, these results indicate that p48 serves an important role during viral replication. The previously presented studies in Chapters 2 and 3 aimed at further characterizing p48 protein with regard to the function of this protein during viral replication. To accomplish this task a series of protease mutant viruses were generated as well as deletions to the p48 coding domain to identify essential functional domains. The results presented in Chapters 2 and 3 provide insights into p48 and p29 contributions to viral RNA accumulation, evidence of an alternative processing pathway for the ORF B polyprotein and mapped two potential functional domains.

The goal of my first project was initially directed at examining if the p48 catalytic residues, Cys341 and His388, are required for p48 to act *in trans* to rescue the Δp48 mutant virus. Mutation of these residues individually and in combination to serine, resulted in the inability of p48 to complement the Δp48 mutant virus. However, when these same mutations were introduced into the coding region of p48 within the CHV-1 virus, the mutant viruses maintained replication viability, and surprisingly, processing still occurred. The processing of p48/ORF B in the mutant viruses is in contrast to observed results for CHV-1 viruses containing mutations to the catalytic residues of protease p29. Mutation of p29 catalytic residue Cys162 individually or in combination with His215 to serine resulted in a loss of ORF A processing. The occurrence of p48/ORF B processing despite mutation of the

catalytic and cleavage site residues indicates that a host protease may be responsible for the observed maturation of p48.

While no host proteases have been previously identified as having a role in CHV-1 polyprotein processing, it is not uncommon for enveloped viruses to use a host protease in virion maturation. Specifically, the protease furin has been identified as having role in the maturation process of both positive and negative single-strand RNA viruses as well as retroviruses (Löving et al., 2012; Volchkov et al., 1998; Zimmer et al., 2001; Zybert et al., 2008). In this regard, one possible scenario is that hypoviruses, due to their intracellular lifecycle, may have initially relied upon the ability of a host protease for polyprotein processing. Since the catalytic residues of the N-terminal leader proteases are not required for infection, these proteases appear to only be necessary for the virus to maintain maximum levels of replication; indicating that protease activity may have evolved to increase replication efficiency. It is possible that hypoviruses still contain the host protease cleavage sites within the viral genome, allowing for p48/ORF B processing in absence of the p48 catalytic residues. One possible way of approaching this question is to generate a *C. parasitica* transformant expressing the first 650 amino acids of ORF B of either WT or mutant p48 with different epitope tags placed at the N- and C-terminals *in trans*. The expressed proteins can then be isolated and examined for processing in the absence of CHV-1 replication. The ability of the p48 mutant polyprotein to exhibit processing and produce different size protein fragments compared to WT p48 would provide evidence of an alternative processing pathway. However, lack of mutant p48

processing would indicate that an unidentified viral protein is responsible for the observed p48 processing during mutant CHV-1 replication.

Recent computational analysis of the p48 predicted secondary structure indicates that the C-terminus of p48 shares a conserved structure with the papain-like protease domain of HC-Pro from turnip mosaic virus (Guo et al., 2011) (Phyre2, Kelley and Sternberg, 2009, http://www.sbg.bio.ic.ac.uk/phyre2/html/page.cgi?id=index). While this was expected, it also raises the possibility that p48 may possess a catalytic triad and not a dyad as previously believed. Recently, the HC-pro proteinase of ZYMV, in contrast HC-Pro of TEV, was shown to contain a catalytic triad, where an aspargine serves as a third catalytic residue in addition to cysteine and histidine (Boonrod et al., 2011). Analysis of the p48 coding domain shows that there are three conserved aspargine residues located between Cys341 and His388, at amino acid positions 347, 348, and 371. While it is doubtful that p48 contains a catalytic triad, based on evidence that p29 contains a catalytic dyad and Cys341 and His388 appear to be conserved in CHV-2 isolates while the aspargine residues are not, this can be confirmed by mutating the individual aspargine residues to isoluecine in context of the previously established CHV-1/p48(341S:388S:418R) mutant and examining p48 processing.

The results presented in Chapter 2 and obtained by Graham and Denison (2006) indicate that while the catalytic residues of the papain-like proteases of CHV-1 and MHV are essential for optimal viral replication, and in the case of MHV, optimal virus infectivity and plaque size, they are not required for viral replication. These results would seem to indicate that viral proteases have evolved over time to increase

the efficiency of viral replication and are not always essential for virus replication. In addition, the results presented in Chapter 2 illustrate the potential dangers in basing conclusions solely on *in vitro* analyses and underline the importance of combining both *in vitro* and *in vivo* approaches to study viral functions.

In an effort to gain further insight into the how p48 contributes to viral replication, a loss of function/gain of function analysis was performed to identify functional domains within p48. It was quite surprising that large regions of the N- and C-terminus of the p48 coding domain could be deleted from the CHV-1/EP713 virus. While two predicted functional domains have been identified, several questions remain, particularly, how these functional domains contribute to virus replication, protein localization, and the ability of p48 to complement the Δp48 mutant virus *in trans*. The ability to determine the crystal structure of p48 would greatly aid in characterizing the predicted functional domains, D1 and D2, and help in understanding what appears to be a built-in redundancy that allows the virus to replicate with either of the two domains present.

To provide additional insight into the functional characteristics of p48, computational analysis was performed to examine D1 and D2. The D1 region appears to contain a helix-turn-helix and the predicted secondary structure shares regions of homology to the known secondary structure of the Tombusvirus coat protein, dehydrogenase, and oxidoreductase (Phyre2) as well as dsDNA and dsRNA binding domains of bacterial, bacteriophage, and viral proteins (HHpred; http://toolkit.tuebingen.mpg.de/hhpred). In addition, the aa regions directly upstream and downstream of D1 were identified as potentially being disordered (DisoPred2,

Ward et al., 2004, http://bioinf.cs.ucl.ac.uk/index. php?id=806), indicating that these regions could be linker regions between the p48 functional domains. Analysis of the p48 protein sequence for the presence of potential transmembrane domains indicated that no significant domains are present (TMHMM, http://www.cbs.dtu.dk/services/TMHMM-2.0/; TMpred, Hofmann and Stoffel, 1993, http://www.ch.embnet.org/software/TMPREDform.html). However, the poliovirus 2C protein, a multifunctional protein involved in viral replication, lacks defined membrane binding domains and has been shown to interact with host membranes during virus replication (Echeverri and Dasgupta, 1995), indicating that the ability of p48 to interact with host membranes or membrane-associated proteins should be further investigated.

Since p48 is essential for virus replication, it would be of interest to determine if p48, and specifically D1, contains a dsRNA binding domain. Interactions between viral proteins and dsRNA have been well established for positive and negative ssRNA viruses of plants and animals. Viral suppressors of RNA silencing and inhibitors of the innate immune response have been demonstrated to interact with either dsRNA or vsRNA (Chu et al., 2000; Vargason et al., 2003; Chapman et al., 2004; Merai et al., 2005; Yang et al., 2011; Bale et al., 2013; Ramos et al., 2013); in addition, poliovirus protein 2C was shown to interact with the RNA structures at the 3' end of the negative strand of viral RNA (Banerjee et al., 1997). In order to determine if p48 does bind dsRNA, an electrophoretic mobility gel shift assay using ^{32}P-labelled positive sense and negative sense RNAs that correspond the 5' and 3' ends of the CHV-1 genome can be performed. In addition, the ability of p48 to bind vsRNAs as a possible mechanism of suppression of RNA silencing should also be explored. The

results of these experiments will provide additional insight into how p48 functions during CHV-1 replication.

As was previously discussed in Chapter 3, phage C1 encodes a lysine, PlyC, in which the subunit, PlyCA, contains two functional domains, a CHAP domain and a GyH domain, that appear to work either synergistically or cooperatively to increase processivity. Furthermore, disruption of either the CHAP domain or the GyH domain does not affect processivity of the undisrupted domain. It is not known if the p48 potential domains function in a similar manner, i.e. where D1 and D2 work in a synergistic manner. However, as mentioned above the internal region of p48 consisting of the D1 domain has the potential to form folds related to dehydrogenase and oxidoreductase enzymes. Determining the crystal structure of p48 would help determine the exact role of both D1 and D2 during viral replication and direct further mutagenesis studies.

The apparent requirement for at least one of the p48 functional domains leads to questions about differences in function and localization between specific mutant p48 proteins. The ability to detect the p48 protein through either cryo-EM and/or confocal microscopy presents some challanges due to the structure and composition of the *C. parastica* hyphae, however, the results would provide insight into the specific functions of the domains. One approach would be to place specific epitope tags within the coding domain of the p48 deletion mutant viruses, p48Δ6, p48Δ16, and p48Δ3Δ14, and introduce the corresponding synthetic RNA transcripts into Δ*dcl*2 spheroplasts. Monoclonal antibodies directed against the specific epitope tags conjugated with gold could be used in combination with cryo-EM to determine if

there is any difference in localization between the p48Δ6, p48Δ16, and p48Δ3Δ14 mutant proteins during CHV-1 infection. In addition, since hypoviruses do not encode structural proteins or form virions, there are no restrictions on the ability to place large fluorescent proteins, such as eGFP, within regions of the CHV-1/EP713 coding strand (Zhang and Nuss, 2008). With recent advances in confocal microscopy strategies, co-localization studies can be used to confirm the cryo-EM results. Moreover, once the localization of WT and mutant p48 is determined, either bimolecular fluorescence complementation or yeast-2-hbrid assays can be employed to examine specific interactions with proteins that localize to the same region as p48.

While two functional domains within the p48 coding region have been identified, it is still unclear how p48 functions *in trans* to complement the Δp48 mutant virus. It would be of interest to generate an EP155 transformant expressing mutant p48 containing a deletion of aa Thr14-Thr167, but still encoding D1 and D2. Since all previous attempts to replicate *in trans* complementation with mutant p48 containing alterations or deletions in one of the functional domains has been unsuccessful, this experiment would indicate whether the two functional domains are essential for complementation of the Δp48 mutant virus.

In conclusion, the studies presented in this dissertation provide new insights into the requirement and functional importance of the CHV-1 p48 catalytic residues and identification of two potential functional domains. While the requirements for *in trans* rescue of the Δp48 mutant virus has not been fully elucidated, the requirement of the p48 catalytic residues for complementation has been established. Examination of the catalytic residues of p48 and p29 *in cis* revealed that protease activity

contributes to viral RNA accumulation. Mutation of the p29 catalytic residues resulted in the loss of ORF A processing, however, mutation of the p48 catalytic and cleavage site residues revealed an alternate processing pathway for p48/ORF B maturation. Furthermore, it appears as though both identified functional domains, D1 and D2, may be required for *in trans* complementation of the Δp48 mutant virus, however, only one domain is required when p48 is supplied *in cis*. The knowledge gained from these studies aid in our understanding of positive sense RNA virus replication mechanisms and direct future research efforts into (i) examining the possibility of alternative processing pathways in plant and animal viruses; (ii) determining how viral protein functional domains can provide redundant functions during replication.

Appendices

Appendix 1 – Primers used to generate p48 and p29 mutant and epitope tagged viruses in Chapter 2

Name	Sequence	Nucleotide Region
1KF	ATCTCTCGGCCATTGTAG	979-996
5KR	CGGGATCAAGAGCGTGGA	4979-4996
p29 protease primers		
p29-162S-F	GGGCAGGGCTACTCGTATCTCTCGGCC	963-990
p29-162S-R	GGCCGAGAGATACGAGTAGCCCTGCCC	963-990
p29-215S-F	GACCATGTTTATTCCGTGGTCGTCGAC	1122-1149
p29-215S-R	GTCGACGACCACGGAATAAACATGGTC	1122-1149
p48 protease primers		
p48-341S-F	CGAAGAGGGTCGAAGCTTCGAGCTCTTGTTC	3128-3158
p48-341S-R	GAACAAGAGCTCGAAGCTTCGACCCTCTTCG	3128-3158
p48-388S-F	GTGACCAATGCGTGAGCATTGTCGCTGGTGAAACC	3268-3302
p48-388S-R	GGTTTCACCAGCGACAATGCTCACGCATTGGTCAC	3268-3302
p48 cleavage site primers		
p48-418R-F	GCCTGACATCCTCGTTAGGGCTGAAGAAGGTTCAGTCGC	3595-3634
p48-418R-R	GCGACTGAACCTTCTTCAGCCCTAACGAGGATGTCAGGC	3595-3634
Δp29 primers		

AscI-p29-F	atcgatggcgcgccGCCTATGGGTGGTCTACATAGG	1-22
	AscI site in undercase, CHV-1/EP713 sequence in uppercase	
1.8KF	CGACGCAAAGATTCAGTGCATAGGG	1812-1836
1.8KR	CCCTATGCACTGAATCTTTGCGTCG	1812-1836

p48-6xHis tag Primers		
p48-His-F	CATCATCACCATCACCACGGTAGCGGTCAGGTCATGGACGGGCCAACATGG	2402-2425
p48-His-R	GTGGTGATGGTGATGATGACCGCTACCTGTTCGCCACACTTCAATAGGTCG	2378-2401
	6xHis tag in black, GSG linker in blue, p48 in red	

p48-Strep-F	TGGTCCCATCCTCAGTTTGAGAAGCAGGTCATGGACGGGCCAACATGG	2402-2425
p48-Strep-R	CTTCTCAAACTGAGGATGGGACCATGTTCGCCACACTTCAATAGGTCG	2378-2401
	strep tag in black, p48 in red	

ORF B-6xHis tag		
Nhe-His-F	GCTCAAGCTAGCGCATCATCACCATCACCACAAGGGTCTAGCTGAACCTGGCC	3468-3489
	NheI site in red, His with GSG linker in green, ORF B in black	

Appendix 2 – Primers used to generate p48 deletion mutant viruses in Chapter 3

N-terminal Deletions

Name	Sequence	Nucleotide Regions	Deletion Region (aa)
p48Δ1-F	CGACCTATTGAAGTGTGGCGAAGTTTTGGCCAGGGCGGCAAC	(2139-2159)-(2337-2357)	14-72
p48Δ1-R	GTTGCCGCCCTGGCCAAAACTTCGCCACACTTCAATAGGTCG	(2139-2159)-(2337-2357)	14-72
p48Δ2-F	CGACCTATTGAAGTGTGGCGATCCTATGTTGACGGGAGACCG	(2139-2159)-(2493-2513)	14-124
p48Δ2-R	CGGTCTCCCGTCAACATAGGATCGCCACACTTCAATAGGTCG	(2139-2159)-(2493-2513)	14-124
p48Δ3-F	CGACCTATTGAAGTGTGGCGAACTGCACAAGTTTCGGTGGCC	(2139-2159)-(2625-2645)	14-168
p48Δ3-R	GGCCACCGAAACTTGTGCAGTTCGCCACACTTCAATAGGTCG	(2139-2159)-(2625-2645)	14-168
p48Δ4-F	CGACCTATTGAAGTGTGGCGAACCTCTCTATTGTCCAACCGA	(2139-2159)-(2802-2822)	14-227
p48Δ4-R	TCGGTTGGACAATAGAGAGGTTCGCCACACTTCAATAGGTCG	(2139-2159)-(2802-2822)	14-227
p48Δ5-F	CGACCTATTGAAGTGTGGCGATCGATAGGATTAAGTCACGAG	(2139-2159)-(2940-2960)	14-273
p48Δ5-R	CTCGTGACTTAATCCTATCGATCGCCACACTTCAATAGGTCG	(2139-2159)-(2940-2960)	14-273
p48Δ6-F	CGACCTATTGAAGTGTGGCGAACCCTTCGGGTGCCGGTCGAA	(2139-2159)-(3111-3121)	14-330
p48Δ6-R	TTCGACCGGCACCCGAAGGGTTCGCCACACTTCAATAGGTCG	(2139-2159)-(3111-3121)	14-330
p48Δ7-F	CGACCTATTGAAGTGTGGCGAACCCCTGCAATTTTCGAC	(2139-2159)-(3171-3191)	14-351
p48Δ7-R	GTCGAAAATTGCAGGGGTTCGCCACACTTCAATAGGTCG	(2139-2159)-(3171-3191)	14-351
p48Δ8-F	CGACCTATTGAAGTGTGGCGAACGATGGACTCGCTCGAAATC	(2139-2159)-(3240-3260)	14-374
p48Δ8-R	GATTTCGAGCGAGTCCATCGTTCGCCACACTTCAATAGGTCG	(2139-2159)-(3240-3260)	14-374
p48Δ9-F	CGACCTATTGAAGTGTGGCGAACCTTCCGGAACTACGATGAA	(2139-2159)-(3300-3320)	14-394
p48Δ9-R	TTCATCGTAGTTCCGGAAGGTTCGCCACACTTCAATAGGTCG	(2139-2159)-(3300-3320)	14-394

Point Mutations Serine to Threonine

p48Δ1-F (T)	CGACCTATTGAAGTGTGGCGAACCTTTGGCCAGGGCGGCAAC	2139-2180

p48Δ1-R (T)	GTTGCCGCCCTGGCCAAAGGTTCGCCACACTTCAATAGGTCG	2139-2180
p48Δ2-F (T)	CGACCTATTGAAGTGTGGCGAACCTATGTTGACGGGAGACCG	2139-2180
p48Δ2-R (T)	CGGTCTCCCGTCAACATAGGTTCGCCACACTTCAATAGGTCG	2139-2180
p48Δ5-F (T)	CGACCTATTGAAGTGTGGCGAACGATAGGATTAAGTCACGAG	2139-2180
p48Δ5-R (T)	CTCGTGACTTAATCCTATCGTTCGCCACACTTCAATAGGTCG	2139-2180

C-terminal Deletions

Name	Sequence	Nucleotide Regions	Deletion Region (aa)
p48Δ11-F	GCTGGTGAAACCTTCCGGAACTACGACATCCTCGTTGGAGCTGAAGAA	(3291-3314)-(3360-3383)	399-413
p48Δ11-R	TTCTTCAGCTCCAACGAGGATGTCGTAGTTCCGGAAGGTTTCACCAGC	(3291-3314)-(3360-3383)	399-413
p48Δ12-F	GACTCGCTCGAAATCAGTCACAGTGACATCCTCGTTGGAGCTGAAGAA	(3246-3269)-(3360-3383)	384-413
p48Δ12-R	TTCTTCAGCTCCAACGAGGATGTCACTGTGACTGATTTCGAGCGAGTC	(3246-3269)-(3360-3383)	384-413
p48Δ13-F	TTCGACAAGAAGCCATTGCTTAAAGACATCCTCGTTGGAGCTGAAGAA	(3183-3206)-(3360-3383)	363-413
p48Δ13-R	TTCTTCAGCTCCAACGAGGATGTCTTTAAGCAATGGCTTCTTGTCGAA	(3183-3206)-(3360-3383)	363-413
p48Δ14-F	CAAGTAACCCCTGCAATTTTCGACGACATCCTCGTTGGAGCTGAAGAA	(3165-3188)-(3360-3383)	356-413
p48Δ14-R	TTCTTCAGCTCCAACGAGGATGTCGTCGAAAATTGCAGGGGTTACTTG	(3165-3188)-(3360-3383)	356-413
p48Δ15-F	AACCATGAGGAGGAGGTTGAGATTGACATCCTCGTTGGAGCTGAAGAA	(3084-3107)-(3360-3383)	330-413
p48Δ15-R	TTCTTCAGCTCCAACGAGGATGTCAATCTCAACCTCCTCCTCATGGTT	(3084-3107)-(3360-3383)	330-413
p48Δ16-F	AAGCCCCATCTCGTCCCCATGGAAGACATCCTCGTTGGAGCTGAAGAA	(3003-3026)-(3360-3383)	306-413
p48Δ16-R	TTCTTCAGCTCCAACGAGGATGTCTTCCATGGGGACGAGATGGGGCTT	(3003-3026)-(3360-3383)	306-413
p48Δ17-F	GCCCAGAAATCTCGCAAGTGGCAGGACATCCTCGTTGGAGCTGAAGAA	(2901-2924)-(3360-3383)	269-413
p48Δ17-R	TTCTTCAGCTCCAACGAGGATGTCCTGCCACTTGCGAGATTTCTGGGC	(2901-2924)-(3360-3383)	269-413
p48Δ18-F	TTGTCATGGACCAGATACGATGGCGACATCCTCGTTGGAGCTGAAGAA	(2763-2786)-(3360-3383)	223-413
p48Δ18-R	TTCTTCAGCTCCAACGAGGATGTCGCCATCGTATCTGGTCCATGACAA	(2763-2786)-(3360-3383)	223-413
p48Δ19-F	AAATGGGATGTCGGCGTGTTCCGTGACATCCTCGTTGGAGCTGAAGAA	(2550-2573)-(3360-3383)	152-413
p48Δ19-R	TTCTTCAGCTCCAACGAGGATGTCACGGAACACGCCGACATCCCATTT	(2550-2573)-(3360-3383)	152-413
p48Δ20-F	ACACCTTTTGGATATCCTGCCGAGGACATCCTCGTTGGAGCTGAAGAA	(2397-2420)-(3360-3383)	101-413
p48Δ20-R	TTCTTCAGCTCCAACGAGGATGTCCTCGGCAGGATATCCAAAAGGTGT	(2397-2420)-(3360-3383)	101-413

p48Δ21-F	ATGACGCTCGATATCATCCAGCCTGACATCCTCGTTGGAGCTGAAGAA	(2250-2273)-(3360-3383)	52-413
p48Δ21-R	TTCTTCAGCTCCAACGAGGATGTCAGGCTGGATGATATCGAGCGTCAT	(2250-2273)-(3360-3383)	52-413

Point Mutations 302, 303 & 337, 338 Glutamic acid to Alanine

Name	Sequence	Nucleotide Regions
p48EE302/303AA-F	CTCGTCCCCATGGCAGCGGCGAAAGAGGCA	3012-3041
p48EE302/303AA-R	TGCCTCTTTCGCCGCTGCCATGGGGACGAG	3012-3041
p48EE337/338AA-F	CGGGTGCCGGTCGCAGCGGGTCGATGTTTC	3117-3146
p48EE337/338AA-R	GAAACATCGACCCGCTGCGACCGGCACCCG	3117-3146

References:

Adams, M.J., T. Candresse, J. Hammond, J.F. Kreuze, G.P. Martelli, S. Namba, N.M. Pearson, K.H. Ryu, and A.M. Vaira. 2012. Family *Alphaflexiviridae*, p904-919, Virus Taxonomy: 9th Report of the International Committee for the Taxonomy of Viruses. A.M.Q. King, M.J. Adams, E.B. Carstens, and E.J. Lefkowitz (ed.) Elsevier Academic Press, London, United Kingdom.

Anagnostakis, S.L. 1982A. Biological Control of Chestnut Blight. Science. 215:466-471

Anagnostakis, S.L. 1982B. The origin of ascogenous nuclei in Endothia parasitica. Genetics. 100: 413-416

Anagostakis, S.L. 1982C. Genetic analyses of Enothia parasitica: linkage data for four single genes and three vegetative compatibility types. Genetics. 102: 25-28

Attoui, H., P.P.C. mertens, J. Becnel, S. Belaganahalli, M. Bergoin, C.P. Brussaard, J.D. Chappell, M. Ciarlet, M. del Vas, T.S. Dermody, P.R. Dormitzer, R. Duncan, Q. Fcang, R. Graham, K.M. Guglielmi, R.M. Harding, B. Hillman, A. Makkay, C. Marzachi, J. Matthijnssens, R.G. Milne, F. Modh Jaafar, H. Mori, A.A. Noordeloos, T. Omura, J.T. Patton, S. Rao, M. Maan, D. Stoltz, N. Suzuki, N.M. Upadyaya, C. Wei, and J. Zhou. 2012. Family *Reoviridae*, p 541-637. Virus Taxonomy: 9th Report of the International Committee for the Taxonomy of Viruses. A.M.Q. King, M.J. Adams, E.B. Carstens, and E.J. Lefkowitz (ed.) Elsevier/Academic Press, London, United Kingdom.

Baird, S.D., M. Turcotte, R.G. Korneluk, and M. Holcik. 2006. Searching for IRES. RNA. 12: 1755-1785

Bale, S. J.P. Julien, Z.A. Bornholdt, A.S. Krois, I.A. Wilson, E.O. Saphire. 2013. Ebolavirus VP35 coats the backbone of double-stranded RNA for interferon antagonism. Journal of Virology. 87: 10385-10388

Banerjee, R., A. Echeverri, and A. Dasgupta. 1997. Poliovirus-encoded 2C polypeptide specifically binds to the 3'-terminal sequences of viral negative-strand RNA. Journal of Virology. 71: 9570-9578.

Barrett, A.J., and N.D. Rawlings. 2001. Evolutionary lines of Cysteine peptidases. Biological Chemistry. 382: 727-733

Biella, S., M.L. Smith, J.R. Aist, P. Cortesi, and M.G. Milgroom. 2002. Programmed cell death correlates with virus transmission in a filamentous fungus. Proceedings of the Royal Society: Biological Sciences. 269: 2269-2276

Boonrod, K., M.W. Füllgrabe, G. Krczal, and M. Wassenegger. 2001. Analysis of the autooroteolytic activity of the reombinant helper component proteinase from zucchini yellow mosaic virus. Biological Chemistry. 392: 937-945.

Buck, K. 1998. Molecular variability of viruses of fungi. Molecular Variability of Fungal Pathogens. P.D. Bridge, Y. Couteaudier, and J.M. Clarkson, editors. CAB International, Wallingford, United Kingdom: 53-72

Caten, C.E. 1972. Vegetative incompatibility and cytoplasmic infection in fungi. Journal of General Microbiology. 72: 221-229

Cerutti, H., and J.A. Casas-Mollano. 2006. On the origin and functions of RNA-mediated silencing: from protists to man. Current Genetics. 50: 81-99

Chang, R. and E. Wang. 2007. Mouse translation elongation factor eEF1A-2 interacts with Prdx-I to preotect cells against apoptotic death binduced by oxidative stress. Journal of Cellular Biochemistry. 100: 267-278

Chapman, E.J., A.I. Prokhnevsky, K. Gopinath, V.V. Dolja, and J.C. Carrington. 2004. Viral RNA silencing suppressors inhibit the microRNA pathway at an intermediate step. Genes and Development. 18:1179-1186.

Chen, B., G.H. Choi, and D.L. Nuss. 1993. Mitotic stability and nuclear inheritance of integrated viral cDNA in engineered hypovirulent strains of the chestnut blight fungus. The EMBO Journal. 12: 2991-2998

Chen, B., G.H. Choi, and D.L. Nuss. 1994. Attenuation of fungal virulence by synthetic infectious hypovirus transcripts. Science. 264:1762-1764

Chen, B., M.G. Craven, G.H. Choi, and D.L. Nuss. 1994. cDNA-derived hypovirus RNA in transformed chestnut blight fungus is spliced and trimmed of vector nucleotides. Virology. 202: 441-448

Chen, B., and D.L. Nuss. 1999. Infectious cDNA Clone of Hypovirus CHV1-Euro7: A Comparative Virology Approach to Investigate Virus-Mediated Hypovirulence of the Chestnut Blight Fungus *Cryphonectria parasitica*. Journal of Virology. 73: 985-992

Chen, B., L.M. Geletka, and D.L. Nuss. 2000. Using Chimeric Hypoviruses to Fine-Tune the Interaction Between a Pathogenic Fungus and Its Plant Host. Journal of Virology. 74:7562-7567

Choi, G.H., D.M. Pawlyk, and D.L. Nuss. 1991. The Autocatalytic Protease p29 Encoded by a Hypovirulence-Associated Virus of the Chestnut Blight Fungus Resembles the Potyvirus-Encoded Protease HC-Pro. Virology. 183:747-752

Choi, G.H., R. Shapira, and D.L. Nuss. 1991B. Cotranslational autoproteolysis involved in gene expression from a double stranded RNA genetic element associated with hypovirulence of the chestnut blight fungus. Proc. Natl. Acad. Sci. USA 88:1167-1171

Choi, G.H. and D.L. Nuss. 1992. Hypovirulence of Chestnut Blight Fungus Conferred by an Infectious Viral cDNA. Science. 257:800-803

Choi, G.H., A.L. Dawe, A. Churbanov, M.L. Smith, M.G. Milgroom, and D.L. Nuss. 2012. Molecular characterization of vegetative incompatibility genes that restrict hypovirus tramission in the chestnut blight fungus *Cryphonectria parasitica*. Genetics. 190:113-127

Chu, M., B,. Desvoyes, M. Turina, R. Noad, and H.B. Scholthof., 2000. Genetic dissection of tomato bushy stunt virus p19-protein-mediated host-dependent symptom induction and systemic invasion. Virology. 266:79-87.

Cochran, M. F. 1990. Back from the brink: Chestnuts. National Geographic. 177:128-140.

Cogoni, C., and G. Macino. 1997. Isolation of quelling-defective (qde) mutants impaired in posttranscriptional transgene-induced gene silencing in *Neurospora crassa*. Proceedings of the National Academy of Sciences of the United States of America. 94: 10233-10238

Cortesi, P. and M.G. Milgroom. 1998. Genetics of vegetative incompatibility in *Cryphonectria parasitica*. Applied and Environmental Microbiology. 64: 2988-2994

Cortesi, P., C.E. McCulloch, H. Song, H. Lin, and M.G. Milgroom. 2001. Genetic control of horizontal virus transmission in the chestnut blight fungus, *Cryphonectria parasitica*. Genetics. 159: 107-118

Craven, M.G., D.M. Pawlyk, G.H. Choi, and D.L. Nuss. 1993. Papain-like protease p29 as a symptom determinant encoded by a hypovirulence-associated virus of the Chestnut Blight fungus. Journal of Virology. 67:9513-9521

Dawe, A.L., and D.L. Nuss. 2001. Hypoviruses and Chestnut Blight: Exploiting viruses to understand and modulate fungal pathogenesis. Annual Reviews Genetics. 35:1-29

Dawe, A.L., and D.L. Nuss. 2013. Hypovirus molecular biology: From Koch's postulates to host self-recognition genes that restrict virus transmission. Advances in Virus Research. 86: 109-147

Dawe, V.H., and C.W. Kuhn. 1983. Isolation and Characterization of a Double-Stranded DNA Mycovirus Infecting the Aquatic Fungus, Rhizidiomyces. Virology. 130:21-28

Day, P., J. Dodds, J. Elliston, A. Jaynes, and S.L. Anagnostakis. 1977. Double-Stranded RNA in *Enothia parasitica*. Phytopathology. 67: 1393-1396

Deng, F., and D.L. Nuss. 2008. Hypovirus Papain-like Protease p48 is Required for Initiation but not for Maintenance of Virus RNA Propagation in the Chestnut Blight Fungus *Cryphonectria parasitica*. Journal of Virology. 82:6369-78

Denison, M.R., B. Yount, S.M. Brockway, R.L. Graham, A.C. Sims, X.T. Lu, and R.S. Baric. 2004. Cleavage between replicase proteins p28 and p65 of Mouse Hepatits Virus is not required for virus replication. Journal of Virology. 78:5957-5965

Diaz-Pendon, J., and S. Ding. 2008. Direct and Indirect Roles of Viral Suppressors of RNA Silencing in Pathogenesis. Annual Review of Phytopathology. 46: 303-326

Ding, S.W. 2010. RNA-based antiviral immunity. Nature Reviews: Immunology. 10: 632-644

Dinman, J.D., T. Icho, and R.B. Wickner. 1991. A -1 ribosomal frameshift in a double-stranded RNA virus of yeast forms a gag-pol fusion protein. Proceedings of the National Academy of Sciences of the United States of America. 88:174-178

Dinman, J.D., and R.B. Wickner. 1994. Translational maintenance of frame: mutants of *Saccharomyces cerevisiae* with altered -1 ribosomal frameshifting efficiencies. Genetics. 136:75-86

Dodds, J.A. 1980. Association of type 1 viral-like dsRNA with club-shaped particles in hypovirulent strains of Endothia parasitica. Virology. 107: 1-12

Doughterty, W.G., and B.L. Semler. 1993. Expression of virus encoded proteinases: functional and structural similarities with cellular enzymes. Microbiology and Molecular Biology Reveiws. 57: 781-822

Echeverri, A. and A. Dasgupta. 1995. Amino terminal regions of poliovirus 2C protein mediate membrane binding. Virology. 208:540-553.

English, J.J., E. Mueller, and D.C. Baulcombe. 1996. Suppression of virus accumulation in transgenic plants exhibiting silencing of nuclear genes. Plant Cell. 8: 179-188

Fahima, T., P. Kazmierczak, D.R. Hansen, P. Pfeiffer, and N.K. Van Alfen. 1993. Membrane-Associated Replication of an Unencapsidated Double-Stranded RNA of the Fungus *Cryphonectria parasitica*. Virology. 195:81-89

Fahima, T., Y. Wu, L. Zhang, and N.K. Van Alfen. 1994. Identification of the putative RNA polymerase of *Cryphonectria hypovirus* in a solubilized replication complex. Journal of Virology. 68: 6116-6119

Feldman, T.S., M.R. Morsey, and M.J. Roossinck. 2012. Are communities of microbial symbionts more diverse than communities of microbial hosts. Fungal Biology. 116: 465-477

Fensterl, V., and G.C. Sen. 2009. Interferons and viral infections. Biofactors. 35: 14-20

Fire, A., S. Xy, M.K. Montgomery, S.A. Kostas, S.E. Driver, and C.C. Mello. 1998. Potent and specific genetic interference by double-stranded RNA in *Caenorhabditis elegans*. Nature. 391: 806-811

Fukuhara, T., and M.J. Gibbs. 2012. Family *Endornaviridae*, p519-521, Virus Taxonomy: 9th Report of the International Committee for the Taxonomy of Viruses. A.M.Q. King, M.J. Adams, E.B. Carstens, and E.J. Lefkowitz (ed.) Elsevier/Academic Press, London, United Kingdom.

Fulci, V., and G. Macino. 2007. Quelling: post-transcriptional gene silencing guided by small RNAs in *Neurospora crassa*. Current Opinion in Microbiology. 10: 199-203

Ghabrial, S.A., K.W. Buck, B.I. Hillman, R.G. Milne. 2005A. Family Partitiviridae, p581-590. Taxonomy: 8th Report of the International Committee for the Taxonomy of Viruses. C.M. Gauquet, M.A. Mayo, J. Maniloff, U. Desselberger, L.A. Ball (ed) Elsevier/Academic Press, London, United Kingdom.

Ghabrial, S.A., D. Jiang, J.R. Caston. 2005B. Family Chrysoviridae. p591-595. Taxonomy: 8th Report of the International Committee for the Taxonomy of Viruses. C.M. Gauquet, M.A. Mayo, J. Maniloff, U. Desselberger, L.A. Ball (ed) Elsevier/Academic Press, London, United Kingdom.

Ghabrial, S.A., and N. Suzuki. 2009. Viruses of plant pathogenic fungi. Annual Review of Phytophathology. 47: 353-384

Gibbs, M.J., R. Koga, H. Moriyama, P. Pfeiffer, and T. Fukuhara. 2000. Phylogenetic analysis of some large double-stranded RNA replicons from plants suggests they evolved from defective single-stranded RNA virus. Journal of General Virology. 81:227-233

Glass, N.L. and K. Dementhon. 2006. Non-self-recognition and programmed cell death in filamentous fungi. Current Opinion in Microbiology. 9: 553-558

Gonen, H., C.E. Smith, N.R. Siegel, C. Kahana, W.C. Merrick, K. Chakraburtty, A.L. Schwartz, and A. Ciechanover. 1994. Protein synthesis elongation factor EP-1 alpha is essential for ubiquitin-dependent degradation of certain N alpha-acetylated proteins and may be subsititued for by the bacterial elongation factor EF-Tu. Proceedings of the National Academy of Sciences of the United States of America. 91: 7648-7652

Goodwin, J., K. Chapman, S. Swaney, T.D. Parks, E.A. Wernsman, and W.G. Dougherty. 1996. Genetic and biochemical dissection of transgenic RNA-mediated virus resistance. Plant Cell. 8: 95-105.

Graham, R.L. and M.R. Denison. 2006. Replication of Murine Hepatitis Virus is regulated by papain-like proteinase 1 processing of nonstructural preoteins 1, 2, and 3. Journal of Virology. 80:11610-11620

Guo, B., J. Lin and K. Ye. 2011. Structure of the autocatalytic cysteine protease domain of potyvirus helper-component proteinase. Journal of Biological Chemistry. 286: 21937-21943

Guo, L., L. Sun, S. Chiba, H. Araki, and N. Suzuki. 2009. Coupled termination/ reinitiation for translation of the downstream open reading frame B of the prototypic hypovirus CHV1-EP713. Nucleic Acids Research. 37:3645-3659

Hansen, D.R., N.K. Van Alfen, K. Gillies, and W.A. Powell. 1985. Naked dsRNA associated with hypovirulence of *Endothia parasitica* is packaged in fungal vesicles. Journal of General Virology. 66: 2605-2614

Herrero, N., S. Sanchez Marquez, I. Zabalgogeazcoa. 2009. Mycoviruses are common among different species of endophytic fungi of grasses. Archives of Virology. 154: 327-330

Hillman, B.I. and R. Esteban. 2012. Family *Narnaviridae*, p1055-1060 Virus Taxonomy: 9th Report of the International Committee for the Taxonomy of Viruses. A.M.Q. King, M.J. Adams, E.B. Carstens, and E.J. Lefkowitz (ed.) Elsevier/Academic Press, London, United Kingdom.

Hillman, B.I., R. Foglia, and W. Yuan. 2000. Satellite and defective RNAs of *Cryphonectria hypovirus* 3-grand haven 2, a virus species in the family *Hypoviridae* with a single open reading frame. Virology. 276:181-189

Hillman, B. I., D. W. Fullbright, D. L. Nuss and N. K. Van Alfen. 1995. Hypoviridae. In virus Taxonomy, ed. FA Murphy, pp. 261-264, New York: Springer Verlag.

Hillman, B.I. and N. Suzuki. 2004. Viruses of the Chestnut Blight Fungus, *Cryphonectria parasitica*. Advances in Virus Research. 63: 423-472

Hiremath, S., B. L'Hostis, S.A. Ghabrial, and R.E. Rhoads. 1986. Therminal structure of hypovirulence-associated dsRNAs in the chestnut blight fungus *Endothia parasitica*. Nucleic Acids Research. 14: 9877-9896

Hofmann, K., and W. Stoffel. 1993. TMbase- A database of membrane spanning proteins segments. Biological Chemistry Hoppe-Seyler. 374:166.

Hollings, M. 1962. Viruses associated with a die-back disease of cultivated mushroom. Nature. 196:962-965

Hollings, M. 1978. Mycoviruses: viruses that infect fungi. Advances in Virus Research. 22: 1-53

Horvath, C.M., M.A. Williams, and R.A. Lamb. 1990. Eukaryotic coupled translation of tandem cistrons: Identification of the influenza B virus BM2 polypeptide. The EMBO Journal. 9: 2639-2647

Hotokezaka, Y., U. Tobben, H. Hotokezaka, K. Van Leyen, B. Beatrix, D.H. Smith, T. Nakamura, and M. Wiedmann. 2002. Interaction of the eukaryotic elongation factor 1A with newly synthesized polypeptides. Journal of Biological Chemistry. 277: 18545-18551

Howitt, R.L.J., R.E. Beever, M.N. Pearson, and R.L.S. Forster. 2006. Genome characterization of a flexuous rod-shaped mycovirus, Botrytis virus X, reveals

high amino acid identity to genes from plant potex-like viruses. Archives of Virology. 151: 563-579

Huang, S., and S.A. Ghabrial. 1996. Organization and expression of the double-stranded RNA genome of *Helminthosporium victoriae* 190S virus, a totivirus infecting a plant pathogenic filamentous fungus. Proceedings of the National Academy of Sciences of the United States of America. 93:12541-12546

Huang, S., A.I. Soldevila, B.A. Webb, and S.A. Ghabrial. 1997. Expression, assembly, and proteolytic processing of *Helminthosporium victoriae* 190S totivirus capsid protein in insect cells. Virology. 234:130-137

Huber, D.H. 1996. Genetic analysis of vegetative incompatibility polymorphisms and horizontal transmission in the chestnut blight fungus, *Cryphonectira parasitica*. Ph.D. Thesis, Michigan State University, East Lansing, MI.

Huber, D.H. and D.W. Fulbright. 1994. Preliminary investigations on the effect of individual genes upon the transmission of dsRNA in *Cryphonectria parasitica*. p15-19. Proceedings of the International Chestnut Conference. M.L. Double, W.L. MacDonald, (ed) West Virginia Press, Morgantown, WV.

Jacob-Wilk, D., M. Turina, and N.K. Van Alfen. 2006. Mycovirus *Cryphonectria* Hypovirus1 elements cofractionate with trans-Golgi Network membranes of the f ungal host *Cryphonectria parasitica*. Journal of Virology. 80:6588-6596

Kang, J., J. Wu, J.A. Bruenn, and C.J. Park. 2001. The H1 double-stranded RNA genome of *Ustilago maydis* virus-H1 encodes a polyprotein that contains structural motifs for capsid polypeptide, papain-like protease and RNA-dependent RNA polymerase. Virus Research. 76:183-189

Kasschau, K., and J. Carrington. 1995. Requirement for HC-Pro processing during genome amplification of Tabacco Etch Potyvirus. Virology. 209: 268-273

Katiyar-Agarwal, S., and H. Jin. 2010. Role of Small RNAs in Host-Microbe Interactions. Annual Review of Phytopathology. 45:225-246

Kelley, L.A., and M.J. Sternberg. 2009. Protein structure prediction on the Web: a case study using the Phyre server. Nature Protocols. 4: 363-371

Kim, S., and P.A. Coulombe. 2010. Emerging role for the cytoskeleton as an organizer and regulator of translation. Nature Reviews: Molecular and Cell Biology. 11: 75-81

Kojima, K.K., T. Matsumoto, and H. Fujiwara. 2005. Eukaryotic translational coupling in UAAUG stop-start codons for the bicistronic RNA translation of the non-long terminal repeat retrotransposon SART1. Molecular Cell Biology. 25: 7675-7686

Koloniuk, I., M.H. El-Habbak, K. Petrzik, and S.A. Ghabrial. 2014. Complete genome sequence of a novel hypovirus infecting Phomopsis longicolla. Archives of Virology. January, 2014

Koonin, E.V., G.H. Choi, D.L. Nuss, R. Shapira, and J.C. Carrington. 1991. Evidence for Common Ancestry of a Chestnut Blight Hypovirulence-associated Double-Stranded RNA and a Group of Positive-strand RNA Plant Viruses. Proceedings of the National Academy of Sciences of the United States of America. 88:10647-10651

Koonin, E.V. and V.V. Dolja. 1993. Evolution and taxonomy of positive-strand RNA viruses: implications of comparative analysis of amino acid sequences. Critical Reviews in Biochemistry and Molecular Biology. 28: 375-430

Kubisiak, T.L. and M.G. Milgroom. 2006. Markers linked to vegetative incompatibility (vic) genes and a region of high heterogeneity and reduced recombination near the mating type locus (MAT) in *Cryphonectria parasitica*. Fungal Genetics and Biology. 43: 453-463

Kumagai, M.H., J. Donson, G. della-Cioppa, D. Harvey, K. Hanley, and L.K. Grill. 1995. Cytoplasmic inhibition of carotenoid biosynthesis with virus-derived RNA. Proceedings of the National Academy of Sciences of the United States of America. 92: 1679-1683

Lakatos, L., T. Csorba, V. Pantaleo, E.J. Chapman, J.C. Carrington, Y.K. Liu, V.V. Dolja, L.F. Calvino, J.J. Lopez-Moya, and J. Burgyan. 2006. Small RNA Binding is a common strategy to suppress RNA silencing by several viral suppressors. The EMBO Journal. 25:2768-2780

Lan, X., Z. Yao, Y. Zhou, J. Shang, H. Lin, D.L. Nuss, and B. Chen. 2008. Deletion of the *cpku80* gene in the Chestnut Blight Fungus, *Cryphonectria parasitica*, enhances gene disruption ffficiency. Current Genetics. 53: 59-66

Li, D., T. Wei, C.M. Abbott, and D. Harrich. 2013. The unexpected roles of eukaryotic translation elongation factors in RNA virus replication and pathogenesis. Microbiology and Molecular Biology Reviews. 77: 253-266

Lin, H., X. Lan, H. Liao, T.B. Parsley, D.L. Nuss, and B. Chen. 2007. Genome Sequence, full-length infectious cDNA clone, and mapping of viral double-stranded RNA

accumulation determinant of hypovirus CHV1-EP721. Journal of Virology. 81: 1813-1820

Lindbo, J.A., L. Silva-Rosales, W.M. Proebsting, W.G. Dougherty. 1993. Induction of a highly specific antiviral state in transgenic plants: implications for regulation of gene expression and virus resistance. Plant Cell. 5: 1749-1759

Linder-Basso, D., J.N. Dynek, and B.I. Hillman. 2005. Genome analysis of *Cryphonectria hypovirus* 4, the most common hypovirus species in North America. Virology. 337:192-203

Liu, Y.P. V.V. Peremyslov, V. Medina, and V.V. Dolja. Tandem leader proteases of Grapevine leafroll-associated virus-2: host-specific functions in the infection cycle. Virology. 383: 291-299

Löving, R., S.R. Wu, M. Sjöberg, B. Lindqvist, H. Garoff. 2012. Maturation cleavage of the murine leukemia vius Env precursor separates the transmembrane subunits to prime it for receptor triggering. Proceedings of the National Academy of Sciences of the United States of America. 109: 7735-7740

Maiti, M. H.C. Lee, and Y. Liu. QIP, a putative exonuclease, interacts with the *Neurospora* Argonaute protein and facilitates conversion of duplex siRNA into single strands. Genes and Development. 21: 590-600

Márquez, L.M., R.S. Redman, R.J. Rodriguez, and M.J. Roossinck. 2007. A virus in a f ungus in a plant: Three –way symbiosis required for thermal tolerance. Science. 315: 513-515

McGowan, S., A.M. Buckle, M.S. Mitchell, J.T. Hoopes, D.T. Gallagher, R.D. Heselpoth, Y. Shen, C.R. Reboul, R.H. Law, V.A. Fischetti, J.C. Whisstock, and D.C. Nelson. 2012. X-ray crystal structure of the streptococcal specific phage lysine PlyC. Proceedings of the National Academy of Sciences of the United States of America. 109:12752-12757.

Merai, Z., X. Kerenyi, A. Molnar, E. Barta, A. Valoczi, G. Bisztray, Z. Havelda, J. Burgyan, and D. Shilhavy. 2005. Aureusvirus P14 is an efficient RNA silencing suppressor that binds double-stranded RNAs without size specificity. Journal of Virology. 79:7217-7226.

Mertens, P.P.C., C.Z. Wei, and B.I. Hillman. 2005. Genus *Mycoreovirus*, Virus Taxonomy: Eighth Report of the International Committee for Taxonomy of Viruses. C.M. Fauquet, M.A. Mayo, J. Maniloff, U. Desselberger, and L.A. Ball (ed), Virus Taxonomy: Eigth Report of the International Committee for

Taxonomy of Viruses. Elsevier/Academic Press, London, United Kingdom. 556-560

Milgroom, M. and P. Cortesi. 2004. Biological control of chestnut blight with hypovirulence: a critical analysis. Annual review of Phytopathology. 42: 311-338

Moffit, E.M., and R.M. Lister. 1975. Application of a Serological Screening Test for Detecting Double-Stranded RNA mycoviruses. Phytopathology. 65: 851-859

Morsy, M.R., J. Oswald, J. He, Y. Tang, and M.J. Roossinck. 2011. Teasing apart a three-way symbiosis: Transcriptome analyses of *Curvularia protuberata* in response to viral infection and heat stress. Biochemical and Biophysical Research Communications. 401: 225-230

Mu, R., T.A. Romero, K.A. Hanley, A.L. Dawe. 2011. Conserved and variable structural elements in the 5′ untranslated region of two hypoviruses from the filamentous fungus *Cryphonectria parasitica*. Virus Research. 161: 203-208

Nakayashiki, H., N. Kadotani, S. Mayama. 2006. Evolution and diversification of RNA silencing proteins in fungi. Journal of Molecular Evolution. 63: 127-135

Newhouse, J.R., H.C. Hoch, and W.L. MacDonald. 1983. The ulrastructure of *Endothia parasitica*. Comparison of a virulent with a hypovirulent isolate. Canadian Journal of Botany. 61: 389-399

Newhouse, J.R., W.L. MacDonald, and H.C. Hoch. 1990. Virus-like particles in hyphae and conidia of European hypovirulent (dsRNA-containing) strains of *Cryphonectria parasitica*. Canadian Journal of Botany. 68: 90-101

Newhouse, J.R. and W.L. MacDonald. 1991. The ultrastructure of hyphal anastomosis between vegetatively compatible and incompatible virulent and hypovirulent strains of *Cryphonectria parasitica*. Canadian Journal of Botany. 69: 602-614

Nolan, T., L. Braccini, G. Azzalin, A. De Toni, G. Macino, and C. Cogoni. 2005. The post-transcriptional gene silencing machinery functions independently of DNA methylation to repress a LINE1-like retrotransposon in *Neurospora crassa*. Nucleic Acids Research. 33: 1564-1573

Nuss, D.L., 1992. Biological control of chestnut blight: an example of virus mediated attenuation of fungal pathogenesis. Microbiol. Reviews. 56:561-576

Nuss, D.L. 2005. Hypovirulence: Mycoviruses at the Fungal-Plant Interface. Nature Reviews Microbiology. 3:632-642

Nuss, DL. 2010. Mycoviruses. Cellular and Molecular Biology of Filamentous Fungi. Borkovich, KA.; Ebbole, DJ., editors. ASM Press; Washington, DC: 145-152

Nuss, D.L. and B.I. Hillman. 2012. Family *Hypoviridae*, p1029-1033, Virus Taxonomy: 9th Report of the International Committee for the Taxonomy of Viruses. A.M.Q. King, M.J. Adams, E.B. Carstens, and E.J. Lefkowitz (ed.) Elsevier/Academic Press, London, United Kingdom.

Paoletti, M., S.J. Saupe, and C. Clave. 2007. Genesis of a fungal non-self recognition repertoire. PLoS One. 2: e283

Parsley, T.B., B. Chen, L.M. Geletka, and D.L. Nuss., 2002. Differential Modulation of Cellular Signaling Pathways by Mild and Severe Hypovirus Strains. Eukaryotic Cell. 1: 401-413

Paul, C.P., and D.W. Fulbright. 1988. Double-stranded RNA molecules from Michigan hypovirulent isolates of Endothia parasitica vary in size and sequence homology. Phytopathology. 78:751-755

Pearson, M.N., R.E. Beever, B. Boine, and K. Arthur. 2009. Mycoviruses of filamentous fungi and their relevance to plant pathology. Molecular Plant Pathology. 10: 115-128

Polashock, J.J., and B.I. Hillman. 1994. A small mitochondrial souble-stranded (ds) RNA element associated with a hypovirulent strain of the chestnut blight fungus and ancestrally related to yeast cytoplasmic T and W dsRNAs. Proceedings of the National Academy of Sciences of the United States of America. 91:8680-8684

Polashock, J.J., P.J. Bedker, and B. I. Hillman. 1997. Movement of a small mitochondrial doube-stranded RNA element of *Cryphonectria parasitica*: ascospore inheritance and implications for mitochondrial recombination. Molecular and General Genetics. 256: 566-571

Powell, M.L., S. Napthine, R.J. Jackson, I. Brierley, and T.D. Brown. 2008. Characterization of the termination-reinitiation strategy employed in the expression of influenza B virus BM2 protein. RNA. 14: 2394-2406

Rae, B.P., B.I. Hillman, J. Tartaglia, and D.L. Nuss. 1989. Characterization of double-stranded RNA genetic elements associated with biological control of chestnut

blight: organization of terminal domains and identification of gene products. The EMBO Journal. 8: 657-663

Ramos, I., E. Carnero, D. Bernal-Rubio, C.W. Seibert, L. Westera, A. Garcia-Sastre, and A. Fernandex-Sesma. 2013. Contribution of double-stranded RNA and CPSF30 binding domains of influenza virus NS1 to the inhibition of type I interferon production and activation of human dendritic cells. Journal of Virology. 87: 2430-2440

Roossinck, M.J. 2011. The good viruses: viral mutualistic cymbioses. Nature Reviews: Microbiology. 9: 99-108

Ruest, L.B. R. Marcotte, and E. Wang. 2002. Peptide elongation factor eEF1A-2/S1 expression in cultured differentiated myotubes and its protective effect against caspase-3-3mediated apoptosis. Journal of Biological Chemistry. 277: 5418-5425

Sasaki, A., M. Onoue, S. Kanematsu, K. Suzaki, M. Miyanishi, N. Suzuki, D.L. Nuss, and K. Yoshida. 2002. Extending chestnut blight hypovirus host range within diaporthales by biolistic delivery of viral cDNA. Molecular Plant-Microbe Interactions. 15: 780-789.

Segers, G.C., R. Van Wezel, X. Zhang, Y. Hong, and D.L. Nuss. 2006. Hypovirus papain-like protease p29 suppresses RNA silencing in the natural fungal host and in a heterologous plant system. Eukaryotic Cell. 5: 896-904

Segers, G.C., X. Zhang, F. Deng, Q Sun, and D.L. Nuss. 2007. Evidence that RNA silencing functions as an antiviral defense mechanism in fungi. Proceedings of the National Academy of Sciences of the United States of America. 104:12902-12906

Shapira, R., and D.L. Nuss. 1991. Gene Expression by a Hypovirulence-Associated Virus of the Chestnut Blight Fungus Involves Two Papain-Like Protease Activities. The Journal of Biological Chemistry. 266:19419-19425.

Shapira, R., G.H. Choi, and D.L. Nuss. 1991A. Virus-like genetic organization and expression strategy for a double-stranded RNA genetic element associated with biological control of chestnut blight. The EMBO Journal. 10:731-739.

Shapira, R., G.H. Choi, B.I. Hilman, and D.L. Nuss. 1991B. The contribution of defective RNAs to the complexity of viral-encoded double-stranded RNA populations present in hypovirulent strains of the chestnut blight fungus *Cryphonectria parasitica*. The EMBO Journal. 10:741-746.

Shiu, P.K. and R.L. Metzenberg. 2002. Meiotic cilencing by unpaired DNA: properties, regulation, and suppression. Genetics. 161: 1483-1495

Smart, C.D., W. Yuan, R. Foglia, D.L. Nuss, D.W. Fulbright, and B.I. Hillman. 1999. *Cryphonectria hypovirus* 3, a virus species in the family *Hypoviridae* with a single open reading frame. Virology. 265: 66-73

Sun, Q., G.H. Choi, and D.L. Nuss. 2009. A Single Argonaute Gene is Required for Induction of RNA Silencing Antiviral Defense and Promotes Viral RNA Recombination. Proceedings of the National Academy of Sciences of the United States of America. 106: 17927-17932.

Supyani, S., B.I. Hillman, and N. Suzuki. 2007. Baculovirus expression of the 11 mycoreovirus-1 genome segments and identification of the guanylyltransferase-encoding segment. Journal of General Virology. 88:342-350

Suzuki, N., D. Chen, and D.L. Nuss. 1999. Mapping of a hypovirus p29 protease symptom determinant domain with sequence similarity to potyvirus HC-Pro protease. Journal of Virology. 73: 9478-9484.

Suzuki, N., M.L. Geletka, and D.L. Nuss. 2000. Essential and dispensable virus encoded replication elements revealed by efforts to develop hypoviruses as gene expression vectors. Journal of Virology. 74: 7568-7577.

Suzuki, N., and D.L. Nuss. 2002. The contribution of p40 to hypovirus-mediated modulation of fungal host phenotype and viral RNA accumulation. Journal of Virology. 76: 7568-7759

Suzuki, N., K. Maruyama, M. Moriyama, and D.L. Nuss. 2003. Hypovirus Papain-Like Protease p29 Functions in *trans* to Enhance Viral Double-Stranded RNA Accumulation and Vertical Transmission. Journal of Virology. 77: 11697- 11707

Tartaglia, J., C.P. Paul, D.W. Fulbright, and D.L. Nuss. 1986. Structural properties of double-stranded RNAs associated with biological control of chestnut blight fungus. Proceedings of the National Academy of Sciences of the United States of America. 83: 9109-9113.

Tsukiyama-Kohara, K., N. Lizuka, M. Kohara, and A. Nomoto. 1992. Internal ribosome entry site within hepatitis C virus RNA. Journal of Virology. 66: 1476-1483

Vargason, J.M., G. Szittya, J. Burgyan, and T.M. Hall. 2003. Size selective recognition of siRNA by an RNA silencing suppressor. Cell. 115:799-811

Volchkov, V.E., H. Feldmann, V.A. Volchkova, H.D. Klenk. 1998. Processing of the ebola virus glycoprotein by the proprotein convertase furin. Proceedings of the National Academy of Sciences of the United States of America. 95: 5762-5767

Wang, J., F. Wang, Y. Feng, K.Mi, Q. Chen, J. Shang, and B. Chen. 2013. Comparative vesicle proteomics reveals selective regulation of protein expression in chestnut blight fungus by a hypovirus. Journal of Proteomics. 78: 221-230

Ward, J.J., J.S. Sodhi, L.J. McGuffin, B.F. Buxton, and D.T. Jones. 2004. Prediction and functional analysis of native disorder in proteins from the three kingdoms of life. Journal of Molecular Biology. 337:635-645

Wickner, R.B., S.A. Ghabrial, M.L. Nibert, J.L. Patterson, and C.C. Wang. Family *Totiviridae*, p639-650. Virus Taxonomy: 9th Report of the International Committee for the Taxonomy of Viruses. A.M.Q. King, M.J. Adams, E.B. Carstens, and E.J. Lefkowitz (ed.) Elsevier/Academic Press, London, United Kingdom.

Xie, J., D. Wei, D. Jiang, Y. Fu, G. Li, S. Ghabrial, and Y. Peng. 2006. Characterization of debilitation-associated mycovirus infecting the plant-pathogenic fungus *Sclerotina sclerotorium*. Journal of General Virology. 87: 241-249

Xie, J., X. Xiao, Y. Fu, H. Liu, J. Cheng, S.A. Ghabrial, G. Li, and D. Jiang. 2011. A novel mycovirus closely related to hypoviruses that infects the plant pathogenic f ungus *Sclerotinia sclerotiorum*. Virology. 418: 49-56

Yaegashi, H., S. Kanematus, and T. Ito. 2012. Molecular characterization of a new hypovirus infecting a phytopathogenic fungus, *Valsa ceratosperma*. Virus Research. 165:143-150

Yang, X., S.H. Tan, Y.J. Teh, and Y.A. Yuan. 2011. Structural implications into dsRNA binding and RNA silencing suppression by NS3 protein of *Rice Hoja Blanca Tenuivirus*. RNA. 17:903-911

Yu, X., B. Li, Y. Fu, J. Xie, J. Cheng, S. Ghabrial, G. Li, X. Yi, and D. Jiang. 2013. Extracellular transmission of a DNA mycovirus and its use as a natural fungicide. Proceedings of the National Academy of Sciences of the United States of America. 110:1452- 1457.

Yu, X., B. Li, Y. Fu, D. Jiang, S. Ghabrial, G. Li, Y. Peng, J. Xie, J. Cheng, J. Huang, and X. Yi. 2010. A geminivirus-related DNA mycovirus that confers hypovirulence to a plant pathogenic fungus. Proceedings of the National Academy of Sciences of the United States of America. 107: 8387-8392.

Zhang, D., M.J. Spiering, A. Dawe, and D.L. Nuss. 2014. Functional evidence for dedicated allorecognition by the vegetative incompatibility loci that restrict mycovirus transmission in the chestnut blight fungus. Genetics. Submitted.

Zhang, X. and D.L. Nuss. 2008. A host dicer is required for defective viral RNA production and recombinant virus vector RNA instability for a positive sense RNA virus. Proceedings of the National Academy of Sciences of the United States of America. 105:16749-16754.

Zhang, X., G.C. Segers, Q. Sun, F. Deng, and D.L. Nuss. 2008. Characterization of hypovirus-derived small RNAs generated in the Chestnut Blight fungus by an inducible DCL-2-dependent pathway. Journal of Virology. 82: 2613-2619.

Zhang, X., D. Shi, and D.L. Nuss. 2013. Variations in hypovirus interactions with the fungal-host RNA-silencing antiviral-defense response. Journal of Virology. 86: 12933-12939.

Zimmer, G., L. Budz, and G. Herrier. 2001. Proteolytic activation of respiratory syncytial virus fustion protein. Cleavage at two furin consensus sequences. Journal of Biological Chemistry. 276: 31642-31650

Zucker, M. 2003. Mfold web server for nucleic acid folding and hybridization prediction. Nucleic Acids Research. 31: 3406-3415

Zucker, M., and A.B. Jacobson. 1998. Using reliability information to annotate RNA secondary structures. RNA. 4: 669-679

Zybert, I.A., H. vand der Ende-Metselaar, J. Wilschut, and J.M. Smit. 2008. Functional importance of dengue virus maturation: infectious properties of immature virions. Journal of General Virology. 89: 3047-3051